STABILITY ANALYSIS AND CONTROL OF STOCHASTIC DYNAMIC SYSTEMS USING POLYNOMIAL CHAOS

A Dissertation

by

JAMES ROBERT FISHER

Submitted to the Office of Graduate Studies of
Texas A&M University
in partial fulfillment of the requirements for the degree of

DOCTOR OF PHILOSOPHY

August 2008

Major Subject: Aerospace Engineering

STABILITY ANALYSIS AND CONTROL OF STOCHASTIC DYNAMIC SYSTEMS USING POLYNOMIAL CHAOS

A Dissertation

by

JAMES ROBERT FISHER

Submitted to the Office of Graduate Studies of
Texas A&M University
in partial fulfillment of the requirements for the degree of

DOCTOR OF PHILOSOPHY

Approved by:

Chair of Committee,	Raktim Bhattacharya
Committee Members,	Srinivas Rao Vadali
	John L. Junkins
	John Hurtado
	Suman Chakravorty
	D.V.A.H.G. Swaroop
Head of Department,	Helen Reed

August 2008

Major Subject: Aerospace Engineering

ABSTRACT

Stability Analysis and Control of Stochastic Dynamic Systems
Using Polynomial Chaos. (August 2008)
James Robert Fisher, B.S., Texas A&M University;
M.S., Texas A&M University
Chair of Advisory Committee: Dr. Raktim Bhattacharya

Recently, there has been a growing interest in analyzing stability and developing controls for stochastic dynamic systems. This interest arises out of a need to develop robust control strategies for systems with uncertain dynamics. While traditional robust control techniques ensure robustness, these techniques can be conservative as they do not utilize the risk associated with the uncertainty variation. To improve controller performance, it is possible to include the probability of each parameter value in the control design. In this manner, risk can be taken for parameter values with low probability and performance can be improved for those of higher probability.

To accomplish this, one must solve the resulting stability and control problems for the associated stochastic system. In general, this is accomplished using sampling based methods by creating a grid of parameter values and solving the problem for each associated parameter. This can lead to problems that are difficult to solve and may possess no analytical solution.

The novelty of this dissertation is the utilization of non-sampling based methods to solve stochastic stability and optimal control problems. The polynomial chaos expansion is able to approximate the evolution of the uncertainty in state trajectories induced by stochastic system uncertainty with arbitrary accuracy. This approximation is used to transform the stochastic dynamic system into a deterministic system that can be analyzed in an analytical framework.

In this dissertation, we describe the generalized polynomial chaos expansion and present a framework for transforming stochastic systems into deterministic systems. We present conditions for analyzing the stability of the resulting systems. In addition, a framework for solving $\mathcal{L}_2$ optimal control problems is presented. For linear systems, feedback laws for the infinite-horizon $\mathcal{L}_2$ optimal control problem are presented. A framework for solving finite-horizon optimal control problems with time-correlated stochastic forcing is also presented. The stochastic receding horizon control problem is also solved using the new deterministic framework. Results are presented that demonstrate the links between stability of the original stochastic system and the approximate system determined from the polynomial chaos approximation. The solutions of these stochastic stability and control problems are illustrated throughout with examples.

To Marin', who believed in me even when I did not.

ACKNOWLEDGMENTS

While this dissertation bears my name, it would never have reached completion without the aid and support of many people. First, I would like to thank Dr. Raktim Bhattacharya who has been a friend and mentor. His creativity and drive have been essential to the completion of this work. Secondly, I would like to thank Dr. Vadali for his guidance throughout my time as a graduate student. My appreciation also goes to Dr. Suman Chakravorty for letting me "bother" him many times to discuss the theoretical implications of the work.

I would also like to thank my friends who have been very supportive and have helped me to maintain my sanity while completing this work. I would especially like to thank Jeff Wischkaemper for always being there to share a laugh or a hardship. As always I must thank my wife Marin' for all the support and love she has shown me during this time. I would never have completed this without her.

Most importantly, I must thank my God, who leads me beside still waters. His patience when I fall short and His comfort when I feel lost have never failed me.

TABLE OF CONTENTS

CHAPTER Page

CHAPTER Page

LIST OF TABLES

LIST OF FIGURES

FIGURE Page

FIGURE Page

FIGURE Page

CHAPTER I

INTRODUCTION

A. Background

Recently there has been a growing interest in combining robust control approaches with stochastic control methods to develop the so called field of *probabilistic robust control*. This field arises from the need to a) understand how stochastic system uncertainties affect state trajectories and, b) exploit it to design less conservative robust control algorithms. Traditional robust control design techniques assume uniformly distributed uncertainty over the parameter space and the controller is designed to be robust for the worst case scenario. In the framework of probabilistic robust control, the binary notion of robustness is discarded and the notion of a risk-adjusted robustness margin tradeoff is adopted. This framework is more practical as in many cases a control system designer may have knowledge of the distribution of the uncertainty in the system parameters, and may be willing to accept a small well defined level of risk in order to obtain larger robustness margins. It is also possible to stabilize the system for all possible parameter values with non-zero probability of occurrence and optimize performance with respect to the probability distribution of the parameters. Both these design philosophies result in less conservative controllers in the probabilistic sense. Therefore, it is important to consider not only the range of parameter values but also the probability density function of the parameters in the controller design.

Many approaches exist for stability analysis and controller design for stochastic systems. In general, many of these approaches tend to take on one of two approaches.

The journal model is *IEEE Transactions on Automatic Control.*

One approach deals with solution of equations of motion that result from Itô's formula [1]. In general, expressions of this type can be difficult to solve and solutions only exist for certain special cases. Furthermore, these types of problems generally deal only with systems with stochastic forcing and not with systems that contain stochastic uncertainty in the parameters directly. In general, these problems tend to involve white noise processes and do not address correlated inputs. The other approach to solving stochastic stability and control problems involves sampling based methods. These methods attempt to approximate a probability distribution by utilizing a large number of points. This is generally accomplished by creating a mesh of values over the support of the distribution and performing simulation and analysis for each of the points in the mesh. In stability analysis for example, conditions for stability might be tested for each of the points to determine if the system is stable for the entire distribution. While this is certainly effective, this requires a large number of computations and therefore can require a large amount of computational time. Furthermore, if such methods are used to determine system trajectories, any changes in initial conditions will void all calculations and require recomputation for each point in the distribution because the trajectories are uniquely determined by their initial conditions.

Much of the previous work has dealt with solving stochastic stability and control problems with either stochastic forcing or probabilistic uncertainty in system parameters. Specifically, problems dealing with stochastic forcing assume that the unknown forcing terms are Gaussian. When this is not the case, it is common to approximate the distribution using a Gaussian closure. The problem of covariance control with Gaussian excitation has also been investigated, by Skelton *et al.* [2]. The problem of parametric uncertainty is treated separately from that of stochastic excitation. Much of the work here deals with the utilization of sampling based methods. Stengel [3]

introduces the idea of probability of stability and uses sampling based methods to ensure robustness and stability in a probabilistic sense [4]. The methodology is applied to nonlinear systems, but requires a genetic algorithm to solve the resulting control problem [5, 6]. In a similar approach Barmish *et al.* uses Monte-Carlo based methods to analyze stability and control problems in an LMI framework [7, 8], however the results are limited to a multidimensional uniform distribution with respect to the uncertain parameters. An additional approach by Polyak *et al.* [9] develops an algorithm to determine a control with guaranteed worst-case cost. This approach also requires the uncertain system parameters to be linear functions of the random variable. Additionally, a probabilistic design is applied to LPV control in [10]. Here, an algorithm is developed that uses sequential random generation of uncertain parameters using the associated probability distribution function to converge to an LPV solution that is satisfied for the entire range of uncertainty. A sampling based technique is also applied to the $\mathcal{H}_\infty$ problem in [11]. In this case a similar sequential solution technique is employed to solve the $\mathcal{H}_\infty$ problem.

The novelty of the framework presented in this work is that *non-sampling* based methods are used to approximate, with arbitrary accuracy, the evolution of uncertainty in state trajectories induced by uncertain system parameters. The framework is built on the polynomial chaos theory which transforms stochastic dynamics into deterministic dynamics in higher dimensional state space. However, this increase in dimensionality is often significantly lower than the sampling based methods for comparably accurate representation of uncertainty. The benefit of this approach is that stochastic linear and nonlinear systems are transformed into deterministic systems and existing stability analysis and control theory can be used for design and analysis.

Polynomial chaos was first introduced in 1938 by Wiener [12] where Hermite polynomials were used to model stochastic processes with Gaussian random variables. As

the concept of chaos would not be developed until decades later, the concept of using these polynomials to model stochastic behavior was termed "Homogeneous Chaos". According to Cameron and Martin [13] such an expansion converges in the $\mathcal{L}_2$ sense for any arbitrary $\mathcal{L}_2$ functional. In terms of stochastic processes, this implies that the expansion is able to converge to any arbitrary stochastic process with a finite second moment. This applies to most physical systems. The original Homogeneous Chaos expansion utilizes Hermite polynomials to model stochastic processes. Though these polynomials can be used to model any stochastic process with arbitrary accuracy, the convergence rate is exponential when they are used to model Gaussian processes [14]. This is because the Hermite polynomials associated with the Homogeneous Chaos expansion are orthogonal with respect to the probability density function (pdf) of a Gaussian distribution. Using this idea and applying it to other types of polynomials, Xiu *et al.* [15] generalized the result of Cameron-Martin to various continuous and discrete distributions using orthogonal polynomials from the so called Askey-scheme [16] and demonstrated $\mathcal{L}_2$ convergence in the corresponding Hilbert functional space. This is popularly known as the generalized polynomial chaos (gPC) framework. In this work, it was demonstrated that when polynomials orthogonal with respect to a given probability distribution are used, the convergence rate for the resulting approximation is exponential even when the process is the solution of a differential equations.

The gPC framework has been applied to applications including stochastic fluid dynamics [17, 18, 19], stochastic finite elements [20], and solid mechanics [21, 22]. In general these works are applied to static problems, though in [20] application to a dynamic system is presented briefly. Application of gPC to control related problems has been surprisingly limited. Furthermore, there have been few if any attempts at developing a generalized framework to understand the dynamics of the deterministic

system obtained from utilizing the expansion. The work of Hover *et al.* [23] addresses stability and control of a bilinear dynamical system, with probabilistic uncertainty on the system parameters. The controller design problem considered involved determining a family of proportional gains to minimize a finite time integral cost functional. Outside of the work of Hover, there has been additional work that has dealt with applying polynomial chaos to estimation and control problems in power electronics [24, 25]. Unfortunately, several of these papers seem to assume that the uncertainty is time varying and governed by white processes, and thus apply the expansion incorrectly as an infinite number of random variables would be required to model such processes.

B. Content of This Dissertation

In this dissertation we focus on the application of the polynomial chaos expansion to stability analysis and control of stochastic linear and nonlinear systems. In particular we assume that the uncertainty in the system dynamics is dependent on random variable, governed by a known probability distribution. The uncertainty may enter the system as linear or nonlinear functions of the random variable which may be governed by any continuous stationary probability distribution. Although it is certainly possible to extend these results to discrete distributions, these have not been treated. The benefit of the gPC approach is that it admits analytical solutions to stochastic stability and control problems. In fact, we will show that known methods for stability and control analysis can be readily applied to stochastic systems in this framework.

The main contribution of this dissertation lies in the application of the gPC expansion to linear and nonlinear stability analysis and control design problems. Conditions for the solution of these problems are written in the gPC framework and

demonstrated with several examples. The work is divided into seven chapters. The second chapter deals with background on probability theory and outlines generalized Polynomial Chaos theory. Many fundamental concepts such as that of a random variable and a σ-algebra will be presented. We will also outline the Homogeneous Chaos framework and show the extension of this concept to other polynomial sets. Finally, a methodology for incorporating correlated noise into the analysis will be presented by means of the Karhunen-Loéve (KL) expansion. This will allow us to analyze systems with correlated process noise uncertainty.

Chapter III deals with modelling and stability analysis of stochastic systems using the generalized Polynomial Chaos framework. The chapter will deal with results for both linear and nonlinear systems. A generalized framework for modelling stochastic linear systems with the gPC expansion is presented. Next, a discussion on the application of the gPC expansion for different types of nonlinearities is presented and system form is presented for polynomial systems. The ability of the expansion to accurately predict the statistics of these systems is demonstrated by application to the non-dimensional longitudinal Vinh's equations with uncertainty in initial conditions. Stability results for linear and nonlinear systems are presented in terms of the gPC framework. For linear systems results are presented for both continuous and discrete time system. These results are verified with examples.

In Chapter IV, we focus on optimal control of stochastic linear and nonlinear systems. For linear systems, we focus on optimal control in the $\mathcal{L}_2$ sense for systems with probabilistic uncertainty in the system parameters. A framework for minimum expectation control is presented and the problem is solved for different feedback structures. Conditions for feasibility and optimality are determined for each of these structures. In addition, the minimum expectation control framework is applied to nonlinear systems and the gPC expansion is used to generate optimal trajectories for

nonlinear stochastic problems. Finally, the KL expansion is used to generate optimal trajectories for systems with colored stochastic forcing.

In Chapter V the gPC methodology is utilized to solve the stochastic receding horizon problem for linear systems. In particular, a proof is presented for stability in terms of the gPC coefficients and several methods of performing receding horizon control for stochastic systems are presented. Examples are presented that highlight the differences in the application of these policies. Chapter VI presents several results that help theoretically justify the usage of the gPC expansion for processes that can be determined by solution of stochastic differential equations. Finally in the last chapter the main contributions of the work are highlighted and areas of future research are presented. Various probability distributions and their corresponding gPC expansions are presented in the appendix along with a methodology for performing analysis with respect to various confidence intervals. The gPC methodology is used to demonstrate a method for solving problems that require properties to be satisfied with a specific probability. Additionally, the gPC expansion is used to solve stochastic problems involving independent random variables governed by different probability distributions.

CHAPTER II

POLYNOMIAL CHAOS

The methodology described in this dissertation utilizes orthogonal functionals to represent 2^{nd} order random processes that are solutions of stochastic dynamic systems. This approach is spectral with respect to the stochastic elements in the dynamic system. It utilizes families of orthogonal polynomials, which we will refer to as Polynomial Chaoses, to approximate the both the functions of random variables which appear in the equations of motion for a dynamic system as well as the actual solution. In this chapter, we define the structure of these orthogonal polynomials and present some of their properties, which will be applied to analyze stochastic stability and control problems.

A. Preliminary Concepts from Probability Theory

Before presenting a formal definition of Polynomial Chaos, we introduce a few important concepts from probability theory.

Let Ω be a set of events. This is a set of all possible outcomes and to these outcomes we will assign probabilities. As we know intuitively, there are relationships between the probability that a event occurs and the probability that it does not. To account for the relationships between events we will need to introduce another set called a σ-algebra [1, 26].

Definition II.1 *A σ-algebra, $\mathcal{B}$ is a non-empty class of subsets of Ω such that*

1. $\Omega \in \mathcal{B}$
2. $B \in \mathcal{B}$ *implies* $B^c \in \mathcal{B}$
3. $B_i \in \mathcal{B}, i \leq 1$ *implies* $\bigcup_{i=1}^{\infty} B_i \in \mathcal{B}$

One example of a σ-algebra is a set made of all possible combinations of elements in Ω. We are now ready to define a probability space [1, 26].

Definition II.2 *A probability space is a triple (Ω,$\mathcal{B}$,P) where*

- Ω *is the sample space*
- $\mathcal{B}$ *is a σ-algebra of subsets of Ω*
- P *is a probability measure, a function $P : \mathcal{B} \mapsto [0, 1]$ such that*
  1. $P(A) \geq 0$ *for all $A \in \mathcal{B}$*
  2. *If $\{A_n, n \geq 1\}$ are events in $\mathcal{B}$ that are disjoint, then*

$$P\left(\bigcup_{n=1}^{\infty} A_n\right) = \sum_{n=1}^{\infty} P(A_n)$$

  3. $P(\Omega) = 1$

In this work we will deal with polynomials which are functions of random variables. These random variables are functions that map between a probability space and the probability space, $(\mathbb{R}^k, \mathcal{B}(\mathbb{R}^k), P)$. We will next define the concept of a random variable. To accomplish this, we first define an inverse image.

Definition II.3 *Suppose Ω_1 and Ω_2 are two sets (Often $\Omega_2 = \mathbb{R}$) and suppose that $\Delta : \Omega_1 \mapsto \Omega_2$. The inverse image of Δ is defined by*

$$\Delta^{-1}(A_2) = \{\omega \in \Omega_1 : \Delta(\omega) \in A_2\}$$

This is similar to a function inverse, but more general as it is defined on sets. The inverse image is defined to be all of the elements of Ω_1 which correspond to elements in Ω_2 when mapped through Δ. We now define a random variable [1, 26]. A random variable is defined between two measurable spaces (a measurable space is the pair $(\Omega, \mathcal{B})$).

Definition II.4 *Suppose* $(\Omega_1, \mathcal{B}_1)$ *and* $(\Omega_2, \mathcal{B}_2)$ *are two measurable spaces and the function* $\Delta : \Omega_1 \mapsto \Omega_2$*. The function* Δ *is said to be a measurable function if for every set* $B_2 \in \mathcal{B}_2$*,*

$$\Delta^{-1}(B_2) \in \mathcal{B}_1$$

Definition II.5 *If* $(\Omega_2, \mathcal{B}_2) = (\mathbb{R}^k, \mathcal{B}(\mathbb{R}^k))$ *in definition II.4, we call the function* Δ *a random variable.*

In the above definition, $\mathcal{B}(\mathbb{R}^k)$ is the σ-algebra generated by all the open subsets of $\mathbb{R}^k$. A random variable is therefore a function that associates a real number (or vector) with outcomes of an experiment or events.

Next, we will define the expectation of a random variable, X [1, 26].

Definition II.6 *Suppose* $(\Omega, \mathcal{B}, P)$ *is a probability space and* $X : (\Omega, \mathcal{B}) \mapsto (\bar{\mathbb{R}}, \mathcal{B}(\bar{\mathbb{R}}))$*, where* $\bar{\mathbb{R}} = [-\infty, \infty]$ *(*X *can have* $\pm\infty$ *in its range). Define the expectation of* X*, written* $\mathbf{E}[X]$ *as the Lebesgue-Stieltjes integral of* X *with respect to* P *or*

$$\mathbf{E}[X] = \int_\Omega X dP = \int_\Omega X(\omega) P(d\omega)$$

The expectation of a random variable is its average value with respect to the probability space from which it maps. In general, we will be dealing with variables that have an associated probability distribution (either continuous or discrete). When this is the case and $P(d\omega) = f(\omega)d\omega$ we can write the expectation operator as

$$\mathbf{E}[X(\omega)] = \int_\Omega X(\omega) f(\omega) d\omega \tag{II.1}$$

when $f(\omega)$ is piecewise continuous and

$$\mathbf{E}[X(\omega)] = \sum_{\{\omega \in \Omega : f(\omega) \neq 0\}} X(\omega) f(\omega) \tag{II.2}$$

when there are discrete events that occur with finite probability. In the discrete case, the summation is over the values of $\omega \in \Omega$ that occur with non-zero probability and $f(\omega)$ is the probability associated the discrete point ω. This discrete formulation will not be utilized in this work as we will mainly be dealing with continuous functions.

B. The Weiner-Askey Polynomial Chaos

One of the major difficulties in incorporating stochastic processes into analysis and control of dynamic systems is the necessity of dealing with abstract measure spaces which are usually infinite dimensional and are difficult to understand physically. In particular it is difficult to understand the behavior of functions defined on this abstract measure space, more specifically the random variables defined on the σ-algebra of random events. In many applications a Monte-Carlo approach is used and the events in the σ-algebra are sampled. This requires a large number of sample points to achieve a good approximation. An alternative methodology is to approximate the function with a Fourier-like series.

1. Askey Hypergeometric Orthogonal Polynomials

To approximate a stochastic process, a set of orthogonal polynomials will be employed. In this section, we will present an overview of the theory of these polynomials as well as provide details on the Askey scheme. There is a wealth of literature on orthogonal polynomials and the interested reader is referred to [27, 28, 29].

a. Generalized Hypergeometric Series

To begin, the generalized hypergeometric series as presented in [30] is introduced. The generalized hypergeometric series, F_s^r, is defined by

$$F_s^r(a_1,\ldots,a_r,b_1,\ldots,b_s,z) = \sum_{k=0}^{\infty} \frac{(a_1)_k \cdots (a_r)_k}{(b_1)_k \cdots (b_s)_k} \frac{z^k}{k!}, \tag{II.3}$$

where the term $(a)_n$ is the Pochhammer symbol defined by

$$(a)_n = \begin{cases} 1, & n = 0, \\ a(a+1)\cdots(a+n-1), & n = 1,2,\ldots \end{cases}. \tag{II.4}$$

The denominator terms, $b_i \in \mathbb{Z}^+$, are positive to ensure that the denominator factors for the series are nonzero. The radius of convergence of the series depends on the relative values of r and s and is given by

$$\rho = \begin{cases} 0 & r > s+1 \\ 1 & r = s+1 \\ \infty & r < s+1 \end{cases} \tag{II.5}$$

While the values in the denominator (b_i) must be greater than zero, the terms in the numerator, a_i, may be negative. When one of the terms is negative, the series terminates at the value of that term. For example, if $a_1 = -m$,

$$F_s^r = \sum_{k=0}^{m} \frac{(-m)_k \cdots (a_r)_k}{(b_1)_k \cdots (b_s)_k} \frac{z^k}{k!} \tag{II.6}$$

When this occurs, the order of z becomes finite resulting in a polynomial that is m^{th} order with respect to z. Table 1 provides a list of some polynomials and their corresponding r and s values.

Table 1. Examples of hypergeometric series

r	s	Hypergeometric Series
0	0	Exponential Series
1	0	Binomial Series
2	1	Gauss Series

b. Properties of Orthogonal Polynomials

In this section, some of the properties of series of orthogonal polynomials will be discussed. Consider a set of polynomials, $\{Q_n(x), n \in \mathcal{N}\}$ where the polynomial $Q_n(x)$ is of degree n and the set $\mathcal{N}$ can be either $\mathcal{N} = \{0, 1, 2, \ldots\}$ if the series is infinite or $\mathcal{N} = \{0, 1, 2, \ldots, N\}$ for a finite series with N being a finite non-negative integer. The system of polynomials is orthogonal with respect to a real positive measure, $\gamma(x)$, if

$$\int_D Q_n(x)Q_m(x)d\gamma(x) = h_n^2\delta_{nm} \tag{II.7}$$

for $n, m \in \mathcal{N}$, where D is the support for the measure, $\gamma(x)$, and the values h_n are positive constants. If $h_n = 1$, we say that the series of polynomials is orthonormal. In general, the measure may have a continuous weighting function $w(x)$ associated with it or may have discrete weight values $w(x_i)$ at the points, x_i. As a result, (II.7) becomes

$$\int_D Q_n(x)Q_m(x)w(x)dx = h_n^2\delta_{nm} \tag{II.8}$$

for the case when the weighting function is continuous and

$$\sum_{i=0}^{N} Q_n(x_i)Q_m(x_i)w(x_i) = h_n^2\delta_{nm} \tag{II.9}$$

when the support is discrete. For the discrete case it is possible that N is finite (positive) or $N = \infty$. In these expressions, $n, m \in \mathcal{N}$. This weighting function will

become important as we continue our development because for certain polynomials the weights are identical to a probability distribution. This will be the foundation of the ideas behind Polynomial Chaos.

An important characteristic of orthogonal polynomials is the fact that any three consecutive polynomials are connected by a recurrent relation involving three terms. There are several different ways to express this relationship. We will write the relation as

$$-xQ_n(x) = A_nQ_{n+1}(x) - (A_n + C_n)Q_n(x) + C_nQ_{n-1}(x), \qquad n \geq 1 \tag{II.10}$$

where the terms $A_n, C_n \neq 0$ and $C_n/A_{n-1} \geq 0$. To initialize the series, $Q_{-1}(x)$ and $Q_0(x)$ are required. These initialized as $Q_{-1}(x) = 0$ and $Q_0(x) = 1$. With these initial polynomials, the rest of the terms can then be computed.

Continuous orthogonal polynomials also satisfy the second order differential equation

$$\alpha(x)f'' + \beta(x)f' + \lambda f = 0 \tag{II.11}$$

where $\alpha(x)$ is a polynomial of second degree and $\beta(x)$ is a polynomial of first degree. The equation is a Sturm-Liouville type of equation, meaning that $\lambda = \lambda_n$ is the eigenvalue of the solution and the corresponding eigenfunctions are the polynomials, $f(x) = f_n(x)$. The eigenvalues, λ, are given by

$$\lambda = \lambda_n = -n\left(\beta' + \frac{n-1}{2}\alpha''\right) \tag{II.12}$$

All orthogonal polynomials can be obtained by continuously applying a differential operator known as the generalized Rodriguez formula. For continuous orthogonal polynomials, the operator takes the form

$$Q_n(x) = \frac{1}{w(x)}\frac{d^n}{dx^n}\left(w(x)\alpha^n(x)\right) \tag{II.13}$$

For the discrete case, the differential relationship in equation (II.11) becomes a difference relationship. To introduce the relationship, we first introduce the forward and backward difference operators

$$\Delta y(x) = y(x+1) - y(x) \qquad \nabla y(x) = y(x) - y(x-1) \tag{II.14}$$

The discrete version of equation (II.11) is given by

$$\alpha(x)\Delta\nabla f(x) + \beta(x)\Delta f(x) + \lambda f(x) = 0 \tag{II.15}$$

Furthermore, for discrete orthogonal polynomials, the Rodriguez formula is found by replacing the derivative operator ($\frac{d}{dx}$) with the backward difference operator, ∇.

c. Askey-Scheme

The Askey-scheme provides a classification for each of the hypergeometric polynomials and also indicates the limit relation between each. The scheme can be represented by the tree-like structure found in figure 1 [30]. The scheme demonstrates the limit relationships between each element in the tree structure. The tree starts with the polynomials of class F_3^4. The Wilson polynomials are discrete polynomials and the Racah polynomials are discrete. The lines represent the polynomials that can be linked to others via limit relationships. The polynomials at the top can be used to obtain the linked polynomials below it by use of a limit. For example, it is possible to obtain Laguerre polynomials from Jacobi polynomials by using

$$\lim_{\beta\to\infty} P_n^{(\alpha,\beta)}\left(1 - \frac{2x}{\beta}\right) = L_n^{(\alpha)}(x) \tag{II.16}$$

and it is possible to obtain Hermite polynomials from Laguerre polynomials

$$\lim_{\alpha\to\infty}\left(\frac{2}{\alpha}\right)^{n/2} L_n^{(\alpha)}\left((2\alpha)^{1/2}x + \alpha\right) = \frac{(-1)^n}{n!}H_n(x) \tag{II.17}$$

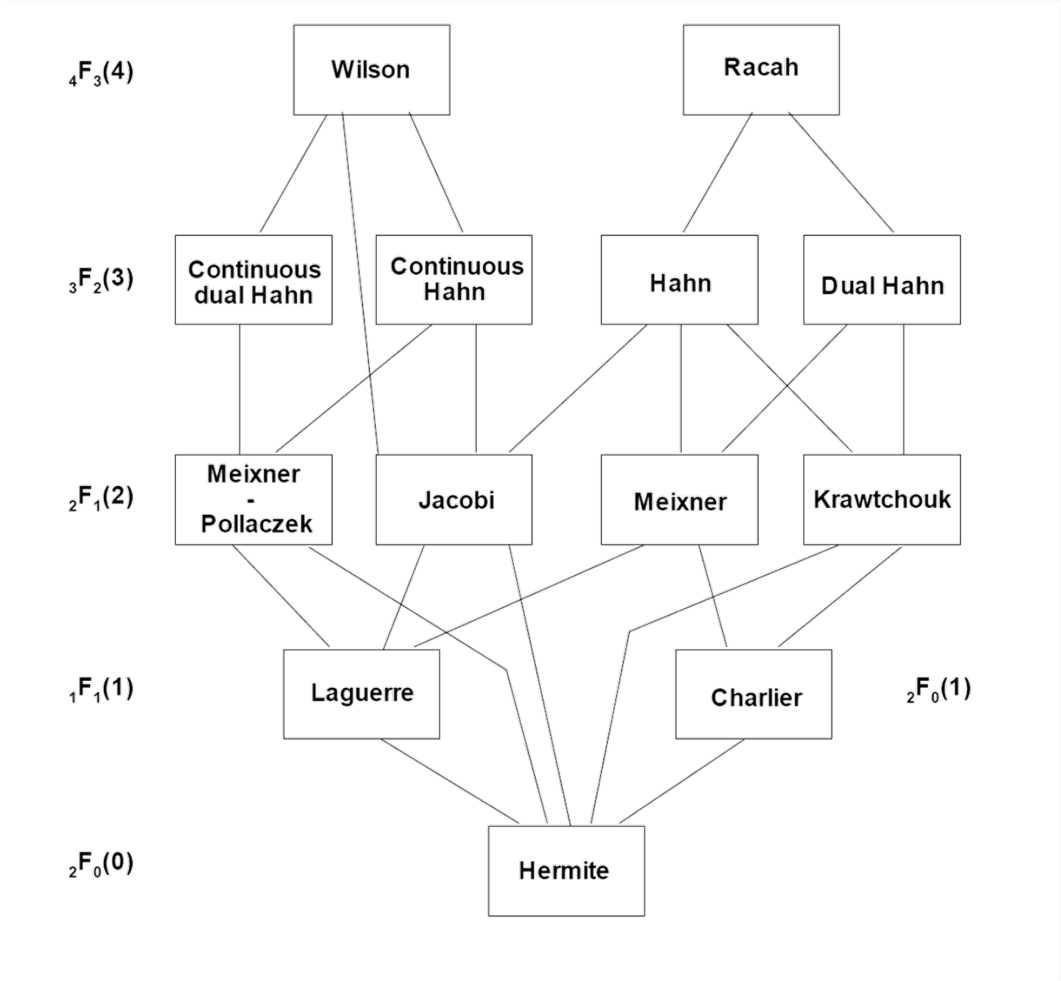

Fig. 1. Askey-Scheme of hypergeometric orthogonal polynomials

2. Homogeneous Chaos

The concept of Homogeneous Chaos was first introduced by Wiener [12] and is an extension of Volterra's work on the generalization of Taylor series to functionals [31, 32, 20]. The Homogenous Chaos utilizes Hermite polynomials to approximate Gaussian random variables. Based on Wiener's ideas, Cameron and Martin used Hermite functionals to create an orthogonal basis for nonlinear functionals and showed that these functionals can approximate any functionals with finite second moment in $\mathcal{L}_2$ and that these functionals in fact converge in the $\mathcal{L}_2$ sense [13]. Therefore,

it is possible to use Hermite-Chaos to expand any second order process, that is a process having finite second moment, in terms of orthogonal polynomials. While the types of processes are limited by the finite second moment requirement, most physical processes do in fact meet this requirement, meaning such a requirement is reasonable.

We now introduce the Homogeneous Chaos. Define the set of all square integrable random variables to be $\mathbf{\Theta}$. Let $\{\xi_i(\theta)\}_{i=1}^{\infty}$ be a set of orthonormal Gaussian random variables and let $\hat{\Gamma}_p$ be the space of all polynomials in $\{\xi_i(\theta)\}_{i=1}^{\infty}$ of degree less than or equal to p. In addition, Γ_p will represent the set of all polynomials in $\hat{\Gamma}_p$ that are orthogonal to the set $\hat{\Gamma}_{p-1}$. The space spanned by Γ_p is denoted $\bar{\Gamma}_p$. This space is a subspace of $\mathbf{\Theta}$ ($\bar{\Gamma}_p \subseteq \mathbf{\Theta}$) and is called the p^{th} Homogeneous Chaos. We call Γ_p the Polynomial Chaos (PC) of order p.

The Polynomial Chaoses are therefore polyvariate orthogonal polynomials of order p of any combination of the random variables $\{\xi_i(\theta)\}_{i=1}^{\infty}$. Because the Polynomial Chaoses must account for all combinations of the random variables, it is therefore clear that the number of chaoses of order p which involve specific random variables in the set increase as p increases. Furthermore, the Polynomial Chaoses are in fact functionals since they are functions of random variables which in turn are functions mapping from the event space to some real number.

The set of Polynomial Chaoses is a linear subspace of square integrable random variables ($\mathbf{\Theta}$). This set, Γ_p, is also a ring with respect to the functional multiplication $\Gamma_p\Gamma_q(x) = \Gamma_p(x)\Gamma_q(x)$. Denote the Hilbert space spanned by the set of random variables $\{\xi_i(\theta)\}_{i=1}^{\infty}$ by $\mathbf{\Theta}(\xi)$ and denote the resulting ring $\mathbf{\Phi}_{\mathbf{\Theta}(\xi)}$. This is the ring of functions generated by $\mathbf{\Theta}(\xi)$. It has been shown that under general conditions, this ring is dense in $\mathbf{\Theta}$ [33]. As a result, any square integrable random variable mapping from Ω to $\mathbb{R}$ can be approximated as closely as desired. We can therefore write any

general second-order random process as

$$X(\theta) = \sum_{p\geq 0} \sum_{n_1+\ldots+n_r=p} \sum_{\rho_1,\ldots,\rho_r} \Gamma_p\left(\xi_{\rho_1}(\theta),\ldots,\xi_{\rho_r}(\theta)\right) \tag{II.18}$$

or as a linear combination of all Polynomial Chaoses (Γ_p) of order $p \geq 0$. The polynomials in equation (II.18) involve r distinct random variables out of $\{\xi_i(\theta)\}_{i=1}^{\infty}$, with the k^{th} random variable having multiplicity n_k, and the total number of random variables involved is equal to the order of the Polynomial Chaos, p. If we assume that the Polynomial Chaoses to be symmetrical with respect to their arguments (symmetrization is always possible [20]), equation (II.18) can be simplified to give the following expression for a random process

$$\begin{aligned} X(\theta) =& a_0\Gamma_0 \\ &+ \sum_{i=1}^{\infty} a_{i_1}\Gamma_1(\xi_{i_1}(\theta)) \\ &+ \sum_{i_1=1}^{\infty}\sum_{i_2=1}^{i_1} a_{i_1 i_2}\Gamma_2(\xi_{i_1}(\theta)\xi_{i_2}(\theta)) \\ &+ \sum_{i_1=1}^{\infty}\sum_{i_2=1}^{i_1}\sum_{i_3=1}^{i_2} a_{i_1 i_2 i_3}\Gamma_3(\xi_{i_1}(\theta)\xi_{i_2}(\theta)\xi_{i_3}(\theta)) + \ldots \end{aligned} \tag{II.19}$$

where $\Gamma_p(\cdot)$ is the Polynomial Chaos of order p. For the case of Homogeneous Chaos with the Gaussian variables, $\boldsymbol{\xi}$ having zero mean and unit variance, these polynomials are Hermite Polynomials and we will henceforth express them as $\Gamma_p = H_p$ (The term $\boldsymbol{\xi} = (\xi_{i_1}, \xi_{i_2}, \ldots, \xi_{i_n})$). These polynomials have the form

$$H_n(\xi_{i_1},\ldots,\xi_{i_n}) = e^{\frac{1}{2}\boldsymbol{\xi}^T\boldsymbol{\xi}}(-1)^n \frac{\partial^n}{\partial\xi_{i_1}\cdots\partial\xi_{i_n}} e^{-\frac{1}{2}\boldsymbol{\xi}^T\boldsymbol{\xi}} \tag{II.20}$$

The values of the upper limits are a reflection of the symmetry of each polynomial with respect to its arguments. The polynomials of different orders are orthogonal as are the polynomials of the same order, but with different arguments. Equation (II.19) is a discrete version of the original Wiener polynomial chaos expression where

the continuous integrals are replaced by summations. For notational convenience, we can write equation (II.19) as

$$X(\theta) = \sum_{i=0}^{\infty} \hat{a}_i \Psi_i(\boldsymbol{\xi}) \tag{II.21}$$

where there is a one-to-one correspondence between $\Psi_i(\boldsymbol{\xi})$ and $H_p(\xi_{i_1}, \ldots, \xi_{i_n})$, and also between the coefficients $\hat{a}_i$ and $a_{i_1 \cdots i_r}$. To help attain some insight into the form of the summation in equation (II.19) as well as into how the Ψ_i's in equation (II.21) relate to the H_n's, consider the following expansion for two random variables.

$$\begin{aligned} X(\theta) = {} & a_0 H_0 + a_1 H_l(\xi_1) + a_2 H_1(\xi_2) \\ & + a_{11} H_2(\xi_1, \xi_1) + a_{12} H_2(\xi_2, \xi_1) + a_{22} H_2(\xi_2, \xi_2) \\ & + a_{111} H_3(\xi_1, \xi_1, \xi_1) + a_{211} H_3(\xi_2, \xi_1, \xi_1) + a_{221} H_3(\xi_2, \xi_2, \xi_1) \\ & + a_{222} H_3(\xi_2, \xi_2, \xi_2) + \ldots \end{aligned} \tag{II.22}$$

The terms in this expansion correspond with the terms in equation (II.21) such that $\hat{a}_0 \Phi_0 = a_0 H_0$, $\hat{a}_1 \Phi_1 = a_1 H_1(\xi_1)$, $\hat{a}_2 \Phi_2 = a_2 H_1(\xi_2)$, and so forth.

The polynomials for the Homogeneous (Hermite) Chaos form an orthogonal basis, which means

$$\langle \Psi_i \Psi_j \rangle = \langle \Psi_i^2 \rangle \delta_{ij} \tag{II.23}$$

where δ_{ij} is the Kronecker delta ($\delta_{ij} = 0$ if $i \neq j$ and $\delta_{ij} = 1$ when $i = j$) and $\langle \cdot, \cdot \rangle$ denotes a weighted inner product. For Hermite Chaos, this is the inner product on the Hilbert space determined by the support of the Gaussian variables

$$\langle f(\boldsymbol{\xi}) g(\boldsymbol{\xi}) \rangle = \int f(\boldsymbol{\xi}) g(\boldsymbol{\xi}) w(\boldsymbol{\xi}) \, d\boldsymbol{\xi} \tag{II.24}$$

where the weighting function is given by

$$w(\boldsymbol{\xi}) = \frac{1}{\sqrt{(2\pi)^n}} e^{-\frac{1}{2}\boldsymbol{\xi}^T \boldsymbol{\xi}} \tag{II.25}$$

The variable n is the size of the random variable vector, $\boldsymbol{\xi}$. This weighting function is equivalent to the probability density function for an n-dimensional independent Gaussian distribution. Therefore, the basis polynomials of the Hermite Chaos are orthogonal with respect to a Gaussian distribution and the variables in the expansion are Gaussian random variables. Therefore, Homogeneous Chaos (Hermite-Chaos) is used in situations where the stochastic uncertainty in the system is known to be Gaussian.

3. Generalized Polynomial Chaos

The Hermite-Chaos discussed in the previous section is very useful for solving stochastic differential equations for systems with Gaussian inputs as well as systems with certain non-Gaussian inputs [20, 18, 21]. While the Cameron-Martin theorem guarantees that this type of polynomial converges to a function with finite second moment in the $\mathcal{L}_2$ sense [13], it does not guarantee the *rate* of convergence. The Homogeneous Chaos for systems with Gaussian inputs has an exponential rate of convergence. This is because the polynomials are orthogonal with respect to the probability distribution of the inputs. For systems without Gaussian inputs, the rate of convergence can be drastically deteriorated [15].

As a result the Wiener-Askey polynomial chaos expansion will be presented. This is a generalization of the original Wiener-Chaos expansion, but uses the complete polynomial basis from the Askey-scheme presented earlier. Let $\{\Delta_i(\theta)\}_{i=1}^{\infty}$ be a set of orthonormal random variables of any continuous distribution. As with Homogeneous

Chaos, we model a second order process in the following manner

$$\begin{aligned} X(\theta) =& a_0 I_0 \\ &+ \sum_{i=1}^{\infty} c_{i_1} I_1(\Delta_{i_1}(\theta)) \\ &+ \sum_{i_1=1}^{\infty} \sum_{i_2=1}^{i_1} c_{i_1 i_2} I_2(\Delta_{i_1}(\theta)\Delta_{i_2}(\theta)) \\ &+ \sum_{i_1=1}^{\infty} \sum_{i_2=1}^{i_1} \sum_{i_3=1}^{i_2} c_{i_1 i_2 i_3} I_3(\Delta_{i_1}(\theta)\Delta_{i_2}(\theta)\Delta_{i_3}(\theta)) + \dots \end{aligned} \tag{II.26}$$

where $I_i(\Delta_{i_1}, \dots, \Delta_{i_n})$ denotes the Wiener-Askey polynomial chaos of order n in terms of the random variables $\mathbf{\Delta} = (\Delta_{i_1}, \dots, \Delta_{i_n})$. Unlike the Homogeneous Chaos expansion where the polynomials were Hermite polynomials, I_i can be any polynomial in the Askey-scheme shown in figure 1. As in the previous section, equation (II.26) can be put into the more notationally convenient form

$$X(\theta) = \sum_{i=0}^{\infty} \hat{c}_i \Phi_i(\mathbf{\Delta}) \tag{II.27}$$

Again, the basis function in equation (II.27) have a one-to-one relationship with the polynomials in equation (II.26) as do the coefficients. Using this formulation and the fact that each basis, Φ_i, is orthogonal, the inner product of any two polynomials becomes

$$\langle \Phi_i \Phi_j \rangle = \langle \Phi_i^2 \rangle \delta_{ij} \tag{II.28}$$

where as before, δ_{ij} is the Kronecker delta and $\langle \cdot, \cdot \rangle$ denotes the weighted inner product on the Hilbert space of the variables, $\mathbf{\Delta}$. Similarly to the previous section, this inner product is defined by

$$\langle f(\mathbf{\Delta}) g(\mathbf{\Delta}) \rangle = \sum_{\mathbf{\Delta}} f(\mathbf{\Delta}) g(\mathbf{\Delta}) w(\mathbf{\Delta}) \tag{II.29}$$

for polynomials with discrete support or

$$\langle f(\boldsymbol{\Delta})g(\boldsymbol{\Delta})\rangle = \int f(\boldsymbol{\Delta})g(\boldsymbol{\Delta})w(\boldsymbol{\Delta})d\boldsymbol{\Delta} \tag{II.30}$$

when the weight function has continuous support. Previously, the weighting function, $w(\boldsymbol{\Delta})$ corresponded to the weight for the Hermite basis, but in this more general setting $w(\boldsymbol{\Delta})$ is the weighting function associated with the particular choice of basis from the Wiener-Askey polynomial chaos.

The choice of basis function for the Wiener-Askey chaos scheme is dependent on the probability distribution that is to be modeled. Several of the polynomials in the Askey-scheme are orthogonal with respect to well-known probability distributions. When modeling a system with uncertainty governed by a specific type of distribution, we can choose the corresponding polynomial in the scheme to model it. Because each type of polynomial from the Askey-scheme forms a complete basis in the Hilbert space determined from their support, each type of polynomial in the Wiener-Askey expansion will converge to an $\mathcal{L}_2$ function in the $\mathcal{L}_2$ sense. This result can be obtained as a general result of the Cameron-Martin Theorem [13, 34]. Table 2 shows some common probability distributions and their corresponding polynomial basis in the Askey-scheme.

Table 2. Correspondence between choice of polynomials and given distribution of $\Delta(\omega)$.

Random Variable Δ	$\phi_i(\Delta)$ of the Wiener-Askey Scheme
Gaussian	Hermite
Uniform	Legendre
Gamma	Laguerre
Beta	Jacobi

The basis functions in table 2 are all orthogonal with respect to their associated distribution. As a result, this gives physical insight into the inner products in equations (II.28-II.30). Therefore, $w(\Delta(\omega))d\Delta = dP(\Delta(\omega))$ where P is the corresponding probability measure. It becomes clear that the inner product is an expectation operator, or

$$\langle f(\Delta)g(\Delta)\rangle = \int f(\Delta)g(\Delta)w(\Delta)d\Delta = \mathbf{E}[f(\Delta)g(\Delta)] \tag{II.31}$$

Therefore, the inner product of the orthogonal polynomial basis functions becomes

$$\mathbf{E}[\Phi_i\Phi_j] = \mathbf{E}[\Phi_i^2]\delta_{ij} \tag{II.32}$$

where the expectation operator has been taken with respect to the probability density function associated with the polynomial basis.

C. Building Sets of Orthogonal Polynomials

While in theory it is easy to assume that all distributions fall into one of the types listed in table 2, in practice this may not be the case. Furthermore, it may not be desirable to use Hermite polynomials in practice as their support is infinite. As a result it is often necessary to generate a set of orthogonal polynomials with desired support. This can be accomplished several ways. One method is the Gram-Schmidt process which we will briefly describe here. This process involves determining a set of orthogonal (not necessarily orthonormal) functions, $\{\Phi_i(x)\}_{i=0}^{\infty}$, from a set of linearly independent functions, $\{u_i(x)\}_{i=0}^{\infty}$ with a given weighting function, $w(x)$ [35]. To begin, let

$$\Phi_0(x) = u_0(x) \tag{II.33}$$

We will build on this function to create orthogonal functions from the linearly independent ones. The order in which we perform the operation with respect to the $u_i's$

is unimportant since each u_i is linearly independent. The next function, $\Phi_1(x)$, can be determined from $\Phi_0(x)$ by subtracting off the projection of $u_1(x)$ onto $\Phi_0(x)$.

$$\Phi_1(x) = u_1(x) - \frac{\langle u_1(x)\Phi_0(x)\rangle}{\langle \Phi_0(x)^2\rangle}\Phi_0(x) \tag{II.34}$$

where $\langle f(x)g(x)\rangle = \int f(x)g(x)w(x)\,dx$. To verify that $\Phi_1(x)$ is in fact orthogonal to $\Phi_0(x)$, consider the inner product

$$\begin{aligned}\langle \Phi_0(x)\Phi_1(x)\rangle &= \langle \Phi_0(x)u_1(x)\rangle - \frac{\langle u_1(x)\Phi_0(x)\rangle}{\langle \Phi_0(x)^2\rangle}\langle \Phi_0(x)\Phi_0(x)\rangle \\ &= \langle \Phi_0(x)u_1(x)\rangle - \langle \Phi_0(x)u_1(x)\rangle = 0\end{aligned}$$

In general, we have

$$\Phi_i(x) = u_i(x) - \sum_{k=0}^{i-1}\frac{\langle u_i(x)\Phi_k(x)\rangle}{\langle \Phi_k(x)^2\rangle}\Phi_k(x) \tag{II.35}$$

This gives us a way to systematically compute and orthogonal basis with respect to some weighting function.

The sets of polynomials from the Askey-scheme can also be generated in this manner. For example, let us consider generation of a set of orthogonal polynomials orthogonal with respect to $w(x) = e^{-x^2/2}$ over the domain $x \in (-\infty, \infty)$. We will take $u_i(x) = x^i$ for $i = 1, \ldots \infty$. The first polynomial, $\Phi_0(x) = u_0(x) = 1$. To find $\Phi_1(x)$,

$$\Phi_1(x) = x - \frac{\langle x \cdot 1\rangle}{\langle 1 \cdot 1\rangle} \tag{II.36}$$

Now $\langle 1, 1\rangle = \int_{-\infty}^{\infty} e^{-x^2}\,dx = \sqrt{2\pi}$ and $\langle x, 1\rangle = \int_{-\infty}^{\infty} xe^{-x^2}\,dx = 0$, so $\Phi_1 = x$. To find $\Phi_2(x)$,

$$\Phi_2(x) = x^2 - \frac{\langle x^2\rangle}{\langle 1\rangle} - \frac{\langle x^3\rangle}{\langle x^2\rangle}x \tag{II.37}$$

where $\langle x^2\rangle = \sqrt{2\pi}$ and $\langle x^3\rangle = 0$. This gives

$$\Phi_2(x) = x^2 - 1 \tag{II.38}$$

This process could be continued for as many terms as desired. Upon examination of the first three terms, it becomes clear that the orthogonalization is recovering the Hermite polynomials, which is what should be expected for the given weight function.

D. Karhunen-Loéve Expansion

The polynomial chaos approach is useful when the statistics of the solution are unknown and for stationary processes. When dealing with time-varying (or spatially varying) processes with known covariance, the Karhunen-Loéve expansion becomes the expansion of choice [36, 1, 20]. In a manner similar to equation (II.21), define an expansion of the form

$$X(t,\omega) = \sum_{n=0}^{\infty} \sqrt{\lambda_n} f_n(t) Z_n(\omega) \tag{II.39}$$

where $\{Z_n(\omega)\}$ is a set of random variables that will be determined, λ_n is a constant, and $\{f_n(t)\}$ is an orthonormal set of deterministic functions. The functions, $Z_n(\omega) : \Omega \mapsto \mathbb{R}$ are random variables and can be written as functions of $\Delta(\omega)$. The functions $f_n(t)$ can be spatial, temporal, or both depending on the elements in the vector t and have support on D. For the present work these will usually be a function of time only. For the present discussion, denote $\bar{X}(t)$ as the expectation of $X(t,\omega)$ over all realizations of the process and let $R(t_1,t_2)$ be the covariance function. The covariance function is symmetric and positive definite. It can be written as

$$R(t_1,t_2) = \sum_{n=0}^{\infty} \lambda_n f_n(t_1) f_n(t_2) \tag{II.40}$$

where λ_n is an eigenvalue of the covariance and $f_n(t)$ is the associated eigenvector or eigenfunction. These quantities are solutions of

$$\int_D R(t_1,t_2) f_n(t_1)\, dt_1 = \lambda_n f_n(t_2) \tag{II.41}$$

The eigenfunctions are orthogonal and can be chosen to satisfy the relationship

$$\int_D f_n(t) f_m(t)\, dt = \delta_{nm} \tag{II.42}$$

The random process, $X(t,\omega)$ can be rewritten as

$$X(t,\omega) = \bar{X}(t) + \sum_{n=0}^{\infty} \sqrt{\lambda_n} f_n(t) Z_n(\omega) \tag{II.43}$$

We wish to determine properties of the functions, $Z_n(\omega)$. Define $\tilde{X}(t,\omega) = \sum_{n=0}^{\infty} \left(\sqrt{\lambda_n}\, f_n(t) Z_n(\omega) \right)$, where $\tilde{X}$ has zero mean and let its covariance function be written as

$$\begin{aligned} R(t_1,t_2) &= \langle \tilde{X}(t_1,\omega) \tilde{X}(t_2,\omega) \rangle \\ &= \sum_{n=0}^{\infty} \sum_{m=0}^{\infty} \sqrt{\lambda_n \lambda_m} f_n(t_1) f_m(t_2) \langle Z_n(\omega) Z_m(\omega) \rangle \end{aligned} \tag{II.44}$$

Multiplying both sides of the above expression by $f_k(t_2)$ and integrating over the domain, D, gives (recall equation (II.41))

$$\begin{aligned} \int_D R(t_1,t_2) f_k(t_2)\, dt_2 &= \sum_{n=0}^{\infty} \sum_{m=0}^{\infty} \sqrt{\lambda_n \lambda_m} \langle Z_n(\omega) Z_m(\omega) \rangle f_n(t_1) f_m(t_2) f_k(t_2) \\ &= \sum_{n=0}^{\infty} \sqrt{\lambda_n \lambda_k} \langle Z_n(\omega) Z_k(\omega) \rangle f_n(t_1) \\ &= \lambda_k f_k(t_1) \end{aligned} \tag{II.45}$$

Multiplying this expression by an additional basis vector $f_j(t)$ and once more integrating over the domain, D gives

$$\sum_{n=0}^{\infty} \langle Z_n(\omega) Z_k(\omega) \rangle \sqrt{\lambda_n \lambda_k} \delta_{nj} = \lambda_k \int_D f_k(t_1) f_j(t_1)\, dt_1 \tag{II.46}$$

therefore

$$\sqrt{\lambda_k \lambda_j} \langle Z_j(\omega) Z_k(\omega) \rangle = \lambda_k \delta_{kj} \tag{II.47}$$

From the previous equation, it becomes clear that

$$\langle Z_j(\omega) Z_k(\omega) \rangle = \delta_{jk} \tag{II.48}$$

Therefore the KL expansion of the function X can be written as

$$X(t,\omega) = \bar{X}(t) + \sum_{n=0}^{\infty} \sqrt{\lambda_n} f_n(t) Z_n(\omega) \tag{II.49}$$

where λ_n and $f_n(t)$ are the eigenvalues and eigenfunctions of the covariance and

$$\langle Z_n(\omega) \rangle = 0 \qquad \langle Z_n(\omega) Z_m(\omega) \rangle = \delta_{mn} \tag{II.50}$$

The expressions for the random variables, $Z_n(\omega)$ can be obtained from

$$Z_n(\omega) = \frac{1}{\sqrt{\lambda_n}} \int_D f_n(t) X(t,\omega)\, dt$$

The KL expansion is able to model a random process with covariance $R(t_1, t_2)$ over *finite time* with arbitrary accuracy. The expansion convergence in the $\mathcal{L}_2$ sense is guaranteed by Mercer's theorem [1]. This expansion is particularly useful because it allows us to represent colored processes in terms of random variables $Z_n(\omega)$. These random variables can be used in conjunction with the gPC expansion described in the previous section to include time-varying processes in our analysis. This will allow us to examine problems such as that of stochastic forcing in the gPC framework. The key is that each term in the KL expansion defines a new random variable that must be included in the PC expansion. This will be discussed in more detail in Chapter IV.

E. Summary

In this chapter, we have covered many of the preliminary concepts that will be utilized throughout the rest of the dissertation. We have presented a general overview of the Polynomial Chaos expansion that will be used to transform stochastic stability and control problems into deterministic problems in higher dimensional space.

CHAPTER III

MODELLING AND STABILITY ANALYSIS OF STOCHASTIC DYNAMIC SYSTEMS

A. Introduction

In this chapter, we apply some of the concepts introduced in the previous chapter to modelling and stability analysis of stochastic dynamic systems. This chapter will deal with analysis of both linear and nonlinear stochastic systems. The first part of the chapter will deal with creating a general framework for modelling of stochastic systems in the generalized Polynomial Chaos framework. A generalized framework will be presented for linear systems as well as nonlinear polynomial systems.

The latter portion of the chapter deals with stability analysis of linear and nonlinear stochastic systems. For linear systems, if the parameters are bounded linear functions of the random variable that governs the uncertainty, then it is only necessary to test the extreme values of the parameters [9]. However, if the uncertainty does not appear linearly, this method is no longer valid. Stability analysis for nonlinear systems is more difficult than for linear systems. In general, for linear systems if in the "worst-case", the system is stable, then the system will be stable for the entire range of possible parameter variations. For nonlinear systems, this may not be true. As a result, we must not only ensure that the system is stable for the worst-case uncertainty, but for the entire parameter distribution. For nonlinear systems in general, stability has been addressed for deterministic systems with stochastic forcing [37, 38]. In our stability discussion, we will restrict our attention to systems with stochastic parameters, i.e. systems with probabilistic uncertainty in system parameters. For such class of systems, sampling based approaches are often used to solve

the stochastic problem in a deterministic setting. The drawback of this approach is that it can result in the solution of very large problems for accurate characterization of uncertainty.

As a result, we apply *non-sampling* based methods to approximate, with arbitrary accuracy, the evolution of uncertainty in state trajectories induced by uncertain system parameters. As mentioned previously, the framework is built on the polynomial chaos theory which transforms stochastic dynamics into deterministic dynamics in higher dimensional state space. We assume that the system uncertainty is a function of random variables governed by known stationary distributions. The benefit of this approach is that stochastic linear and nonlinear systems are transformed into deterministic systems and existing system theory can be used for stability analysis.

B. Wiener-Askey Polynomial Chaos

Let $(\Omega, \mathcal{F}, P)$ be a probability space, where Ω is the sample space, $\mathcal{F}$ is the σ-algebra of the subsets of Ω, and P is the probability measure. Let $\Delta(\omega) = (\Delta_1(\omega), \cdots, \Delta_d(\omega)) : (\Omega, \mathcal{F}) \to (\mathbb{R}^d, \mathcal{B}^d)$ be an $\mathbb{R}^d$-valued continuous random variable, where $d \in \mathbb{N}$, and $\mathcal{B}^d$ is the σ-algebra of Borel subsets of $\mathbb{R}^d$. A general second order process $X(\omega) \in \mathcal{L}_2(\Omega, \mathcal{F}, P)$ can be expressed by polynomial chaos as

$$X(\omega) = \sum_{i=0}^{\infty} x_i \phi_i(\Delta(\omega)) \tag{III.1}$$

where ω is the random event and $\phi_i(\Delta(\omega))$ denotes the gPC basis of degree p in terms of the random variables $\Delta(\omega)$. The functions $\{\phi_i\}$ are a family of orthogonal basis in $\mathcal{L}_2(\Omega, \mathcal{F}, P)$ satisfying the relation

$$\int_{\mathcal{D}_{\Delta(\omega)}} \phi_i \phi_j w(\Delta(\omega))\, d\Delta(\omega) = h_i^2 \delta_{ij} \tag{III.2}$$

where δ_{ij} is the Kronecker delta, h_i is a constant term corresponding to $\int_{\mathcal{D}_\Delta} \phi_i^2 w(\Delta)\, d\Delta$, $\mathcal{D}_\Delta$ is the domain of the random variable $\Delta(\omega)$, and $w(\Delta)$ is a weighting function. Henceforth, we will use Δ to represent $\Delta(\omega)$. For random variables Δ with certain distributions, the family of orthogonal basis functions $\{\phi_i\}$ can be chosen in such a way that its weight function has the same form as the probability density function $f(\Delta)$. When these types of polynomials are chosen, we have $f(\Delta) = w(\Delta)$ and

$$\int_{\mathcal{D}_\Delta} \phi_i \phi_j f(\Delta)\, d\Delta = \mathbf{E}[\phi_i \phi_j] = \mathbf{E}[\phi_i^2]\delta_{ij} \tag{III.3}$$

where $\mathbf{E}[\cdot]$ denotes the expectation with respect to the probability measure $dP(\Delta(\omega)) = f(\Delta(\omega))d\Delta(\omega)$ and probability density function $f(\Delta(\omega))$. The orthogonal polynomials that are chosen are the members of the Askey-scheme of polynomials [16], which forms a complete basis in the Hilbert space determined by their corresponding support. Table 3 summarizes the correspondence between the choice of polynomials for a given distribution of Δ [15].

Table 3. Correspondence between choice of polynomials and given distribution of $\Delta(\omega)$.

Random Variable Δ	$\phi_i(\Delta)$ of the Wiener-Askey Scheme
Gaussian	Hermite
Uniform	Legendre
Gamma	Laguerre
Beta	Jacobi

C. Stochastic Linear Dynamics and Polynomial Chaos

Define a linear stochastic system in the following manner

$$\dot{x}(t,\Delta) = A(\Delta)x(t,\Delta) + B(\Delta)u(t,\Delta) \tag{III.4}$$

where $x \in \mathbb{R}^n, u \in \mathbb{R}^m$. For the case of a discrete time system, the system is defined as

$$x(k+1,\Delta) = A(\Delta)x(k,\Delta) + B(\Delta)u(k,\Delta) \tag{III.5}$$

The system has probabilistic uncertainty in the system parameters, characterized by $A(\Delta)$ and $B(\Delta)$, which are matrix functions of random variable $\Delta \equiv \Delta(\omega) \in \mathbb{R}^d$ with certain *stationary* distributions. Due to the stochastic nature of (A, B), the system trajectory will also be stochastic. The control $u(t)$ may be deterministic or stochastic, depending on the implementation.

Let us represent components of $x(t,\Delta), A(\Delta)$ and $B(\Delta)$ as

$$x(t,\Delta) = \begin{bmatrix} x_1(t,\Delta) & \cdots & x_n(t,\Delta) \end{bmatrix}^T \tag{III.6}$$

$$A(\Delta) = \begin{bmatrix} A_{11}(\Delta) & \cdots & A_{1n}(\Delta) \\ \vdots & & \vdots \\ A_{n1}(\Delta) & \cdots & A_{nn}(\Delta) \end{bmatrix} \tag{III.7}$$

$$B(\Delta) = \begin{bmatrix} B_{11}(\Delta) & \cdots & B_{1m}(\Delta) \\ \vdots & & \vdots \\ B_{n1}(\Delta) & \cdots & B_{nm}(\Delta) \end{bmatrix} \tag{III.8}$$

By applying the Wiener-Askey gPC expansion to $x_i(t,\Delta), A_{ij}(\Delta)$ and $B_{ij}(\Delta)$, we get

$$\hat{x}_i(t,\Delta) = \sum_{k=0}^{p} x_{i,k}(t)\phi_k(\Delta) = \mathbf{x}_i(t)^T\Phi(\Delta) \tag{III.9}$$

$$\hat{u}_i(t,\Delta) = \sum_{k=0}^{p} u_{i,k}(t)\phi_k(\Delta) = \mathbf{u}_i(t)^T\Phi(\Delta) \tag{III.10}$$

$$\hat{A}_{ij}(\Delta) = \sum_{k=0}^{p} a_{ij,k}\phi_k(\Delta) = \mathbf{a}_{ij}^T\Phi(\Delta) \tag{III.11}$$

$$\hat{B}_{ij}(\Delta) = \sum_{k=0}^{p} b_{ij,k}\phi_k(\Delta) = \mathbf{b}_{ij}^T\Phi(\Delta) \tag{III.12}$$

where $\mathbf{x}_i(t), \mathbf{a}_{ij}, \mathbf{b}_{ij}, \Phi(\Delta) \in \mathbb{R}^p$ are defined by

$$\mathbf{x}_i(t) = \begin{bmatrix} x_{i,0}(t) & \cdots & x_{i,p}(t) \end{bmatrix}^T \tag{III.13}$$

$$\mathbf{u}_i(t) = \begin{bmatrix} u_{i,0}(t) & \cdots & u_{i,p}(t) \end{bmatrix}^T \tag{III.14}$$

$$\mathbf{a}_{ij} = \begin{bmatrix} a_{ij,0}(t) & \cdots & a_{ij,p}(t) \end{bmatrix}^T \tag{III.15}$$

$$\mathbf{b}_{ij} = \begin{bmatrix} b_{ij,0}(t) & \cdots & b_{ij,p}(t) \end{bmatrix}^T \tag{III.16}$$

$$\Phi(\Delta) = \begin{bmatrix} \phi_0(\Delta) & \cdots & \phi_p(\Delta) \end{bmatrix}^T \tag{III.17}$$

When $u_i(t, \Delta)$ is a feedback control, it follows that it must also be probabilistic (depending on the implementation), and if the control is not probabilistic, this implies $u_i(t) = u_{i,0}(t)$ with all other coefficients as zero.

The number of terms p is determined by the dimension, d, of Δ and the order, r, of the orthogonal polynomials $\{\phi_k\}$, satisfying $p + 1 = \frac{(d+r)!}{d!r!}$. The coefficients $a_{ij,k}$ and $b_{ij,k}$ are obtained via Galerkin projection onto $\{\phi_k\}_{k=0}^p$ given by

$$a_{ij,k} = \frac{\langle A_{ij}(\Delta), \phi_k(\Delta) \rangle}{\langle \phi_k(\Delta)^2 \rangle} \tag{III.18}$$

$$b_{ij,k} = \frac{\langle B_{ij}(\Delta), \phi_k(\Delta) \rangle}{\langle \phi_k(\Delta)^2 \rangle} \tag{III.19}$$

The inner product or ensemble average $\langle \cdot, \cdot \rangle$, used throughout this work, utilizes the weighting function associated with the assumed probability distribution, as listed in table 3. The $n(p+1)$ time varying coefficients, $\{x_{i,k}(t)\}; i = 1, \cdots, n; k = 0, \cdots, p$, are obtained by substituting the approximated solution in the governing equation (eqn.(III.4)) and conducting Galerkin projection on the basis functions $\{\phi_k\}_{k=0}^p$, to

yield $n(p+1)$ *deterministic* linear differential equations, given by

$$\dot{\mathbf{X}} = \mathbf{A}\mathbf{X} + \mathbf{B}\mathbf{U} \tag{III.20}$$

for the continuous time case. For the discrete time case the projection yields the linear difference equations

$$\mathbf{X}(k+1) = \mathbf{A}\mathbf{X}(k) + \mathbf{B}\mathbf{U} \tag{III.21}$$

In both expressions, $\mathbf{X} \in \mathbb{R}^{n(p+1)}$, $\mathbf{A} \in \mathbb{R}^{n(p+1)\times n(p+1)}$, $\mathbf{B} \in \mathbb{R}^{n(p+1)\times m}$, and

$$\mathbf{X} = \begin{bmatrix} \mathbf{x}_1^T & \mathbf{x}_2^T & \cdots & \mathbf{x}_n^T \end{bmatrix}^T \tag{III.22}$$

$$\mathbf{U} = \begin{bmatrix} \mathbf{u}_1^T & \mathbf{u}_2^T & \cdots & \mathbf{u}_m^T \end{bmatrix}^T \tag{III.23}$$

While it is possible to derive many forms for the $\mathbf{A}$ and $\mathbf{B}$ matrices, a convenient form can be obtained in the following manner. Define $\hat{e}_{ijk} = \frac{\langle \phi_i, \phi_j \phi_k \rangle}{\langle \phi_i^2 \rangle}$. The linear equations of motion can be expressed as

$$\dot{x}_{i,l} = \sum_{j=1}^{n} \sum_{k=0}^{p} \sum_{q=0}^{p} a_{ij,k} x_{j,q} \hat{e}_{lkq} + \sum_{j=1}^{m} \sum_{k=0}^{p} \sum_{q=0}^{p} b_{ij,k} u_{j,q} \hat{e}_{lkq}$$

Here we will only deal with continuous time systems as the development in the discrete time is identical. Define the matrix Ψ_k as

$$\Psi_k = \begin{bmatrix} \hat{e}_{0k0} & \hat{e}_{0k1} & \cdots & \hat{e}_{0kp} \\ \hat{e}_{0k1} & \hat{e}_{1k1} & \cdots & \hat{e}_{1kp} \\ \vdots & \vdots & \ddots & \vdots \\ \hat{e}_{0kp} & \hat{e}_{1kp} & \cdots & \hat{e}_{pkp} \end{bmatrix} \tag{III.24}$$

The matrices $\mathbf{A}$ and $\mathbf{B}$ can be written as

$$\mathbf{A} = \begin{bmatrix} \mathbf{A}_{11} & \mathbf{A}_{12} & \cdots & \mathbf{A}_{1n} \\ \mathbf{A}_{21} & \mathbf{A}_{22} & \cdots & \mathbf{A}_{2n} \\ \vdots & \vdots & \ddots & \vdots \\ \mathbf{A}_{n1} & \mathbf{A}_{n2} & \cdots & \mathbf{A}_{nn} \end{bmatrix} \tag{III.25}$$

$$\mathbf{A}_{ij} = \sum_{k=0}^{p} a_{ij,k} \Psi_k \tag{III.26}$$

$$\mathbf{B} = \begin{bmatrix} \mathbf{B}_{11} & \mathbf{B}_{12} & \cdots & \mathbf{B}_{1m} \\ \mathbf{B}_{21} & \mathbf{B}_{22} & \cdots & \mathbf{B}_{2m} \\ \vdots & \vdots & \ddots & \vdots \\ \mathbf{B}_{n1} & \mathbf{B}_{n2} & \cdots & \mathbf{B}_{nm} \end{bmatrix} \tag{III.27}$$

$$\mathbf{B}_{ij} = \sum_{k=0}^{p} b_{ij,k} \Psi_k \tag{III.28}$$

More convenient expressions for $\mathbf{A}$ and $\mathbf{B}$ are given by

$$\mathbf{A} = \sum_{k=0}^{p} A_k \otimes \Psi_k \tag{III.29}$$

$$\mathbf{B} = \sum_{k=0}^{p} B_k \otimes \Psi_k \tag{III.30}$$

where $\otimes$ is the Kronecker product and the matrices A_k, B_k are the projections of $A(\Delta), B(\Delta)$ on the polynomial chaos basis functions. Therefore, transformation of a stochastic linear system with $x \in \mathbb{R}^n, u \in \mathbb{R}^m$, with p^{th} order gPC expansion, results in a *deterministic* linear system with increased dimensionality equal to $n(p+1)$.

Example: Consider the system

$$\dot{x}(t, \Delta) = a(\Delta) x(t, \Delta)$$

where $a(\Delta) = \bar{a}_0 + \bar{a}_2 \Delta^2$ with $\Delta \in [-1, 1]$ governed by a uniform distribution and $\bar{a}_i$,

$i = 0, 2$ is known. Because Δ is governed by a uniform distribution, we use Legendre polynomials to model each of the processes. For this example, we will use up to order 3. The expansion of x is therefore $x(t, \Delta) = \sum_{i=0}^{3} x_i(t)\phi_i(\Delta)$ and the expansion of $a(\Delta)$ is $a(\Delta) = \sum_{i=0}^{3} a_i\phi_i(\Delta)$. The first 3 Legendre polynomials (unnormalized) are given by

$$\begin{aligned}
\phi_0 &= 1 \\
\phi_1 &= \Delta \\
\phi_2 &= \frac{3}{2}\Delta^2 - \frac{1}{2} \\
\phi_3 &= \frac{5}{2}\Delta^3 - \frac{3}{2}\Delta
\end{aligned}$$

It is clear from the form of $a(\Delta)$ that it can be expressed as

$$a(\Delta) = (\bar{a}_0 + \frac{1}{3}\bar{a}_2)\phi_0 + \frac{2}{3}\bar{a}_2\phi_2$$

The equation of motion then becomes

$$\sum_{j=0}^{3} \dot{x}_j\phi_j = \left(\sum_{k=0}^{3} a_k\phi_k\right)\left(\sum_{i=0}^{3} x_i\phi_i\right) = \sum_{i=0}^{3}\sum_{k=0}^{3} a_k x_i \phi_k\phi_i$$

If we take the projection of both sides onto ϕ_j and divide by $\langle\phi_j^2\rangle$ we obtain

$$\begin{aligned}
\dot{x}_j &= \frac{1}{\langle\phi_j^2\rangle}\sum_{i=0}^{3}\sum_{k=0}^{3} a_k x_i \langle\phi_k\phi_i\phi_j\rangle \\
&= \frac{1}{\langle\phi_j^2\rangle}\left(\sum_{k=0}^{3} a_k \begin{bmatrix} \langle\phi_k\phi_j\phi_0\rangle & \langle\phi_k\phi_j\phi_1\rangle & \langle\phi_k\phi_j\phi_2\rangle & \langle\phi_k\phi_j\phi_3\rangle \end{bmatrix}\right)\mathbf{X}
\end{aligned}$$

where $\mathbf{X} = \begin{bmatrix} x_0 & x_1 & x_2 & x_3 \end{bmatrix}^T$. The structure above can be easily identified as the j^{th} row of the Ψ_k matrix described in the previous section in (III.24). Now, because there are only two non-zero coefficients in the expansion of $a(\Delta)$, our equations of

motion now can be written as

$$\dot{\mathbf{X}} = (a_0\Psi_0 + a_2\Psi_2)\,\mathbf{X} = \left((\bar{a}_0 + \frac{1}{3}\bar{a}_2)\Psi_0 + \frac{2}{3}\bar{a}_2\Psi_2\right)\mathbf{X}$$

In this manner we are able to describe the dynamics of the stochastic linear system. The procedure can be repeated for any order of polynomial to obtain better approximations.

D. Stochastic Nonlinear Dynamics and Polynomial Chaos

As was done in the previous section, let $(\Omega, \mathcal{F}, P)$ be a probability space, where Ω is the sample space, $\mathcal{F}$ is the σ-algebra of the subsets of Ω, and P is the probability measure. We again let $\Delta(\omega) = (\Delta_1(\omega), \cdots, \Delta_d(\omega)) : (\Omega, \mathcal{F}) \to (\mathbb{R}^d, \mathcal{B}^d)$ be an $\mathbb{R}^d$-valued continuous random variable, where $d \in \mathbb{N}$, and $\mathcal{B}^d$ is the σ-algebra of Borel subsets of $\mathbb{R}^d$.

1. Preliminaries

In the previous section, the gPC expansion was used to transform linear stochastic differential equations into higher dimensional linear ordinary differential equations. In this section we will explore a similar transformation of the nonlinear problem. Here we consider certain types of nonlinearities that may be present in the system model. The nonlinearities considered here are rational polynomials, transcendental functions and exponentials. We outline the process for representing these nonlinearities in terms of polynomial chaos expansions.

If x, y are random variables with gPC expansions similar to eqn.(III.9) then the gPC expansion of the expression xy can be written as

$$xy = \sum_{i=0}^{p}\sum_{j=0}^{p} x_i y_j \phi_i \phi_j$$

The gPC expansion of x^2 can be derived by setting $y = x$ in the above expansion to obtain

$$x^2 = \sum_{i=0}^{p} \sum_{j=0}^{p} x_i x_j \phi_i \phi_j$$

Similarly x^3 can be expanded as

$$x^3 = \sum_{i=0}^{p} \sum_{j=0}^{p} \sum_{k=0}^{p} x_i x_j x_k \phi_i \phi_j \phi_k$$

This approach can be used to derive the gPC expansions of any multi-variate whole rational monomial in general.

The gPC expansion of fractional rational monomials of random variables is illustrated using the expression $z = \frac{x}{y}$. If x, y are random variables then z is also a random variable with gPC expansions similar to eqn.(III.9). The expansions of x, y are known. The gPC expansions of z can be determined using the following steps. Rewrite

$$z = \frac{x}{y} \text{ as } yz = x$$

Expanding yz and x in terms of their gPC expansions gives

$$\sum_{i=0}^{p} \sum_{j=0}^{p} z_i y_j \phi_i \phi_j = \sum_{k=0}^{p} x_k \phi_k$$

To determine the unknown z_i we project both sides of the equation on the subspace basis to obtain a system of $p+1$ linear equations

$$\frac{1}{\langle \phi_k, \phi_k \rangle} \sum_{i=0}^{p} \sum_{j=0}^{p} z_i y_j \langle \phi_i \phi_j \phi_k \rangle = x_k, \; k = 0, \ldots, p$$

to solve for the p unknowns z_i. This can be generalized to obtain the gPC expansion of any fractional rational monomial.

For dynamic systems that can be expressed as polynomial systems with stochastic coefficients, we can develop a framework for obtaining the gPC expansion. The gPC

methodology is useful because it preserves the order of polynomial systems. In other words, a q^{th}-order polynomial remains a q^{th}-order polynomial after the substitution. While the order of the dynamics is preserved, as with linear systems the number of states is increased.

2. Stochastic Polynomial Systems

Consider a system of the form

$$\dot{x}_i(t,\Delta) = \sum_{j=1}^{m} a_{ij}(\Delta)\mathbf{x}^{\alpha_j}(t,\Delta) \tag{III.31}$$

where m represents the number of terms in the expression, $i = 1,\ldots,n$ represents the number of states, a_{ij} are the coefficients, $\mathbf{x} = [x_1 \ \cdots \ x_n]^T$, and $\alpha_j = [\alpha_{j1} \ \cdots \ \alpha_{jn}]^T$ with $\alpha_{jk} \in \mathbb{N}^+$ is a vector containing the order of each term in the monomial. For example the term given by $x_1^2 x_2^3 x_3 = \mathbf{x}^\alpha$ with $\alpha = [2 \ 3 \ 1]^T$. Note that without loss of generality, this vector does not need to depend upon i because we can add zeros to a_{ij} for any terms that do not appear in the equations of some state x_i. To apply the gPC expansion to this equation of motion, we write

$$x_i(t,\Delta) = \sum_{k=0}^{p} x_{i,k}(t)\phi_k(\Delta) \tag{III.32}$$

$$a_{ij}(\Delta) = \sum_{k=0}^{p} a_{ij,k}\phi_k(\Delta) \tag{III.33}$$

where these forms are familiar as they are identical to those of the linear system.

These expressions can be utilized to derive the equations of motion in a fashion

similar to that utilized in the previous section. Consider the term

$$a_{ij}(\Delta)\mathbf{x}^{\alpha_j}(t,\Delta) = \sum_{k=0}^{p}\sum_{k_{11}=0}^{p}\cdots\sum_{k_{1\alpha_{j1}}}^{p}\sum_{k_{21}=0}^{p}\cdots\sum_{k_{n\alpha_{jn}}}^{p}\Big[a_{ij,k}x_{1,k_{11}}\cdots x_{1,k_{1\alpha_{j1}}}x_{2,k_{21}}\cdots x_{n,k_{n\alpha_{jn}}}\phi_k\cdots\phi_{k_{n\alpha_{jn}}}\Big]$$

While this expression involves a large number of summations (the number depends upon the order of each polynomial term), clearly, the order of the polynomial in terms of the vector $\mathbf{x}$ is preserved; however, the number of terms in the polynomial has increased dramatically. As was done in the linear case, the equations of motion can be projected onto each polynomial subspace to obtain a system of ordinary differential equations in terms of our coefficients. Each equation of motion is then given by

$$\dot{x}_{i,q} = \sum_{j=1}^{m}\sum_{\mathbf{k}=0}^{p}\Big[\hat{e}_{q,k,k_{11},\ldots,k_{n\alpha_{jn}}}a_{ij,k}\prod_{r=1}^{n}\prod_{m=1}^{\alpha_{jr}}x_{rk_m}\Big] \tag{III.34}$$

where

$$\hat{e}_{q,k,k_{11},\ldots,k_{n\alpha_{jn}}} = \frac{1}{\langle\phi_q^2\rangle}\langle\phi_q\phi_k\phi_{k_{11}}\cdots\phi_{k_{n\alpha_{jn}}}\rangle$$

and $\sum_{\mathbf{k}=0}^{p}[\cdot] = \sum_{k=0}^{p}\sum_{k_{11}=0}^{p}\cdots\sum_{k_{n\alpha_{jn}}=0}^{p}[\cdot]$. As an example, consider a polynomial of the form $ax_1^2x_2$ with x_1, x_2, and a as random variables. For this term, $\alpha = [2\ \ 1]^T$. The gPC expansion of this term is written as

$$ax_1^2x_2 = \sum_{\mathbf{k}=0}^{p}a_kx_{1,k_{11}}x_{1,k_{12}}x_{2,k_{21}}\phi_k\phi_{k_{11}}\phi_{k_{12}}\phi_{k_{21}}$$

In general, we can write the expanded system in the following form

$$\dot{\mathbf{X}} = \sum_{j=1}^{\hat{m}}\hat{\mathbf{a}}_{ij}\mathbf{X}^{\hat{\alpha}_j} \tag{III.35}$$

where $\mathbf{X}$ has been previously defined in (III.22). The term, $\hat{m}$, represents the new number for terms based on the addition of more variables, $\hat{\mathbf{a}}_{ij}$ is the coefficient of each new term, and $\hat{\alpha}_j$ contains the orders of each of the monomials. The stochastic

polynomial dynamics are thus written as deterministic polynomial dynamics of state dimension $\mathbb{R}^{n(p+1)}$.

When nonlinearities involve non polynomial functions, such as transcendental functions and exponentials, difficulties occur during computation of the projection on the gPC subspace. The corresponding integrals may not have closed form solutions. In such cases, the integrals either have to be numerically evaluated or these nonlinearities are first approximated as polynomials using Taylor series expansions and then the projections are computed using methods described above. While Taylor series approximation is straightforward and generally computationally cost effective, it can become severely inaccurate when higher order gPC expansions are required to represent the physical variability. A more robust algorithm is presented by Debusschere *et al.*[39] for any non polynomial function $u(x)$ for which $\frac{du}{dx}$ can be expressed as a rational function of $x, u(x)$.

3. Nonlinear Systems Example

In this section we will outline a brief example that demonstrates the ability of the gPC expansion to accurately capture the statistics of even nonlinear systems. We will consider uncertainty in initial conditions as parametric uncertainty will be considered as part of another example in a later section.

Consider the following set of longitudinal non-dimensionalized Vinh's equations for a vehicle passing through the atmosphere.

$$\begin{aligned}
\dot{h} &= V \sin\gamma \\
\dot{V} &= -\rho V^2 \frac{R_0}{2B_c} - \frac{gR_0}{V_c^2}\sin\gamma \\
\dot{\gamma} &= \frac{gR_0}{V_c^2}\cos\gamma\frac{V^2-1}{V} + \rho\frac{R_0}{2B_c}V\frac{L}{D} \\
\dot{x} &= V\cos\gamma
\end{aligned}$$

In these equations, V represents the non-dimensionalized velocity, h represents the non-dimensionalized altitude, γ is the flight path angle and x is the non-dimensionalized lateral distance. The term R_0 represents the radius of the body (in this case the Mars), B_c is the ballistic coefficient, g is the acceleration due to gravity at the surface of the body, and V_c is the circular orbit velocity of the body which can be approximated as $\sqrt{gR_0}$. Finally, $\frac{L}{D}$ is the lift to drag ratio. For the purposes of this example we will assume that this is a constant. The density, ρ is a function of the altitude given by

$$\rho = \rho_0 e^{(\frac{h_2 - hR_0}{h_1})}$$

For the purposes of this example we assume that the vehicle is entering the atmosphere of Mars, meaning $R_0 = 3397\,km$, $g = 3.7116\,m/s^2$, $\rho_0 = 0.0019\,km/m^3$, $h_1 = 9.8\,km$, and $h_2 = 20\,km$. The vehicle is assumed to have a ballistic coefficient of $72.8\,kg/m^2$ and a lift to drag ratio of 0.3.

For this example, we will consider initial condition uncertainty in the altitude parameter. Assume that the initial condition uncertainty appears as a linear perturbation to the nominal initial condition and that the value of the perturbation is governed by a beta distribution with 20% uncertainty. In other words, at the start of the simulation the height of the vehicle is unknown and the starting altitude may be anywhere within 20% of the mean value. The α and β parameters of the beta distribution are chosen to be equal and to be 2. This produces a Gaussian-like curve with the highest probability associated with the mean. The total range of uncertainty is governed by a single random variable. We will utilize the gPC expansion for each

of the states to obtain the equations

$$\begin{aligned}
\sum_{i=0}^{p} \dot{h}_i \phi_i &= \left(\sum_{i=0}^{p} V_i \phi_i\right) \sin\left(\sum_{j=0}^{p} \gamma_j \phi_j\right) \\
\sum_{i=0}^{p} \dot{V}_i \phi_i &= -\rho \frac{R_0}{2B_c} \sum_{i=0}^{p} \sum_{j=0}^{p} V_i V_j \phi_i \phi_j - \frac{g R_0}{V_c^2} \sin\left(\sum_{i=0}^{p} \gamma_i \phi_i\right) \\
\sum_{i=0}^{p} \dot{\gamma}_i \phi_i &= \frac{g R_0}{V_c^2} \cos\left(\sum_{i=0}^{p} \gamma_i \phi_i\right) \left(\sum_{i=0}^{p} V_j \phi_j - \frac{1}{\sum_{k=0}^{p} V_k \phi_k}\right) + \rho \frac{R_0}{2B_c} \frac{L}{D} \sum_{i=0}^{p} V_i \phi_i \\
\sum_{i=0}^{p} \dot{x}_i \phi_i &= \left(\sum_{i=0}^{p} V_i \phi_i\right) \cos\left(\sum_{j=0}^{p} \gamma_j \phi_j\right)
\end{aligned}$$

Additionally, since ρ is a function of the altitude it must also be written as a gPC variable.

$$\rho = \rho_0 e^{\left(\frac{h_2 - \left(\sum_{i=0}^{p} h_i \phi_i\right) R_0}{h_1}\right)}$$

The gPC variables in this equation are all written with respect to the random variable that governs the initial condition uncertainty. These equations are non-linear and non-polynomial. This means that we have no means of determining gPC projections for the system directly. As a result, at each time step numerical integration will be used to perform the Galerkin projection and determine the equations of motion. The initial condition can be written as

$$h(0) = h_0 + \Delta$$

The other initial conditions are assumed to be known perfectly for this example so we write $V(0) = V_0$, $\gamma(0) = \gamma_0$, and $x(0) = x_0$. It is easy to write the other initial conditions as functions of the same or additional random variables. Adding additional random variables adds more dimensionality to the problem. To test the accuracy of the gPC expansion we examine the time response of each set of states for a polynomial order of $p = 7$.

Figures 2(a) and 2(b) demonstrate the response of the body's altitude and veloc-

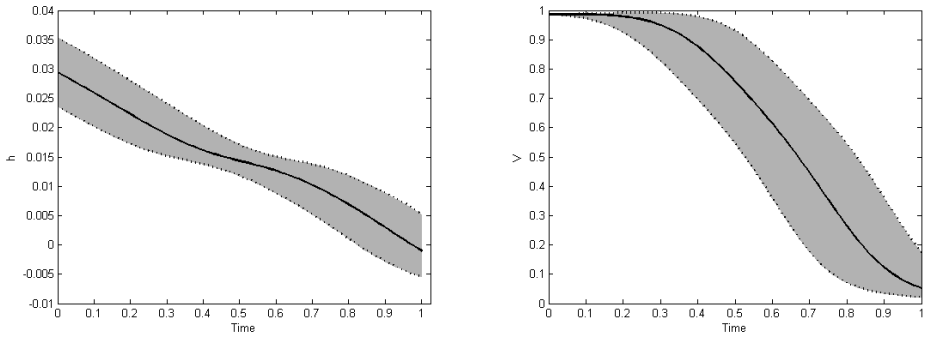

(a) Time response of altitude with 20% uncertainty in h_0

(b) Time response of velocity with 20% uncertainty in h_0

Fig. 2. Altitude and velocity response for longitudinal Vinh's equations with uncertainty in h_0

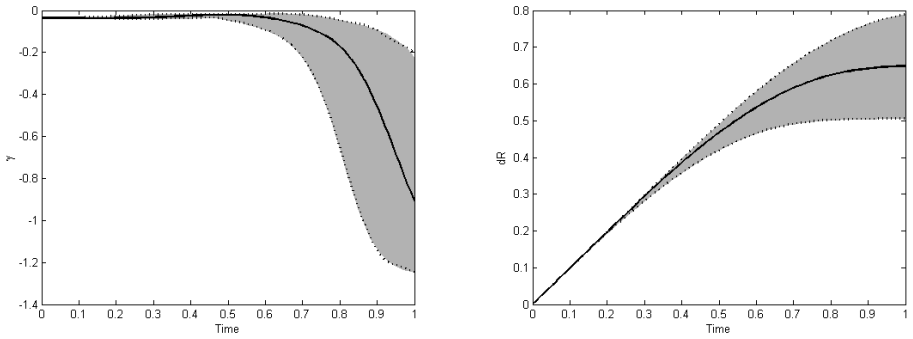

(a) Time response of γ with 20% uncertainty in h_0

(b) Time response of dR with 20% uncertainty in h_0

Fig. 3. γ and horizontal position response for longitudinal Vinh's equations with uncertainty in h_0

ity over time due to the uncertainty in the initial value for the altitude. Figures 3(a) and 3(b) show the response of γ and the horizontal position respectively. In these figures the gray area represents the trajectories generated through Monte-Carlo. The Monte-Carlo trajectories are generated by successive solution of the equations of motion with different initial conditions which have values governed by a Beta distri-

bution. The solid black line in the figures represents the predicted mean value from

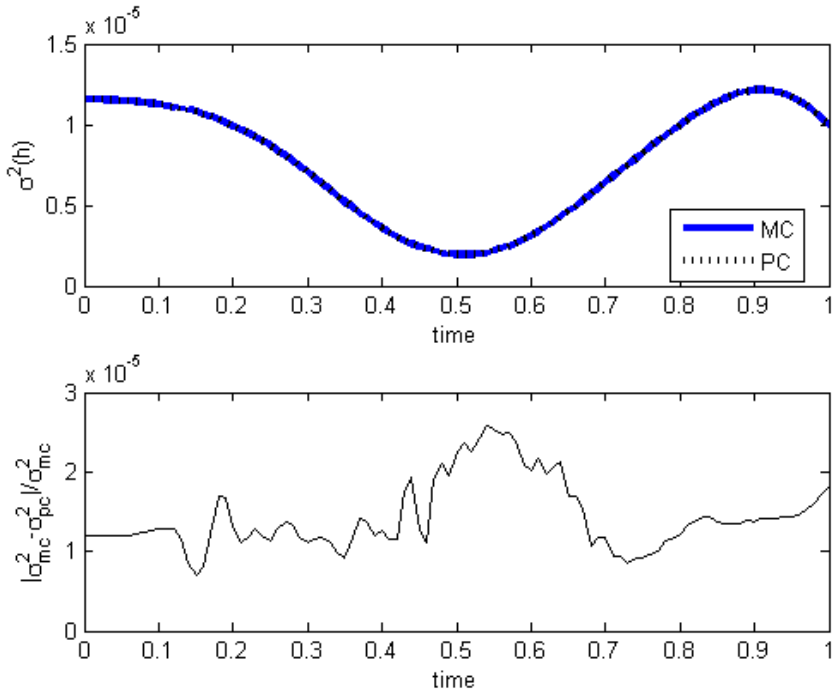

Fig. 4. Variance of altitude response for Monte-Carlo and gPC predicted trajectories

gPC and the dashed lines on the edges represent the maximum and minimum trajectory values predicted from gPC. The figures demonstrate that the predictions of the mean as well as the uncertainty bounds are very accurate. As the evolution of the equations demonstrate, the initial condition uncertainty in h results in uncertainty in all of the other parameters as time progresses. The uncertainty in γ is very large (57 degrees) by the time the body is nearing the surface (h = 0). Despite the large uncertainty, the gPC approximation is able to capture the bounds very accurately. To further demonstrate the accuracy of the expansion, consider figures 4 and 5. The top portions of these figures show the variance of the altitude and velocity respectively. In each of the figures it is clear that the variance obtained from Monte-Carlo simulation and that obtained by the gPC approximation are very close.

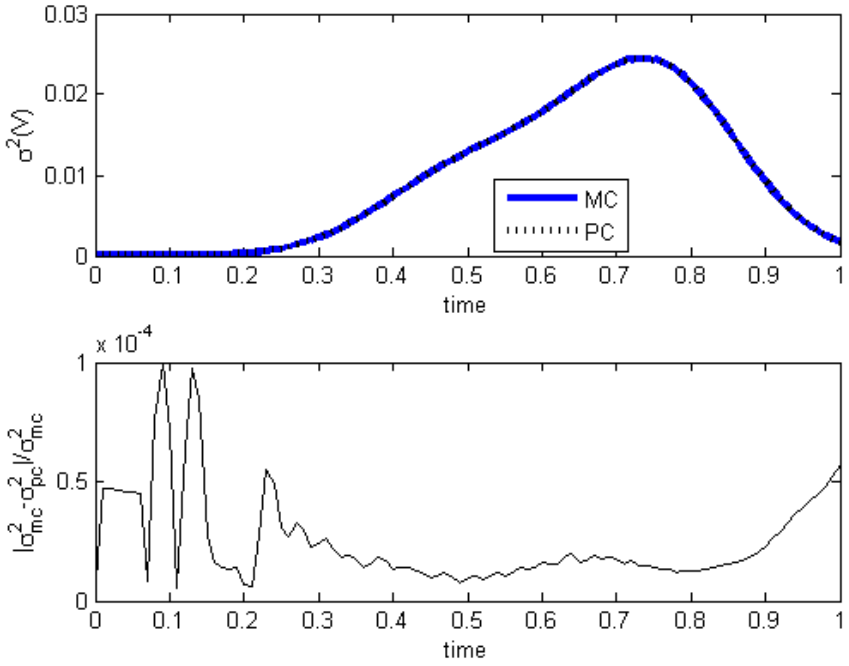

Fig. 5. Variance of velocity response for Monte Carlo and gPC predicted trajectories

As an additional comparison, the bottom portions of figures 4 and 5 show the normalized error between the variances predicted by Monte-Carlo simulation and those predicted by the gPC approximation. In each case the errors in predicted variance are at least four orders of magnitude smaller than the actual variance. The largest errors are observed when the variance is near zero. This is because the actual variance error is beginning to approach the tolerances of the integration scheme.

Next, we quantify the relationship between the observed error and the number of terms used in the polynomial chaos expansion. In particular, it has been observed that the expansion converges exponentially [15], but we wish to verify this. Figure 6 shows the errors between the predicted altitude mean and variance values for gPC versus the Monte-Carlo results. The figure shows the trends in these errors as the polynomial order is increased. It is important to note that the error in the variance

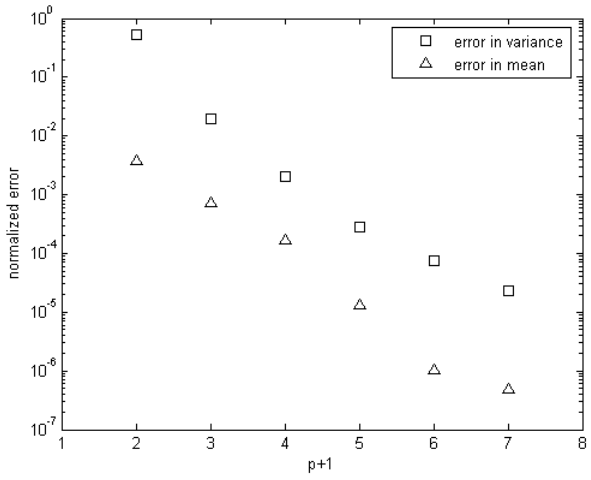

Fig. 6. Altitude mean and variance errors between gPC and Monte-Carlo for various polynomial orders

prediction is higher that of the predicted mean for the same polynomial order. This is to be expected as the variance is second order while the mean is first order. A more accurate prediction of the variance will therefore require higher order polynomials. As an example of this, consider a trajectory that can be completely modeled with three polynomials. We can write this trajectory as $x_t(\Delta) = x_0\phi_0 + x_1\phi_1 + x_2\phi_2$. The mean of the trajectory is simply x_0. Therefore, only a single gPC term is needed to capture the mean, though with differential equations higher-order terms can influence the evolution of x_0 meaning these will be required to accurately predict the mean. To compute the variance, we need to compute

$$\begin{aligned}\mathbf{E}[(x - \mathbf{E}[x])^2] &= \mathbf{E}[(x_1\phi_1 + x_2\phi_2)^2] = \mathbf{E}[x_1^2\phi_1^2 + x_1x_2\phi_1\phi_2 + x_2^2\phi_2^2] \\ &= x_1^2\langle\phi_1^2\rangle + x_2^2\langle\phi_2^2\rangle\end{aligned}$$

The first term, x_0, is cancelled from the expression because it is the mean. So, we can see that even while the mean can be captured accurately with just one term, to capture the variance we indeed need all three terms. Therefore, to predict the

variance with high accuracy, we will require polynomials of higher order than would be needed to produce equivalent accuracy in the mean. Fortunately, figure 6 shows that the errors associated with the gPC approximation go to zero exponentially as the order of the polynomials is increased. This means that we will require only a few polynomials to obtain a high accuracy. In fact, accuracy to 3 significant figures is nearly obtained for third order polynomials (corresponding to $p + 1 = 4$). While the errors will continue to decrease indefinitely as the polynomial order is increased, this might not always be observed in practice. If higher order terms were added to figure 6, the errors would remain constant and no improvement would be observed past $p+1 = 8$. This is because the errors in the variance are approaching the integration tolerances of the solver. If higher accuracy is required, the solver accuracy should be increased.

E. Stochastic Stability Analysis of Linear Systems

By representing the stochastic system in a deterministic framework, we are able to analyze stability properties of the stochastic system using tools developed for deterministic systems. This enables definition of stability conditions in terms of the augmented state vector, which results in a larger linear matrix inequality (LMI), as opposed to many smaller LMI's in the case of sampling based approaches.

Proposition III.1 *The system in (III.20) with* $u = 0$ *is stable if and only if there exists a* $P = P^T > 0$ *such that*

$$\mathbf{A}^T P + P\mathbf{A} \leq 0$$

Proof Choose $V = \mathbf{X}^T P \mathbf{X}$ and utilize the standard Lyapunov argument. ■

For the discrete time case, we have a similar result.

Proposition III.2 *The system in (III.21) with* $u = 0$ *is stable if and only if there exists a* $P = P^T > 0$ *such that*

$$\mathbf{A}^T P \mathbf{A} - P \leq 0$$

Proof Choose $V = \mathbf{X}^T P \mathbf{X}$ and again utilize the standard Lyapunov argument. ■

This result is presented to demonstrate the power of the approach to enable the study of system stability in terms of well known methodologies.

Remark III.3 *The number of polynomials should be chosen to accurately represent the stochastic process in finite dimensional process, as the validity of the stability arguments only relates to the approximated random process.*

Remark III.4 *The stability condition in the previous propositions only guarantee stability of the Galerkin projection of the linear system. This is an approximation and as such does not guarantee that the original stochastic system is indeed stable for all* Δ*. For more discussion see Chapter VI.*

The closed-loop stability of a system can be analyzed by utilizing similar arguments.

Proposition III.5 *Given a feedback control* $u(t, \Delta) = Kx(t, \Delta)$*, the feedback gain* K *asymptotically stabilizes the projection of the family of systems, parameterized by* Δ*, if the condition*

$$\mathbf{A}^T P + P\mathbf{A} + (K^T \otimes I_{p+1})\mathbf{B}^T P + P\mathbf{B}(K \otimes I_{p+1}) < 0$$

is satisfied for some $P = P^T > 0$.

Proof First, let us look at $u(t, \Delta) = Kx(t, \Delta)$. When $x(t, \Delta)$ is approximated by a gPC expansion, $u(t, \Delta) = K\hat{x}(t, \Delta)$, and

$$u_i(t, \Delta) = \sum_{l=0}^{p} u_{i,l}\phi_l = \sum_{j=1}^{n}\sum_{k=0}^{p} k_{ij} x_{j,k}\phi_k$$

By projecting, we find that

$$\mathbf{U} = (K \otimes I_{p+1})\mathbf{X} \tag{III.36}$$

Therefore, the closed loop system is given by

$$\dot{\mathbf{X}} = \mathbf{A}\mathbf{X} + \mathbf{B}(K \otimes I_{p+1})\mathbf{X}$$

Using the Lyapunov function $V = \mathbf{X}^T P \mathbf{X}$, where $P = P^T > 0$, and taking its derivative implies that the system is asymptotically stable (exponentially stable since this is a linear system) if

$$\mathbf{X}^T \left(\mathbf{A}^T P + P\mathbf{A} + (K \otimes I_{p+1})\mathbf{B}P + P\mathbf{B}(K \otimes I_{p+1}) \right) \mathbf{X} < 0.$$

This completes the proof. ■

For discrete time, we can formulate a similar proposition.

Proposition III.6 *Given a feedback control $u(k, \Delta) = Kx(k, \Delta)$, the feedback gain K asymptotically stabilizes the projection of the family of systems, parameterized by Δ, if the condition*

$$\left(\mathbf{A}^T + (K^T \otimes I_{p+1})B^T \right) P \left(\mathbf{A} + \mathbf{B}(K \otimes I_{p+1}) \right) - P < 0$$

is satisfied for some $P = P^T > 0$. Determination of stability can be solved via the LMI feasibility problem

$$\begin{bmatrix} P & \left(\mathbf{A}^T + (K^T \otimes I_{p+1})\mathbf{B}^T \right) P \\ P \left(\mathbf{A} + \mathbf{B}(K \otimes I_{p+1}) \right) & P \end{bmatrix} > 0$$

Proof As was determined in the previous proposition, $\mathbf{U} = (K \otimes I_{p+1})\mathbf{X}$. To analyze the stability we use the Lyapunov function $V(k) = \mathbf{X}(k)^T P \mathbf{X}(k)$. For stability of linear systems with a Lyapunov function of this form we require $V(k+1) - V(k) < 0$.

It is simple to see that substitution of $\mathbf{X}(k+1)$ in terms of $\mathbf{X}(k)$ yields

$$\mathbf{X}^T(k)\left(\left(\mathbf{A}^T + (K^T \otimes I_{p+1})B^T\right)P\left(\mathbf{A} + \mathbf{B}(K \otimes I_{p+1})\right) - P\right)\mathbf{X}(k) < 0$$

which implies that if $P = P^T \succ 0$ is found, the system is stable. Using Schur Complements, it is easy to write this condition as an LMI [40]. This completes the proof. ■

This result allows us to test the stability of a control law for a family of systems by the analysis of a single deterministic system. It does not make sense to examine marginal stability ($\lambda(\mathbf{A}) = 0$ for continuous and $|\lambda_i(\mathbf{A})| = 1$ for discrete systems) for these systems because any inaccuracy in the approximation of the system could lead to instability. Therefore, the amount of uncertainty in the approximation should be considered when analyzing stability margins. It is also worth noting that for stability analysis, the probability density function being considered is not important. For the system to be stable with probability one, it must be stable for any parameter values that occur with non-zero probability. Thus, for a continuous pdf the system must be stable over the entire support with non-zero measure. For certain types of distributions this can be impractical. For example, when considering a Gaussian distribution the polynomial support is for $\Delta \in (-\infty, \infty)$, meaning that it could be practically impossible to ensure stability with finite probability. In such cases it is more practical to consider stability metrics such as 6σ.

F. Linear Stability Example

Here we consider a flight control problem, based on an F-16 aircraft model, where a feedback control K has been designed for the nominal system. We wish to verify the robustness of the controller in the presence of parametric uncertainty in the F-

16 model. For simplicity, we assume that the variation in the system parameters are dependent on a single random variable, Δ, i.e. the variation in these parameters is not independent. In general, these parameters could be independent random processes. In this example, we consider the short-period approximation of an F-16. The model is given by

$$\dot{x} = Ax + Bu$$

$$y = Cx$$

where the state vector $x = [\alpha \;\; q \;\; x_e]^T$; α is the angle of attack, q is the pitch rate, and x_e is an elevator state which captures actuator dynamics. The control, $u = \delta_{ec}$, is the elevator command in degrees. The matrix parameters are

$$A = \begin{bmatrix} -0.6398 & 0.9378 & -0.0014 \\ (-1.5679) & (-0.8791) & (-0.1137) \\ 0 & 0 & -20.2000 \end{bmatrix}$$

$$B = \begin{bmatrix} 0 & 0 & 20.2 \end{bmatrix}^T$$

$$C = \begin{bmatrix} 0 & \frac{180}{\pi} & 0 \end{bmatrix}$$

The values in parenthesis are assumed to be uniformly distributed with 10% deviation about their nominal values. A frequency-domain control has been designed based on feedback of q for the nominal system. The control is of the form

$$u = \frac{0.3122s + 0.5538}{s^2 + 2.128s + 1.132} q$$

which is designed to be a pitch-rate tracking controller. This is converted to state-space form (A_c, B_c, C_c) and augmented to the system to arrive at the closed loop

system

$$\dot{x}_a = A_{cl}x_a + B_{cl}u$$

where

$$A_{cl} = \begin{bmatrix} A & BC_c \\ B_cC & A_c \end{bmatrix}$$

$$B_{cl} = \begin{bmatrix} \mathbf{0} \\ B_c \end{bmatrix}$$

The accuracy of the gPC based approach, for finite dimensional approximation of linear stochastic dynamics, can be inferred from figure 7. The circles (black) represent the eigenvalues of the gPC system with ten terms. The solid (red) dots represent the eigenvalues of the system obtained by sampling the stochastic system over Δ. It is interesting to note that the range of eigenvalues of the stochastic system is accurately captured by the eigenvalues of the gPC system. It should be noted that $\lambda(\mathbf{A})$ does not give the distribution of eigenvalues of the actual system. This would require the solution of a different problem. Regardless, this gives us confidence in the use of polynomial chaos for stability analysis and control of stochastic dynamical systems. Furthermore, we are able to understand how the uncertainty in system trajectories evolve over time. Figure 8 shows the pitch rate response of the system in the presence of ±10% system uncertainty in the aforementioned parameters. The predicted mean and trajectory bounds from gPC are represented by the dark solid and dashed lines respectively. The Monte-Carlo responses of each system are depicted in gray. We observe that the bounds predicted by the gPC system are in excellent agreement with the responses of the Monte-Carlo simulations. As an additional point of comparison, figure 9 shows the normalized errors in the mean and variance for the pitch rate response of the aircraft. This figure is generated for $p = 3$. This demonstrates that

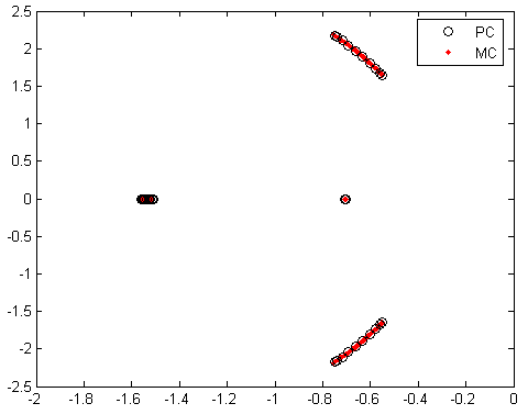

Fig. 7. Closed loop eigenvalue distributions of short-period mode for ±20% parameter uncertainty

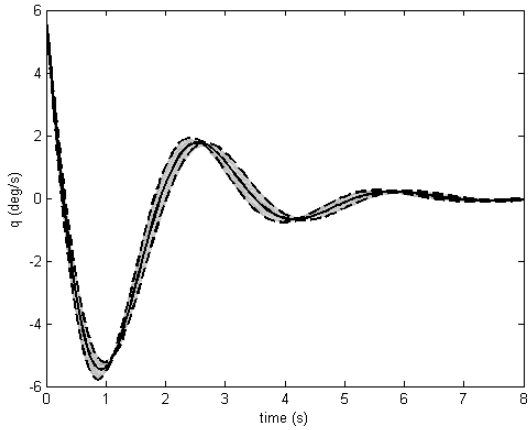

Fig. 8. Predicted and Monte-Carlo system response to ±10% parameter uncertainty

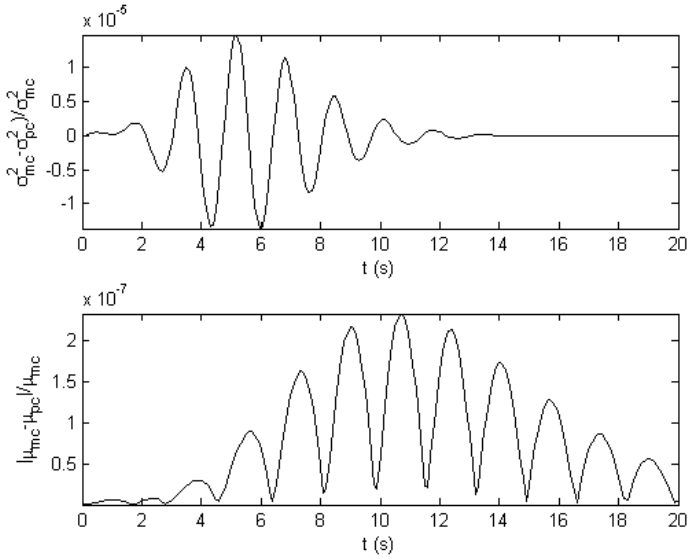

Fig. 9. Normalized mean and variance errors between gPC prediction and Monte Carlo observation

for linear systems, high accuracy can be obtained with a relatively small number of polynomials. In this manner, we are able to predict the statistical behavior of the system through simulation of the gPC system, which is computationally far superior than Monte-Carlo methods.

G. Stability of Nonlinear Systems

1. Methodology

In the section on nonlinear modelling, we showed that stochastic polynomial systems of n variables could be modelled as deterministic polynomial systems of the same order with $n(p+1)$ variables. Transforming stochastic dynamic systems into deterministic systems allows us to utilize previously existing techniques to test the stability of such a system. Because the resulting system is deterministic, any stability technique for nonlinear systems can be utilized to analyze the stability of the projected gPC system.

In general, for nonlinear systems the number of polynomials required to approximate the system behavior (especially if extreme accuracy in variance is required) can be large. For this reason, it can become difficult to analyze the stability of the system using traditional analytical techniques. The larger set of system dynamics makes numerical or "automated" stability analysis tools much more attractive. One such technique is Sum-of-Squares (SOS) programming. We can utilize the SOS framework to discuss the stability of these new polynomials. For details on this approach, see [41, 42, 43] Let $\mathcal{X}(\mathbf{X})$ be a vector of monomials with the property that $\mathcal{X} = 0$ if and only if $\mathbf{X} = 0$. Define a function

$$V = \mathcal{X}^T P \mathcal{X} \tag{III.37}$$

Furthermore, define a function $W(\mathbf{X})$ that is positive definite in X and is a sum-of-squares polynomial in terms of monomials of $\mathbf{X}$.

Proposition III.7 *The approximation of the family of polynomial systems is stable when a function, V, can be found such that*

$$V(\mathbf{X}) - W(\mathbf{X}) \quad \text{is} \quad \text{SOS} \tag{III.38}$$

$$-\dot{V}(\mathbf{X}) \quad \text{is} \quad \text{SOS} \tag{III.39}$$

Proof For proof see[41]. ■

Remark III.8 *This result is straight-forward but powerful. It enables the analysis of uncertainty in nonlinear systems in an algorithmic manner that does not require case-by-case analysis of the various changes in the terms. The drawback is that stability is only proven for the approximation governed by the projected system and not for the actual stochastic system.*

2. Example

For linear systems with parametric uncertainty appearing linearly in the parameters (as in the previous example), it is possible to determine system stability by examining the stability of the vertex set [9]. While for many nonlinear systems, this may be the case, one cannot in general assume that the stability of the vertex set implies stability of the nonlinear system over the entire range. As a result, it becomes even more important to ensure that stability is guaranteed for the entire distribution of parameters. The gPC methodology, in this context, is very useful in the analysis of stability for uncertain nonlinear systems. Proof of stability for the gPC system ensures that the stochastic nonlinear system is stable for the entire distribution of parameter uncertainty with non-zero measure. This is exemplified by the following analysis. Consider the system

$$\begin{aligned} \dot{x}_1 &= x_2 \\ \dot{x}_2 &= -x_1 + a(\Delta)x_2^3 \end{aligned}$$

we want to understand the stability of this system when a is uncertain and its value is based on a uniform distribution around a mean value of -0.5. For this case, we consider the distribution that varies by ± 0.4 ($a(\Delta) \in [-0.9, -0.1]$). The nominal system is stable, and by utilizing SOSTOOLS (see[44, 45]), we are able to show stability and obtain a Lyapunov function of the form

$$V = .79602x_1^2 + .70839x_2^2$$

To verify the stability of the system, we introduce the gPC expansion and determine the stability of the deterministic system. The deterministic system is another polynomial system of the same order, but with increased dimensionality. To demonstrate the

methodology, stability certificates were generated for various values of p, the number of gPC expansions. For a specific case of $p = 4$, the Lyapunov function is given by,

$$V = Z^T Q Z$$

where $Z = [x_{23}\ \ x_{22}\ \ x_{21}\ \ x_{20}\ \ x_{13}\ \ x_{12}\ \ x_{11}\ \ x_{10}]^T$, and

$$Q = \begin{bmatrix} Q_{11} & 0 \\ 0 & Q_{22} \end{bmatrix}$$

The sub-matrices are given by

$$Q_{11} = \begin{bmatrix} 0.5230 & 0.1472 & -0.0659 & 0.0239 \\ 0.1472 & 0.6272 & 0.1509 & -0.0949 \\ -0.0659 & 0.1509 & 0.6814 & 0.1377 \\ 0.0239 & -0.0949 & 0.1377 & 0.7589 \end{bmatrix}$$

$$Q_{22} = \begin{bmatrix} 0.6581 & 0.0510 & -0.0242 & 0.0086 \\ 0.0510 & 0.7073 & 0.0590 & -0.0385 \\ -0.0242 & 0.0590 & 0.7376 & 0.0567 \\ 0.0086 & -0.0385 & 0.0567 & 0.7772 \end{bmatrix}$$

It is interesting to note that for this system, the structure of the Q matrix takes a block diagonal form. The Lyapunov function for the gPC system retains the original structure, i.e. it is also block diagonal. This suggests ways of examining stability and generating certificates for gPC systems. It is important to note that the number of terms in the certificate increases significantly as more coefficients are added. If the structure of the Lyapunov function is unknown, then guessing all possibilities of monomials can lead to problem formulations with large numbers of variables, which are extremely computationally intensive in the SOSTOOLS framework.

H. Summary

In this chapter we have presented a generalized framework for the analysis of stochastic linear and nonlinear systems within the gPC framework. A general formulation for writing a stochastic system in terms of a higher dimensional deterministic system was presented for linear systems as well as nonlinear polynomial systems. Stability problems for linear systems with stochastic parameter uncertainty have been reduced to the solution of an LMI feasibility problem. For nonlinear polynomial systems, stability problems are solved using a sum of squares programming approach. The chapter also presents several examples that highlight the application of the new deterministic stability conditions to analysis of linear and nonlinear stability problems.

CHAPTER IV

OPTIMAL CONTROL OF STOCHASTIC SYSTEMS

A. Introduction

In the previous chapter, the discussion was centered around modelling and stability analysis of linear and nonlinear stochastic systems. We now take some of the same concepts and apply these ideas to the study of control design of stochastic systems. In this chapter we will use the modelling results from the previous chapter to solve linear and nonlinear stochastic optimal control problems.

As mentioned previously, control of stochastic systems is receiving a heightened amount of attention as of late. The more prevalent approaches in the literature tend to utilize sampling based methods. For linear systems, the work of Barmish *et al.* utilizes Monte-Carlo based methods to analyze stability and control problems in an LMI framework [7, 8]. The results are somewhat limited, however as they can only be applied to systems where the uncertain parameters are governed by a uniform distribution. Polyak *et al.* [9] develops an algorithm to determine a control with guaranteed worst-case cost. Unfortunately, this approach is also limited to systems with uncertainty governed by a uniform distribution and appearing linearly in the parameters. A sampling based technique is also applied to the $\mathcal{H}_\infty$ problem in [11]. These sampling based results are extended to linear parameter varying (LPV) control problems in [10].

For linear problems we are interested in obtaining optimal *feedback* laws for unconstrained infinite horizon optimal control problems. We will also examine finite-horizon constrained problems for both linear and nonlinear systems.

The main focus of this chapter is on optimal control in the $\mathcal{L}_2$ sense for linear and

nonlinear systems with probabilistic uncertainty in system parameters. It is assumed that the probability density functions of these parameters are known. These parameters may enter the system dynamics in any manner. In the beginning of the chapter, we address minimum expectation feedback control for linear systems. We will discuss the formulation of the stochastic $\mathcal{L}_2$ optimal problem of the Bolza type in terms of the polynomial chaos expansion. To solve this problem we will consider several different feedback structures for continuous and discrete time systems. Several examples will be presented to highlight the various feedback laws. The latter part of the chapter deals with the transformation of finite-time constrained open-loop stochastic optimal control problems to equivalent deterministic optimal control problems in higher dimensional state space. These problems are solved using standard numerical methods available for deterministic optimal control problems. For these problems, uncertainty is assumed to be in the system parameters as well as in stochastic forcing terms. We will assume that for each type of uncertainty, the probability distribution function is known. In particular, nonlinear dynamical systems are considered though the methodology could easily be applied to linear systems.

B. Stochastic LQR Design

In this section we address feedback control of linear stochastic dynamical systems with probabilistic system parameters, in the gPC framework. Here we consider optimal control with respect to expected value of a quadratic cost function, that depends on the state and control vectors. We will examine the solution of this problem for both deterministic and stochastic feedback control laws, and highlight salient features of each.

1. Minimum Expectation Control

Minimum expectation optimal trajectories are obtained by minimizing the following cost function, which is analogous to the Bolza form,

$$\min_u \mathbf{E}\left[\int_0^\infty (x^T Q x + u^T R u) dt\right] \tag{IV.1}$$

where $x \equiv x(t) \in \mathbb{R}^n, u \equiv u(t) \in \mathbb{R}^m$, $Q = Q^T > 0, R = R^T > 0, S = S^T > 0$. For discrete time systems, the following cost function is used

$$\min_u \mathbf{E}\left[\sum_{k=0}^{\infty} x^T(k) Q x(k) + u^T(k) R u(k)\right] \tag{IV.2}$$

For scalar x, the quantity $\mathbf{E}[x^2]$ in terms of its gPC expansions is given by

$$\mathbf{E}[x^2] = \sum_{i=0}^{p}\sum_{j=0}^{p} x_i x_j \int_{\mathcal{D}_\Delta} \phi_i \phi_j f d\Delta = \mathbf{x}^T W \mathbf{x} \tag{IV.3}$$

where $\mathcal{D}_\Delta$ is the domain of Δ , x_i are the gPC expansions of x, $f \equiv f(\Delta)$ is the probability distribution of Δ; $W \in \mathbb{R}^{(p+1)\times(p+1)} = \{w_{ij}\}$, with $w_{ij} = \int_{\mathcal{D}_\Delta} \phi_i \phi_j f d\Delta = \mathbf{E}[\phi_i^2]\delta_{ij}$ (note: W is a diagonal matrix), and $\mathbf{x} = (x_0 \cdots x_p)^T$. Because the polynomials of the PC expansion or orthogonal, we can write

$$W = \texttt{diag}\left(\langle\phi_0^2\rangle, \langle\phi_1^2\rangle, \ldots, \langle\phi_p^2\rangle\right) \tag{IV.4}$$

where $\texttt{diag}(\cdot)$ is a diagonal matrix with its diagonal terms given by the values in parenthesis. The expression $\mathbf{E}[x^2]$ can be generalized for $x \in \mathbb{R}^n$ where $\mathbf{E}[x^T x]$ is given by

$$\mathbf{E}[x^T x] = \mathbf{X}^T (I_n \otimes W)\mathbf{X} \tag{IV.5}$$

$I_n \in \mathbb{R}^{n\times n}$ is the identity matrix and $\otimes$ is the Kronecker product, and $\mathbf{X}$ is given by eqn.(III.22). The cost function in eqn.(IV.1) can now be written in terms of the gPC

expansions as

$$\min_u J = \min_u \int_0^\infty \left(\mathbf{X}^T Q_{\bar{x}} \mathbf{X} + \mathbf{E}\left[u^T R u\right]\right) dt \tag{IV.6}$$

where $Q_{\bar{x}} = Q \otimes W$. The discrete time cost becomes

$$\min_u J_d = \min_u \sum_{k=0}^{\infty} \left(\mathbf{X}^T(k) Q_{\bar{x}} \mathbf{X}(k) + \mathbf{E}\left[u^T(k) R u(k)\right]\right) \tag{IV.7}$$

The expected value of $u^T R u$ will depend upon the control implementation discussed in subsection 2. It is also possible to write variance control and moment control problems in a similar fashion. This is discussed in more detail in section C.

2. Feedback Solutions

In this section, we will discuss conditions for optimality for various feedback structures as they apply to a quadratic cost of the form developed in the previous section.

a. Augmented Deterministic State Feedback with Constant Deterministic Gain

The first implementation we will discuss involves the assumption that the control is probabilistic and augmented state vector $\mathbf{X}$ is used for feedback. If we assume $u = \sum_{k=0}^{p} u_{i,k}(t)\phi_k(\Delta)$

$$\mathbf{E}\left[u^T R u\right] = \mathbf{U}^T R_{\bar{u}} \mathbf{U} \tag{IV.8}$$

where $R_{\bar{u}} = R \otimes W$.

Proposition IV.1 *The cost function in eqn. (IV.6) is minimized with a control of the form*

$$\mathbf{U} = -R_{\bar{u}}^{-1} \mathbf{B}^T P \mathbf{X} \tag{IV.9}$$

where $P \in \mathbb{R}^{n(p+1)\times n(p+1)}$ *is the solution to the Riccatti equation*

$$\mathbf{A}^T P + P\mathbf{A} - P\mathbf{B} R_{\bar{u}}^{-1} \mathbf{B}^T P + Q_{\bar{x}} = 0 \tag{IV.10}$$

Proof As per the usual solution to the LQR problem, we can write the cost function as $J = \mathbf{X}^T P \mathbf{X}$. From Euler-Lagrange (by substituting for the Lagrange multiplier), we obtain $0 = R_{\bar{u}}\mathbf{U} + \mathbf{B}^T P \mathbf{X}$, giving

$$\mathbf{U} = -R_{\bar{u}}^{-1}\mathbf{B}^T P \mathbf{X}$$

where $\mathbf{U}$ is defined by eqn.(III.23). Substituting this into the cost function and taking the derivative of both sides gives

$$\dot{P} + \mathbf{A}^T P - P\mathbf{B}R_{\bar{u}}^{-1}\mathbf{B}^T P + P\mathbf{A} - P\mathbf{B}R_{\bar{u}}^{-1}\mathbf{B}^T P = -Q_{\bar{x}} - P\mathbf{B}R_{\bar{u}}^{-1}\mathbf{B}^T P$$

For the infinite horizon problem $\dot{P} = 0$, completing the proof. ■

Remark IV.2 *The solution to this expression yields a constant gain matrix, but implementation requires knowledge of gPC expansions of the states. The control vector* $\mathbf{U} = -R_{\bar{u}}^{-1}\mathbf{B}^T P \mathbf{X}$ *with*

$$\mathbf{U} = \begin{bmatrix} \mathbf{u}_1(t)^T & \mathbf{u}_2(t)^T & \cdots & \mathbf{u}_m(t)^T \end{bmatrix}^T \tag{IV.11}$$

defines $u(t, \Delta) = \{\mathbf{u}_i(t)^T \Phi(\Delta)\}_{i=1}^m$, *a family of control laws, parameterized by* Δ. *Appropriate* $u(t)$ *can be determined based on the knowledge of* Δ, *as a result* Δ *must also be known during implementation.*

Remark IV.3 *This control scheme can also be used to simultaneously design optimal controls for all* Δ. *This is equivalent to solving the LQR problem for each value of* Δ. *This will be demonstrated numerically in an example in the next section.*

For discrete time systems, the equivalent control strategy is outlined in the following proposition

Proposition IV.4 *The cost function in eqn. (IV.7) is minimized with a control of the form*

$$\mathbf{U}(k) = -\left(R_{\bar{u}} + \mathbf{B}^T P \mathbf{B}\right)^{-1} \mathbf{B}^T P \mathbf{A} \mathbf{X}(k) \tag{IV.12}$$

where $P \in \mathbb{R}^{n(p+1)\times n(p+1)}$ *is the solution to the Riccatti equation*

$$P = Q_{\bar{x}} + \mathbf{A}^T \left(P - PB(R_{\bar{u}} + \mathbf{B}^T P \mathbf{B})^{-1} \mathbf{B}^T P\right) \mathbf{A} \tag{IV.13}$$

Proof Again, following the solution to the LQR problem we can write the cost function as $J_k = \mathbf{X}^T(k) P(k) \mathbf{X}(k)$. Examining the cost at time k in terms of the cost at $k+1$ gives

$$\mathbf{X}^T(k) P(k) \mathbf{X}(k) \quad = \quad \mathbf{X}^T(k) Q_{\bar{x}} \mathbf{X}(k) + \mathbf{U}^T(k) R_{\bar{u}} \mathbf{U}(k) + \mathbf{X}^T(k+1) P(k+1) \mathbf{X}(k+1)$$

But the cost at time $k+1$ can be written as a function of the state and control at time k as

$$\mathbf{X}^T(k+1) P(k+1) \mathbf{X}(k+1) = \left(\mathbf{U}^T(k) \mathbf{B}^T + \mathbf{X}^T(k) \mathbf{A}^T\right) P(k+1) \left(\mathbf{A}\mathbf{X}(k) + \mathbf{B}\mathbf{U}(k)\right)$$

From this expression, we can see that

$$\mathbf{U}(k) = -\left(R_{\bar{u}} + \mathbf{B}^T P(k+1) \mathbf{B}\right)^{-1} \mathbf{B}^T P(k+1) \mathbf{A} \mathbf{X}(k)$$

where $P(k+1)$ is the solution of

$$P(k) = Q_{\bar{x}} + \mathbf{A}^T \left(P(k+1) - P(k+1) B(R_{\bar{u}} + \mathbf{B}^T P(k+1) \mathbf{B})^{-1} \mathbf{B}^T P(k+1)\right) \mathbf{A}$$

For the infinite horizon problem we have that $P(k+1) = P(k) = P$ and this completes the proof. ■

Remark IV.5 *As in the continuous time case, implementation requires both knowledge of the gPC expansion of the states as well as knowledge of* Δ*. Furthermore,*

solution of this equation can be written in terms of an LMI using the Schur Complement.

b. Stochastic State Feedback with Constant Deterministic Gain

In this formulation, the state trajectory $x(t,\Delta)$ is used to generate the control law that is not explicitly parameterized by Δ. This approach does not require estimation of the gPC expansions of the state and hence doesn't require the knowledge of Δ. We propose feedback of the form

$$u(t,\Delta) = Kx(t,\Delta) \tag{IV.14}$$

where K is a deterministic constant gain. Once again the control is stochastic, due to stochastic state trajectory, and enters the cost function as $\mathbf{E}[u^T Ru]$. The control vector in gPC framework then becomes

$$\mathbf{U} = (K \otimes I_{p+1})\,\mathbf{X}. \tag{IV.15}$$

In this manner, we are selecting a feedback structure that results in a problem similar to the output feedback problem in traditional control. The modified cost function becomes

$$J = \int_0^\infty \mathbf{X}^T \left(Q_{\bar{x}} + \left(K^T \otimes I_{p+1}\right) R_{\bar{u}} \left(K \otimes I_{p+1}\right)\right) \mathbf{X} dt \tag{IV.16}$$

for the continuous case and

$$J_d = \sum_{k=0}^{\infty} \mathbf{X}^T(k) \left(Q_{\bar{x}} + \left(K^T \otimes I_{p+1}\right) R_{\bar{u}} \left(K \otimes I_{p+1}\right)\right) \mathbf{X}(k) \tag{IV.17}$$

for the discrete time case.

Proposition IV.6 *For a feedback law of the form in eqn.(IV.14), the cost function*

in eqn.(IV.16) is minimized for a matrix $K \in \mathbb{R}^{m\times n}$ *solving*

$$\mathbf{A}^T P + P\mathbf{A} + P\mathbf{B}(K \otimes I_{p+1}) + (K^T \otimes I_{p+1})\mathbf{B}^T P + Q_{\bar{x}} + (K^T \otimes I_{p+1})R_{\bar{u}}(K \otimes I_{p+1}) = 0 \tag{IV.18}$$

subject to $P = P^T > 0$. *Furthermore, a solution exists for some* $Q_{\bar{x}}$ *and* $R_{\bar{u}}$ *if the feasibility condition*

$$\mathbf{A}^T P + P\mathbf{A} + (K^T \otimes I_{p+1})\mathbf{B}^T P + P\mathbf{B}(K \otimes I_{p+1}) < 0 \tag{IV.19}$$

is satisfied.

Proof Let $J = \mathbf{X}^T P \mathbf{X}$. Taking the derivative of the cost function gives rise to the matrix equation

$$\dot{P} + P\mathbf{A} + P\mathbf{B}(K \otimes I_{p+1}) + \mathbf{A}^T P + (K^T \otimes I_{p+1})\mathbf{B}^T P = -Q_{\bar{x}} - (K^T \otimes I_{p+1})R_{\bar{u}}(K \otimes I_{p+1})$$

For an infinite time interval, let $\dot{P} \to 0$, giving the first condition. Now, we must show the second part of the proposition. The feasibility condition implies that we can select some stabilizing gain, K and that we can select some $M = M^T > 0$, and find a $P = P^T > 0$ such that

$$\mathbf{A}^T P + P\mathbf{A} + (K^T \otimes I_{p+1})\mathbf{B}^T P + P\mathbf{B}(K \otimes I_{p+1}) = -M$$

Select $M = \hat{M} \otimes W$. Let $\hat{M} = Q + K^T R K$. Because K makes the system Hurwitz, use of Lyapunov's theorem guarantees the existence of a P. This completes the proof. ■

Remark IV.7 *The bilinear matrix inequality (BMI) in eqn.(IV.19) does not have any analytical solution and must be solved numerically to obtain* K *and* P. *The BMI can be solved using solvers such as PENBMI [46].*

Proposition IV.8 *For a feedback law of the form in eqn.(IV.14), the cost function in eqn.(IV.17) is minimized for a matrix $K \in \mathbb{R}^{m\times n}$ solving*

$$Q_{\bar{x}} + (K^T \otimes I_{p+1})R_{\bar{u}}(K \otimes I_{p+1}) + ((K^T \otimes I_{p+1})\mathbf{B}^T + \mathbf{A}^T)P(\mathbf{A} + \mathbf{B}(K \otimes I_{p+1})) - P = 0$$

subject to $P = P^T > 0$. Furthermore, a solution exists for some $Q_{\bar{x}}$ and $R_{\bar{u}}$ if the feasibility condition

$$\left((K^T \otimes I_{p+1})\mathbf{B}^T + \mathbf{A}^T\right) P \left(\mathbf{A} + \mathbf{B}(K \otimes I_{p+1})\right) - P < 0 \tag{IV.20}$$

is satisfied.

Proof Let $J = \mathbf{X}^T P \mathbf{X}$. Examining the cost function at time k, as was done previously, gives rise to the matrix equation

$$P(k) = Q_{\bar{x}} + (K^T \otimes I_{p+1})R_{\bar{u}}(K \otimes I_{p+1}) + \left((K^T \otimes I_{p+1})\mathbf{B}^T + \mathbf{A}^T\right) P(k+1) \left(\mathbf{A} + \mathbf{B}(K \otimes I_{p+1})\right)$$

For an infinite time interval, let $P(k+1) = P(k) = P$, giving the first condition. The feasibility condition implies that we can select some stabilizing gain, K and that we can select some $M = M^T > 0$, and find a $P = P^T > 0$ such that

$$\left((K^T \otimes I_{p+1})\mathbf{B}^T + \mathbf{A}^T\right) P \left(\mathbf{A} + \mathbf{B}(K \otimes I_{p+1})\right) - P = -M$$

As in the previous proposition, select $M = \hat{M} \otimes W$. Let $\hat{M} = Q + K^T R K$. Because K makes the system stable, use of Lyapunov's theorem guarantees the existence of a P. This completes the proof. ■

Remark IV.9 *The condition in proposition IV.8 can also be written as a bilinear matrix inequality though this is less intuitive. The BMI has the form*

$$\begin{bmatrix} Y & (K^T \otimes I_{p+1})(R_{\bar{u}} + \mathbf{B}^T P \mathbf{B}) \\ (R_{\bar{u}} + \mathbf{B}^T P \mathbf{B})(K \otimes I_{p+1}) & R_{\bar{u}} + \mathbf{B}^T P \mathbf{B} \end{bmatrix} \geq 0$$

where

$$Y = Q_{\bar{x}} + \mathbf{A}^T P \mathbf{A} + (K^T \otimes I_{p+1})\mathbf{B}^T P \mathbf{A} + \mathbf{A}^T P \mathbf{B}(K \otimes I_{p+1}) - P$$

Remark IV.10 *Unlike in the previous design, the variation in the state trajectories directly maps to a corresponding deterministic control and does not require explicit knowledge of* Δ*. This can lead to computational benefits during implementation. This feedback structure mimics the traditional robust control approach where a single controller guarantees robust performance for the entire range of parameter variation. The advantage here is that it admits any arbitrary distribution, where traditional robust control is limited to uniform distribution only.*

At first glance it would seem that these bilinear equations could be reduced to linear equations through standard substitutions as in [40]. This is not the case, however, because the Kronecker product creates more equations than unknowns. Such substitutions require an inverse to solve for the gain, K, but such a procedure would not preserve the Kronecker structure.

c. Stochastic State Feedback with Stochastic Gain

This section deals with the optimality of a control law that involves feedback of the form $u = K(\Delta)x(t, \Delta)$, where the constant gain depends on the random variable Δ. In terms of the gPC expansions, $K(\Delta)$ can be written as $K(\Delta) = \{k_{ij}(\Delta)\}$ and $k_{ij}(\Delta) = \sum_{h=0}^{p} k_{ij,h}\phi_h(\Delta)$. This feedback structure is also analogous to output feedback control, but with increased degree of freedom. Implementation of this control law requires knowledge of Δ. To determine the values $u_{i,j}$, we project the control onto the polynomial subspace

$$u_{i,l} = \frac{1}{\langle \phi_l^2 \rangle} \sum_{j=1}^{n} \sum_{h=0}^{p} \sum_{q=0}^{p} k_{ij,h} x_{j,q} \langle \phi_l, \phi_h \phi_q \rangle$$

giving

$$\mathbf{U} = \left(\sum_{h=0}^{p} K_k \otimes \Psi_h \right) \mathbf{X} = \mathbf{K}\mathbf{X} \tag{IV.21}$$

When the control K is not a function of Δ, this corresponds to $k_{ij,h} = 0$ for $h \geq 1$. The matrix $\Psi_0 = I_{p+1}$, so the previous case is recovered. The cost function is written in terms of this feedback strategy as

$$J = \int_0^\infty \mathbf{X}^T \left(Q_{\bar{x}} + \mathbf{K}^T R_{\bar{u}} \mathbf{K} \right) \mathbf{X} dt \tag{IV.22}$$

Proposition IV.11 *The feedback law in eqn.(IV.21) optimally drives the system to the origin with respect to the cost function in eqn.(IV.22) for $K(\Delta)$ solving*

$$\mathbf{A}^T P + P\mathbf{A} + P\mathbf{B}\mathbf{K} + \mathbf{K}^T \mathbf{B}^T P + Q_{\bar{x}} + \mathbf{K}^T R_{\bar{u}} \mathbf{K} = 0 \tag{IV.23}$$

subject to $P = P^T > 0$. Furthermore, a solution exists for some $Q_{\bar{x}}$ and $R_{\bar{u}}$ if the feasibility condition

$$\mathbf{A}^T P + P\mathbf{A} + \mathbf{K}^T \mathbf{B}^T P + P\mathbf{B}\mathbf{K} < 0 \tag{IV.24}$$

is satisfied.

Proof The proof is similar to the previous proposition and is therefore omitted. ■

For the discrete time case, the cost function becomes

$$J_d = \sum_{k=0}^{\infty} \mathbf{X}^T(k) \left(Q_{\bar{x}} + \mathbf{K}^T R_{\bar{u}} \mathbf{K} \right) \mathbf{X}(k) \tag{IV.25}$$

Proposition IV.12 *The feedback law in eqn.(IV.21) optimally drives the system to the origin with respect to the cost function in eqn.(IV.25) for $K(\Delta)$ solving*

$$Q_{\bar{x}} + \mathbf{K}^T R_{\bar{u}} \mathbf{K} + (\mathbf{K}^T \mathbf{B}^T + \mathbf{A}^T) P (\mathbf{A} + \mathbf{B}\mathbf{K}) - P = 0$$

subject to $P = P^T > 0$. *Furthermore, a solution exists for some* $Q_{\bar{x}}$ *and* $R_{\bar{u}}$ *if the feasibility condition*

$$(\mathbf{A}^T + \mathbf{K}^T\mathbf{B}^T)P(\mathbf{A} + \mathbf{B}\mathbf{K}) - P < 0 \tag{IV.26}$$

is satisfied.

Proof The proof is similar to the previous proposition for a discrete time optimal control policy and is therefore omitted. ■

Remark IV.13 *This control strategy provides more flexibility for solving the necessary condition for optimality at the expense of more complexity in implementation, i.e. the necessity for knowledge of* Δ.

d. Deterministic Control with Augmented State Feedback

In this feedback structure, the augmented gPC states of the stochastic system are used to derive a deterministic control. This corresponds to a control with $u_i(t, \Delta) = u_{i,0}$. As a result, the system $\mathbf{B}$ matrix becomes

$$\hat{\mathbf{B}} = \begin{bmatrix} b_{11,1} & b_{12,1} & \cdots & b_{1m,1} \\ b_{11,2} & b_{12,2} & \cdots & b_{1m,2} \\ \vdots & \vdots & & \vdots \\ b_{11,p} & b_{12,p} & \cdots & b_{1m,p} \\ b_{21,1} & b_{22,1} & \cdots & b_{2m,1} \\ \vdots & \vdots & & \vdots \\ b_{n1,p} & b_{n2,p} & \cdots & b_{nm,p} \end{bmatrix}$$

or $\hat{\mathbf{B}}$ can be written in the form of eqn.(III.27), where

$$\hat{\mathbf{B}}_{ij} = \sum_{k=0}^{p} b_{ij,k}\delta_{1k}$$

The δ_{1k} is a vector of zeros with a 1 at the k^{th} position. Since u is a deterministic control,

$$\mathbf{E}[u^T R u] = u^T R u \tag{IV.27}$$

Unlike previous cases, the dimension of $\hat{\mathbf{B}}$ is $n(p+1)\times m$ instead of $n(p+1)\times m(p+1)$. The optimal control problem for this case involves selecting a control structure of the form

$$u = K\mathbf{X} \tag{IV.28}$$

where $K \in \mathbb{R}^{m\times n(p+1)}$.

Proposition IV.14 *Assume the matrix pair* $(\mathbf{A}, \hat{\mathbf{B}})$ *is stabilizable. The control law in eqn.(IV.28) with a gain given by*

$$K = -R^{-1}\hat{\mathbf{B}}^T P \tag{IV.29}$$

where $P = P^T > 0$ *is the solution of the algebraic Riccatti equation*

$$\mathbf{A}^T P + P\mathbf{A} - P\hat{\mathbf{B}}R^{-1}\hat{\mathbf{B}}^T P + Q_{\bar{x}} = 0 \tag{IV.30}$$

and optimizes the performance index in eqn.(IV.6) for a deterministic feedback law.

Proof This is the solution to the standard LQR problem. ■

The above result gives a feedback law for the continuous time case. We now give a result for the discrete time case.

Proposition IV.15 *Assume the matrix pair* $(\mathbf{A}, \hat{\mathbf{B}})$ *is stabilizable. The control law in eqn.(IV.28) with a gain given by*

$$K = -(R + \hat{\mathbf{B}}^T P \hat{\mathbf{B}})^{-1}\hat{\mathbf{B}}^T P\mathbf{A} \tag{IV.31}$$

where $P = P^T > 0$ *is the solution of the algebraic Riccatti equation*

$$P = Q_{\bar{x}} + \mathbf{A}^T \left(P - P\hat{\mathbf{B}}(R + \hat{\mathbf{B}}^T P \hat{\mathbf{B}})^{-1} \hat{\mathbf{B}} P \right) \mathbf{A} \tag{IV.32}$$

and optimizes the performance index in eqn.(IV.7) for a deterministic feedback law.

Proof This is the solution to the standard LQR problem. ■

Remark IV.16 *The solution to this control problem maps* $\mathbf{X}$*, the gPC expansions of the states, directly to deterministic control* $u(t)$*. Hence, knowledge of* Δ *is necessary to compute* $\mathbf{X}$ *during implementation.*

As the number of PC terms is increased, the system becomes less controllable with respect to a single deterministic control vector ($u_{i,0}$). However, if the system is stabilizable with respect to the feedback, then the higher-order uncontrollable PC states will decay to zero as well. Thus a solution to the optimization problem still exists. This type of system dynamics (with respect to the control input matrix, $\hat{\mathbf{B}}$) is important because the system would behave in this manner under the influence of open-loop optimal control. Therefore, if the system is stabilizable with respect to $\mathbf{K}$, then an open-loop optimal solution may exist. If the pair $(\mathbf{A}, \hat{\mathbf{B}})$ is not stabilizable, then stochastic feedback may be needed and the approaches of the previous propositions will be required.

3. Examples

a. Deterministic State Feedback Example

As a simple example, consider the following model of an F-16 aircraft at high angle of attack

$$\dot{x} = Ax + Bu$$

with states $x = [V \quad \alpha \quad q \quad \theta \quad T]^T$ where V is the velocity, α the angle of attack, q the pitch rate, θ its angle, and T is the thrust. The controls, $u = [\delta_{th} \quad \delta_e]^T$, are the elevator deflection δ_e, and the throttle δ_{th}. The A and B matrices are given by

$$A = \begin{bmatrix} 0.1658 & -13.1013 & (-7.2748) & -32.1739 & 0.2780 \\ 0.0018 & -0.1301 & (0.9276) & 0 & -0.0012 \\ 0 & -0.6436 & -0.4763 & 0 & 0 \\ 0 & 0 & 1 & 0 & 0 \\ 0 & 0 & 0 & 0 & -1 \end{bmatrix}$$

$$B = \begin{bmatrix} 0 & -0.0706 \\ 0 & -0.0004 \\ 0 & -0.0157 \\ 0 & 0 \\ 64.94 & 0 \end{bmatrix}$$

Similar to the analysis of Lu[11], the terms in parenthesis in the A matrix are assumed to be uncertain and are functions of a *single* random variable, Δ. The uncertainty in these terms is assumed to be distributed uniformly by ±20% about the nominal values −7.2748 and 0.9276 respectively. This uncertainty corresponds to the uncertainty in the damping term C_{xq}. The control design objective is to keep the aircraft at trim, given perturbation in the initial condition, in the presence of such parametric uncertainty. This is accomplished with an LQR design, using the control law in eqn.(IV.9), which results in a Δ parameterized family of optimal feedback gains. We compare the performance of the stochastic LQR design with Monte-Carlo designs, where LQR designs were performed for a family of systems *sampled* over uniformly distributed Δ. The cost function for the Monte-Carlo designs is kept identical to that in the stochastic design, i.e. matrices Q and R were the same for all the designs.

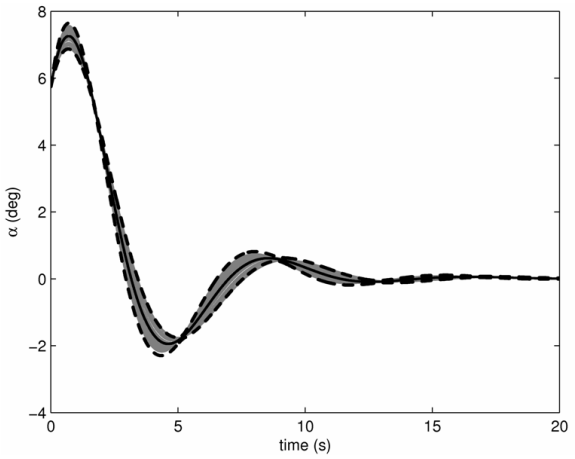

Fig. 10. Family of α trajectories from Monte-Carlo and predicted mean and uncertainty from PC.

Figure 10 shows the performance of the Monte-Carlo LQR designs, represented in gray, as well as the performance of the gPC based design. The variance and mean of the state trajectories, computed from the gPC expansions, are shown as dashed and solid line respectively. We observe that the statistics obtained from stochastic LQR design are consistent with those obtained from the Monte-Carlo simulations. The key advantage in the gPC based design framework is that the stochastic control design problem is solved *deterministically* and by a *single* design. The controller obtained is statistically similar to the family of LQR designs over the sample set of Δ, but synthesized in a computationally efficient and statistically consistent manner. If the LQR problem is solved for each value of Δ and the expected cost is computed, this gives

$$\begin{aligned}\mathbf{E}[J] &= \mathbf{E}[x(\Delta)^T P(\Delta) x(\Delta)] \\ &= \int_\Delta \sum_{i=0}^{p}\sum_{j=0}^{p}\sum_{k=0}^{p} x_i^T P_j x_k \phi_i \phi_j \phi_k \, f \, d\Delta \\ &= \mathbf{X}^T \left(\sum_{k=0}^{p} P_k \otimes W_k \right) \mathbf{X} = \mathbf{X}^T P_{mc} \mathbf{X} \end{aligned} \tag{IV.33}$$

where we define $e_{ijk} = \langle \phi_i \phi_j \phi_k \rangle$ and let $W_k = W_k^T$ be defined by

$$W_k = \begin{bmatrix} e_{00k} & e_{01k} & \cdots & e_{0nk} \\ e_{10k} & e_{11k} & \cdots & e_{1nk} \\ \vdots & & \ddots & \vdots \\ e_{n0k} & e_{n1k} & \cdots & e_{nnk} \end{bmatrix}$$

The term, W_0 corresponds to W in eqn.(IV.5). The question naturally arises, "How does the gPC solution relate to the expected cost of solving the LQR problem for each value of Δ?" To determine this relationship we consider the two cost functions and more specifically, their corresponding P matrices. The matrix, P_{mc}, has the same dimensionality as the solution of the Riccatti equation in eqn.(IV.10). Comparing the cost incurred by the controller in equation (IV.9), $J = \mathbf{X}^T P \mathbf{X}$, with the expected cost of each LQR solution, $\mathbf{X}^T P_{mc} \mathbf{X}$, we expect P to tend to P_{mc} as the number of terms in the PC expansion is increased. To compare these two matrices, we solve the traditional LQR problem for a large sample of Δ and obtain the corresponding matrix $P(\Delta)$. This is then projected onto the polynomial chaos basis functions, giving P_k, and P_{mc} is then calculated. Figure 11 shows the Frobenius norm of $P_{mc} - P$ as a

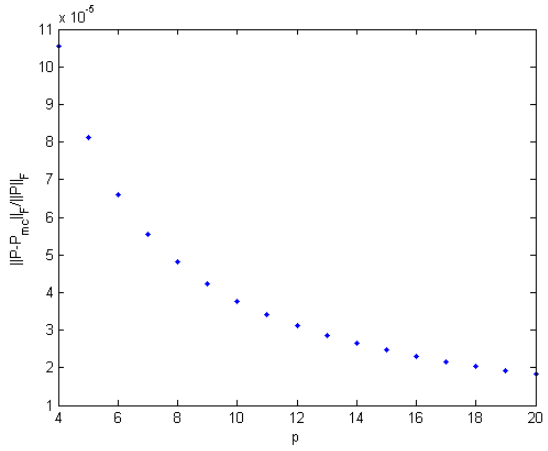

Fig. 11. Frobenius norm of $P_{mc} - P$ normalized by $\|P\|_F$

function of the number of terms included in the gPC expansion. We can see that P tends to the projection of the Monte-Carlo solution exponentially as the number of terms is increased. This means that the LQR solution we obtain for the gPC system for the control in eqn.(IV.9) represents the solution of the LQR problem at each value of Δ when its uncertainty is uniform in distribution. A formal exposition of this observation will be addressed in our future work.

b. Stochastic State Feedback with Constant Gain Example

The previous example demonstrates the ability of the gPC framework to be used to perform optimal control design over a distribution of parameters but requires knowledge of $x_{i,j}$, the gPC expansions of the state vector, as well as Δ. In many systems it may not be feasible to measure or estimate Δ, but rather to utilize a constant feedback solution that is optimal with respect to the distribution of the uncertain parameters. For these cases, the control design in eqn.(IV.14) is used where the gain is calculated as the solution of a BMI. As an example of this design approach consider the following problem.

$$A = \begin{bmatrix} 2+\Delta & 2 \\ -3 & -4 \end{bmatrix} B = \begin{bmatrix} 1 \\ 1 \end{bmatrix}$$
$$C = \begin{bmatrix} 1 & 0 \end{bmatrix}$$

where $\Delta \in [-1, 1]$ is a random variable. We wish to design a single control that stabilizes the system and minimizes the expected cost. Solving the resulting BMI for the optimization condition yields the desired control. In addition to the minimum expectation solution proposed in this work, we also design an optimal control using standard LQR for the nominal system, i.e. $\Delta = 0$. Figure 12 shows the closed loop eigenvalues for both control laws. There is a much larger distribution of system

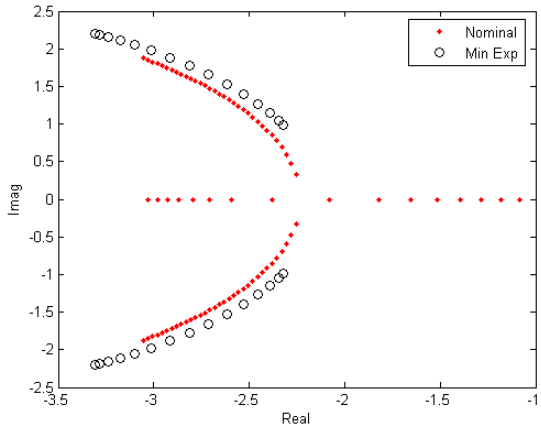

Fig. 12. Closed loop eigenvalues of minimum expectation control and nominal optimal control

eigenvalues for the nominal control law, and the system behavior varies significantly over the range of the random variable, Δ. This example demonstrates the benefit of optimizing with respect to a distribution as opposed to a single nominal point. Figure 13 shows the cost of each control law for given values of Δ. As an additional comparison, the cost for minimizing the worst case is shown as well. With respect

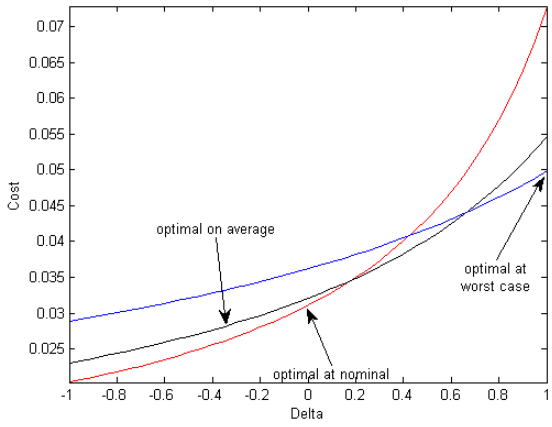

Fig. 13. Comparison of cost of nominal and minimum expectation control as a function of Δ

to the distribution of the parameters, the expected cost of the gPC solution is lower, though the nominal optimal solution is optimal at $\Delta = 0$, which is expected.

Utilizing a uniform distribution for parameter uncertainty does not always result in a realistic representation. If the uncertainty in a parameter is represented by a uniform distribution, this means that knowledge of the value is limited to a range, but there is no value more likely than another. In practice, parameter values exhibit more Gaussian behavior, however the support of the Gaussian distribution is $\Delta \in (-\infty, \infty)$, making them impractical for use in stability analysis. There are two approaches that can be used to alleviate this problem. The distribution can be truncated and new orthogonal polynomials generated through an algorithm such as Gram-Schmidt

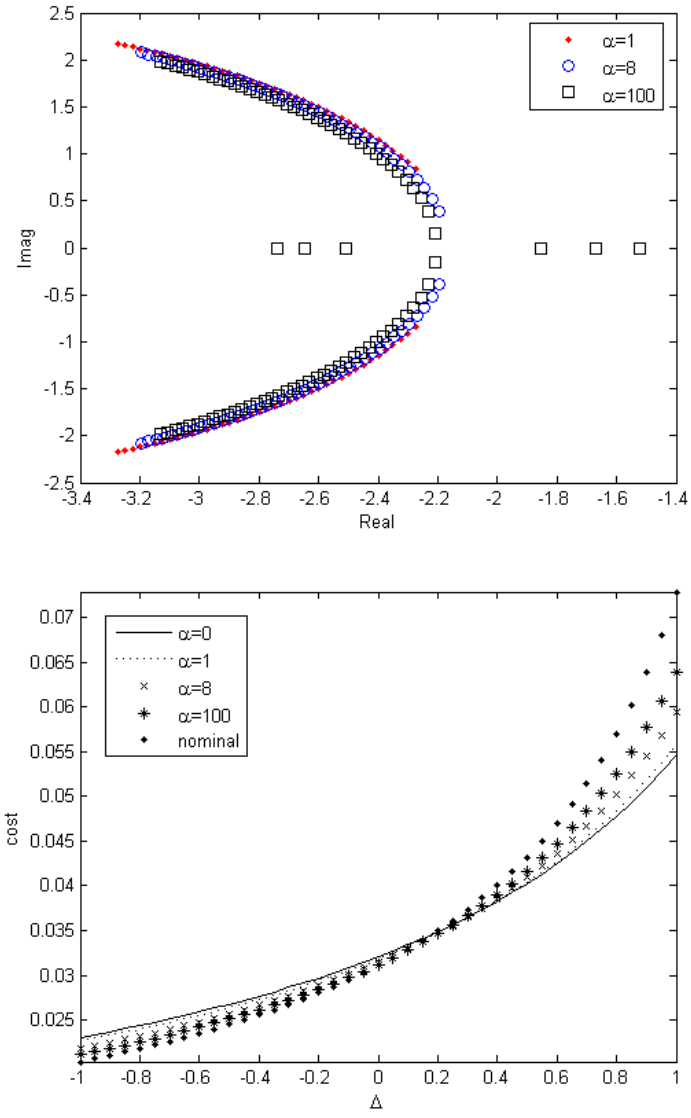

Fig. 14. Closed loop eigenvalues of minimum expectation control for Beta distribution (top). Cost functions associated with various values of α as a function of Δ (bottom)

orthogonalization, or a similar distribution with finite support can be used. For this example, we chose a Beta distribution with $\alpha = \beta$ as this produces a Gaussian like curve with support on $\Delta \in [-1, 1]$. The two parameters, α and β are varied on the line $\alpha = \beta$ and optimal controllers are generated. Figure 14 shows the closed

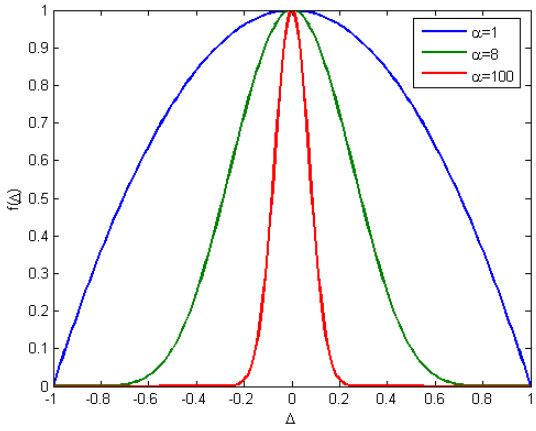

Fig. 15. Beta distribution for various values of $\alpha = \beta$. Distribution approaches δ function as $\alpha \to \infty$.

loop eigenvalue locations of the system for values of Δ between -1 and $+1$. The eigenvalue locations are generated for several values of α. As α is increased, the range of eigenvalues increases and in the limiting case, these become the eigenvalues of the closed loop system with the nominal design. The corresponding distribution curves are shown in figure 15. As $\alpha = \beta \to \infty$, the distribution, weighted properly, becomes a δ function, or a single point with probability one. Finding an optimal control for the nominal case is then equivalent to finding the optimal expectation control for a system where the probability distribution is $f(\Delta) = \delta(\Delta = 0)$. As the value of α is decreased, to zero, the distribution widens and tends to a uniform distribution. Figure 14 also depicts the cost function for various values of α. As the value of α is increased from 0 (corresponding to a uniform distribution) to ∞ (corresponding to the nominal case), the corresponding pointwise cost evolves from that of a uniform distribution to the cost associated with the nominal design. As α is increased, the extreme values of Δ occur with lower probability, making it acceptable to take more risk for these values.

C. Optimal Control with Probabilistic System Parameters

In this section we discuss generation of trajectories for dynamical systems in the optimal control theoretic framework. Optimality with probabilistic uncertainty in system parameters results in stochastic optimal control problems. In this section, we derive two standard cost functions that are encountered in stochastic optimal control problems, in terms of the polynomial chaos expansions. Here we consider minimum expectation and minimum variance cost functions. In the following analysis, we assume $x(t)$ is stochastic and $u(t)$ is deterministic.

1. Minimum Expectation Trajectories

Minimum expectation optimal trajectories are obtained by minimizing the following cost function, analogous to the Bolza form,

$$\min_u \ \mathbf{E}\left[\int_0^{t_f} (x^T Q x + u^T R u)dt + x_f^T S x_f\right] \tag{IV.34}$$

where $x \equiv x(t) \in \mathbb{R}^n, u \equiv u(t) \in \mathbb{R}^m$ and $x_f = x(t_f), Q = Q^T > 0, R = R^T > 0, S = S^T > 0$. Unlike the cost function in equation (IV.1), this function is finite time and also has a terminal cost function. Following steps similar to those for the infinite horizon problem in the previous section, the cost function in eqn.(IV.34) can now be written in terms of the gPC expansions as

$$\min_u \ \int_0^{t_f} \left[\mathbf{X}^T Q_{\bar{x}} \mathbf{X} + u^T R u\right] dt + \mathbf{X}_f^T S_{\bar{x}} \mathbf{X}_f \tag{IV.35}$$

where $Q_{\bar{x}} = Q \otimes W, S_{\bar{x}} = S \otimes W$ and $\mathbf{X}_f = \mathbf{X}(t_f)$.

2. Minimum Covariance Trajectories

For $x \in \mathbb{R}$, the variance $\sigma^2(x)$ in terms of the gPC expansions is given by

$$\sigma^2(x) = \mathbf{E}[x - \mathbf{E}[x]]^2 = \mathbf{E}[x^2] - \mathbf{E}^2[x] = \mathbf{x}^T W \mathbf{x} - \mathbf{E}^2[x]$$

where

$$\mathbf{E}[x] = \mathbf{E}\left[\sum_{i=0}^{p} x_i \phi_i\right] = \sum_{i=0}^{p} x_i \mathbf{E}[\phi_i] = \sum_{i=0}^{p} x_i \int_{\mathcal{D}_\Delta} \phi_i f d\Delta$$

or

$$\mathbf{E}[x] = \mathbf{x}^T F, \quad \text{where } F = \begin{bmatrix} \int_{\mathcal{D}_\Delta} \phi_0 f d\Delta \\ \vdots \\ \int_{\mathcal{D}_\Delta} \phi_p f d\Delta \end{bmatrix}$$

Therefore, σ^2 for scalar x can be written in a compact form as

$$\sigma^2 = \mathbf{x}^T (W - FF^T)\mathbf{x} \tag{IV.36}$$

which may enter the cost function in integral form or as final cost.

The covariance of a vector process $x(t) : \mathbb{R} \mapsto \mathbb{R}^n$ is given by

$$\begin{aligned} C_{xx}(t) &= \mathbf{E}[(x(t) - \bar{x}(t))\,(x(t) - \bar{x}(t))^T] \\ &= \mathbf{E}[(x(t)x(t)^T] - \bar{x}(t)\bar{x}(t)^T \end{aligned}$$

where

$$\bar{x}(t) = \mathbf{E}[x(t)] = \begin{pmatrix} \mathbf{x}_1^T \\ \vdots \\ \mathbf{x}_n^T \end{pmatrix} F$$

and $\mathbf{x}_i$ is defined by eqn.(III.13). Therefore

$$\begin{aligned}\bar{x}(t)\bar{x}(t)^T &= \begin{pmatrix} \mathbf{x}_1^T \\ \vdots \\ \mathbf{x}_n^T \end{pmatrix} FF^T \begin{pmatrix} \mathbf{x}_1^T \\ \vdots \\ \mathbf{x}_n^T \end{pmatrix}^T \\ &= \begin{bmatrix} \mathbf{x}_1^T FF^T \mathbf{x}_1 & \cdots & \mathbf{x}_1^T FF^T \mathbf{x}_n \\ \vdots & & \vdots \\ \mathbf{x}_n^T FF^T \mathbf{x}_1 & \cdots & \mathbf{x}_n^T FF^T \mathbf{x}_n \end{bmatrix}\end{aligned}$$

Similarly,

$$\mathbf{E}[xx^T] = \begin{bmatrix} \mathbf{x}_1^T W \mathbf{x}_1 & \cdots & \mathbf{x}_1^T W \mathbf{x}_n \\ \vdots & & \vdots \\ \mathbf{x}_n^T W \mathbf{x}_1 & \cdots & \mathbf{x}_n^T W \mathbf{x}_n \end{bmatrix}$$

Therefore, in terms of gPC coefficients, C_{xx} can be written as

$$C_{xx} = \begin{bmatrix} \mathbf{x}_1^T (W - FF^T) \mathbf{x}_1 & \cdots & \mathbf{x}_1^T (W - FF^T) \mathbf{x}_n \\ \vdots & & \vdots \\ \mathbf{x}_n^T (W - FF^T) \mathbf{x}_1 & \cdots & \mathbf{x}_n^T (W - FF^T) \mathbf{x}_n \end{bmatrix} \tag{IV.37}$$

An important metric for covariance analysis is $\mathbf{Tr}[C_{xx}]$, which can be written in a compact form as,

$$\mathbf{Tr}[C_{xx}] = \mathbf{X}^T Q_{\sigma^2} \mathbf{X} \tag{IV.38}$$

where $Q_{\sigma^2} = I_n \otimes (W - FF^T)$.

3. Example - Van der Pol Oscillator

In this section we apply the polynomial chaos approach to solve an example stochastic optimal control problem based on the Van der Pol oscillator, which highlights numerical solution of stochastic optimal control problems. Consider the well known

forced Van der Pol oscillator model

$$\left.\begin{aligned} \dot{x}_1 &= x_2 \\ \dot{x}_2 &= -x_1 + \mu(\Delta)(1 - x_1^2)x_2 + u \end{aligned}\right\} \tag{IV.39}$$

where μ is a random variable with uniform distribution in the range $\mu(\Delta) \in [0, 1]$. For uniform distribution the basis functions are Legendre polynomials and $\mathcal{D}_\Delta = [-1, 1]$. Since the dimension of Δ in this case is one, p is equal to the order of the Legendre polynomial. For this example we chose $p = 4$. Representing the gPC expansions of x_1, x_2, μ similar to eqn.(III.9), the dynamics of the Van der Pol oscillator in terms of the gPC expansions can be written as

$$\begin{aligned} \dot{x}_{1,m} &= x_{2,m} \\ \dot{x}_{2,m} &= -x_{1,m} + \frac{1}{\langle \phi_m, \phi_m \rangle} \left(\sum_{i=0}^{p} \sum_{j=0}^{p} \mu_i x_{2,j} e_{ijm} - \right. \\ &\qquad \left. \sum_{i=0}^{p} \sum_{j=0}^{p} \sum_{k=0}^{p} \sum_{l=0}^{p} \mu_i x_{1,j} x_{1,k} x_{2,l} e_{ijklm} + \langle u, \phi_m \rangle \right) \end{aligned}$$

for $m = \{0, \cdots, p\}$; where $e_{ijm} = \langle \phi_i \phi_j \phi_m \rangle$ and $e_{ijklm} = \langle \phi_i \phi_j \phi_k \phi_l \phi_m \rangle$. Note that the projection $\langle u, \phi_m \rangle = u$ for $m = 0$, and $\langle u, \phi_m \rangle = 0$ for $m = \{1, \cdots, p\}$. Therefore the deterministic control only enters the equation for $x_{2,0}$.

The stochastic optimal control problem for this example is posed as

$$\min_{u(t)} \mathbf{E}\left[\int_0^5 (x_1^2 + x_2^2 + u^2) dt \right] \tag{IV.40}$$

subject to stochastic dynamics given by eqn.(IV.39) and constraints

$$\begin{aligned} x_1(0) &= 3 \\ x_2(0) &= 0 \\ \mathbf{E}[x_1(5)] &= 0 \\ \mathbf{E}[x_2(5)] &= 0 \end{aligned}$$

In the posed problem, we have assumed that there is no uncertainty in the initial condition of the states and the terminal equality constraint is imposed on the expected value of the states at final time. In terms of the gPC expansions, the constraints are

$$\left.\begin{aligned} x_{1,0}(0) &= 3 \\ x_{1,m}(0) &= 0,\ m = \{1, \cdots, p\} \\ x_{2,m}(0) &= 0,\ m = \{0, \cdots, p\} \\ \mathbf{E}[x_1(5)] = x_{1,0}(5) &= 0 \\ \mathbf{E}[x_2(5)] = x_{2,0}(5) &= 0 \end{aligned}\right\} \tag{IV.41}$$

The optimal control problem was solved using OPTRAGEN [47], a MATLAB toolbox that transcribes optimal control problems to nonlinear programming problems using B-Spline approximations. The resulting nonlinear programming problem was solved using SNOPT [48]. Figure (16(a)) shows the trajectories of the optimal solution in the subspace spanned by B-Splines. The solid (red) state trajectories are the mean trajectories of $x_1(t), x_2(t)$ and they satisfy the constraints defined by eqn.(IV.41). The dashed (blue) state trajectories are the remaining gPC expansions of $x_1(t), x_2(t)$. The suboptimal cost for these trajectories is 15.28 and took 10.203 seconds to solve for in MATLAB environment. The trajectories were approximated using B-Splines consisting of ten 5^{th} order polynomial pieces with 4^{th} order smoothness at the knot points.

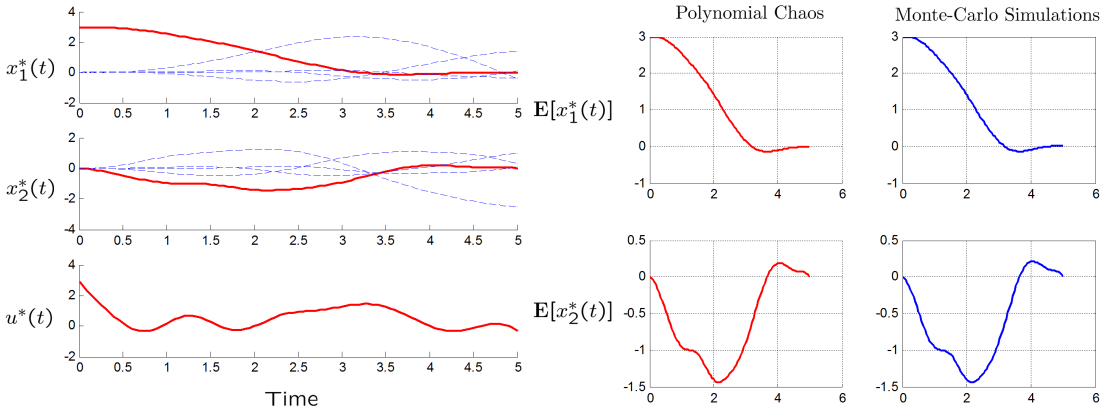

(a) Optimal gPC trajectories for the Van der Pol oscillator

(b) Verification of stochastic optimal control law using Monte-Carlo simulations.

Fig. 16. Comparison of trajectories obtained from gPC expansions and Monte-Carlo simulations.

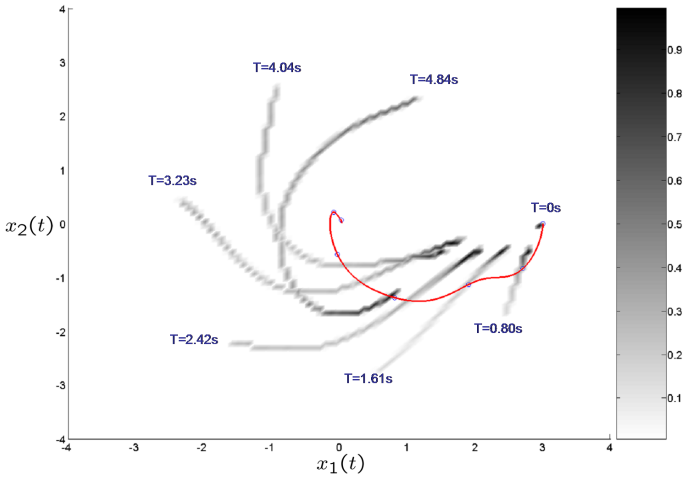

(a) Evolution of pdf and mean trajectory.

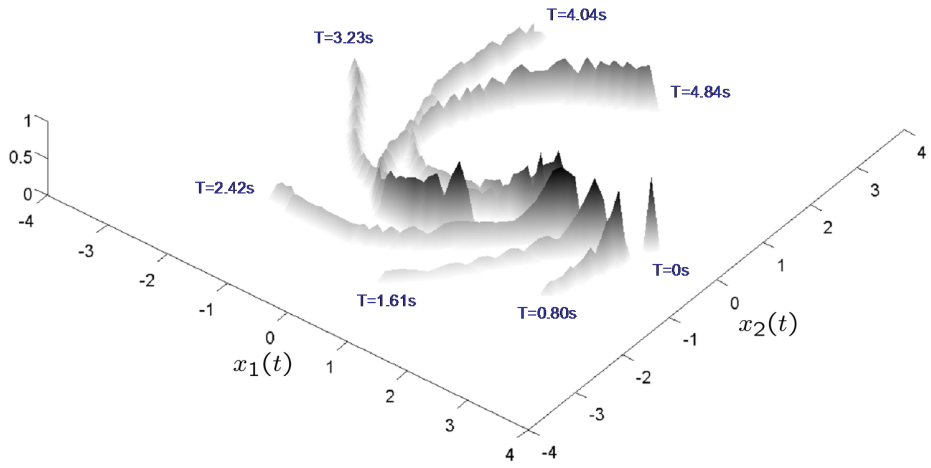

(b) Evolution of uncertainty in state due to uncertainty in μ.

Fig. 17. Evolution of the probability density function of the state trajectories due to $\mu(\Delta)$. The solid (red) line denotes the expected trajectory of (x_1, x_2). The circles (blue) denote time instances, on the mean trajectory, for which the snapshots of pdf are shown.

To verify the optimal control law for the stochastic system, we applied $u^*(t)$ to the Van der Pol oscillator for various values of μ, uniformly distributed over the interval $[0, 1]$, and computed the expected value of the state trajectories from the Monte-Carlo simulations. Figure (16(b)) shows the comparison of the expected trajectories $\mathbf{E}[x_1^*(t)], \mathbf{E}[x_2^*(t)]$, obtained from gPC and Monte-Carlo methods. The trajectories are identical. Thus, the generalized polynomial chaos framework provides a powerful set of tools for solving stochastic optimal control problems.

Figure (17) shows the evolution of uncertainty in state trajectories due to uncertainty in μ. The evolution of probability density functions (pdf), obtained via sampling, are shown in fig. (17(b)). The mean trajectory with the time varying pdf is shown in fig. (17(a)). From these figures, it can be inferred that the trajectories satisfy the terminal constraint in an average sense. However, *none of the individual trajectories arrive at the origin.* This is not surprising, as the constraints were only imposed on the expected value of the trajectories. For nonlinear systems the uncertainty evolves in a non-Gaussian manner. Therefore, analysis based on expectation can lead to erroneous interpretations and it is important to include higher order moments in the analysis. For this problem, localization of the state about the origin at final time can be achieved by including a terminal cost or constraint related to the covariance at final time.

Figure (18) shows the probability density function at final time when a terminal constraint $\mathbf{Tr}[C_{xx}] < 0.2$ was imposed in the optimal control problem. Figure (18) also shows the probability density function, at final time, obtained without the terminal constraint. It is clear from the figure that inclusion of terminal covariance based constraint has localized the covariance about the origin. Although none of the trajectories for $\mu \in [0, 1]$, even for the constrained case, arrive at the origin.

This terminal constraint however incurred a higher cost of 128.79. The state and

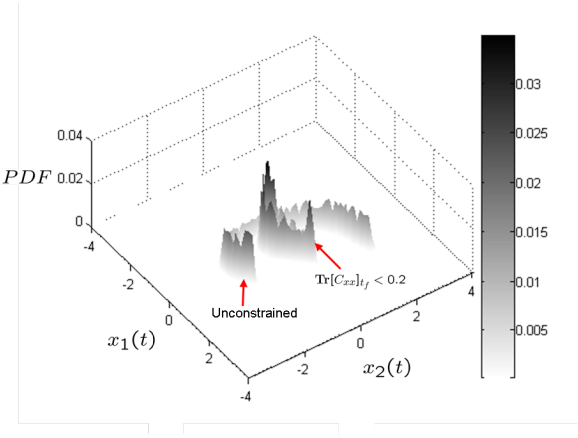

Fig. 18. PDF at final time, due to the terminal constraint based on covariance.

control trajectories are shown in fig. (19(a)). We observe that introduction of terminal constraint $\mathbf{Tr}[C_{xx}] < 0.2$ results in higher control magnitudes. The optimal control obtained in this case also agrees with the Monte-Carlo simulations over $\mu \in [0, 1]$, and is shown in fig. (19(b)).

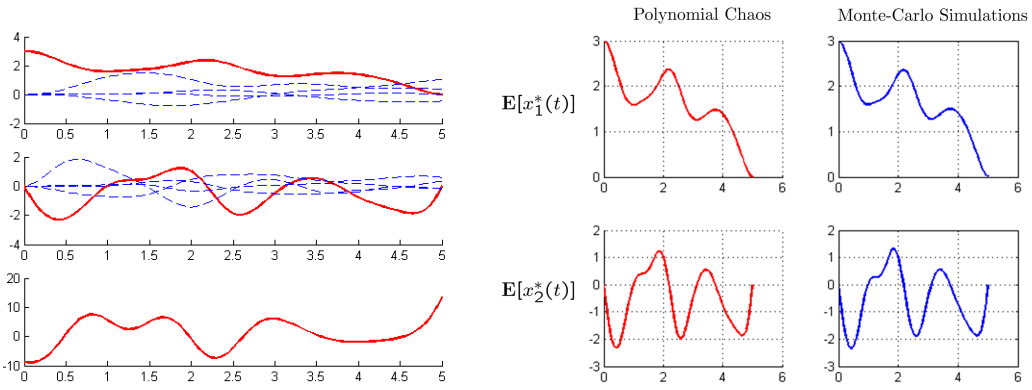

(a) Optimal gPC trajectories for the Van der Pol oscillator with terminal covariance constraint

(b) Verification of stochastic optimal control law using Monte-Carlo simulations.

Fig. 19. Comparison of trajectories obtained from gPC expansions and Monte-Carlo simulations.

D. Optimal Control with Stochastic Forcing

In this section we consider optimal control of dynamical systems with stochastic forcing. The stochastic forcing is assumed to be a random process with known covariance. Such processes can be approximated using the Karhunen-Loéve expansion functions [20]. If the correlation window of the forcing function is zero, i.e. if it is white noise, then the number of terms of the expansion will be infinite. For this reason, we assume that the stochastic forcing function has a non-zero correlation window, making it amenable for finite dimensional approximation. This is not an unrealistic assumption as there are many disturbance inputs in engineering systems with non-zero correlation windows. One notable example is the Dryden gust model which uses colored (correlated) noise inputs. The gPC expansion used in the previous sections of the paper does not utilize information related to the correlation of the noise inputs. When this information is known the Karhunen-Loéve (KL) expansion is used to include this time based information in the dynamics. This is accomplished by adding additional random variables to the system in the following manner. Let $Z(t,\omega)$ be a zero-mean random process with known covariance function $R(t_1,t_2)$, the KL expansion is given by

$$Z(t,\omega) = \sum_{k=1}^{\infty} \sqrt{\lambda_k} f_k(t) \Delta_k \tag{IV.42}$$

where Δ_k is a random variable governed by the distribution that governs $Z(t,\omega)$. For example, if $Z(t,\omega)$ is a correlated Gaussian process, each random variable, Δ_k is governed by a Gaussian distribution. The functions, $f_k(t)$ are eigenfunctions of the covariance function or

$$\int_a^b R(t_1,t_2) f_k(t_2)\, dt_2 = \lambda_k f_k(t_1) \tag{IV.43}$$

The scalars, λ_k, are the associated eigenvalues of the orthonormal functions $f_k(t)$.

This expansion is important because it allows us to write a correlated stochastic process as a summation of random variables with time-varying coefficients. Coupling this expansion with the projection techniques of the gPC gives a means of solving optimization problems with stochastic forcing. To return to the example of the Van der Pol Oscillator, consider the oscillator forced with the stochastic forcing function $w(t,\Delta)$. The dynamics of the oscillator are then governed by

(IV.44)

$$\begin{aligned} \dot{x}_1 &= x_2 \\ \dot{x}_2 &= -x_1 + \mu(\Delta_0)\left(1 - x_1^2\right)x_2 + u + w(t,\Delta) \end{aligned} \tag{IV.45}$$

where Δ_0 corresponds to the random variable associated with uncertainty in μ. The change in notation will become clear in the following text. The covariance of $w(t,\Delta)$ is given by

$$R_w(t_1,t_2) = e^{-a|t_1-t_2|} \tag{IV.46}$$

This covariance can be obtained by passing white noise through a first order filter with time constant a. To determine the new set of approximate dynamics, we first expand $w(t,\Delta)$ with its truncated KL expansion as

$$w(t,\Delta) = \sum_{k=1}^{M} \sqrt{\lambda_k} f_k(t) \Delta_k \tag{IV.47}$$

The time derivative of x_2 then becomes

$$\dot{x}_2 = \mu(\Delta_0)\left(1 - x_1^2\right)x_2 + u + \sum_{k=1}^{M} \sqrt{\lambda_k} f_k(t) \Delta_k \tag{IV.48}$$

The reason for the notation Δ_0 now becomes clear. Each term in the KL expansion adds a new random variable to the equations of motion so that we now have a vector of random variables, $\mathbf{\Delta} = \begin{bmatrix} \Delta_0 & \Delta_1 & \cdots \Delta_k \end{bmatrix}$. Expanding our state variables in terms

of KL gives

$$x_i(t,\Delta) = x_{i,0}(t,\Delta_0) + \sum_{k=1}^{M} f_{x_i,k}(t)\chi_{i,k} \tag{IV.49}$$

Because the covariance of x is not known, the new random variables are written in terms of a new gPC expansion. For simplicity, the two summations in the previous equation are combined into one single summation that starts with $k = 0$. Then we write each $\chi_{i,k}$ as a gPC expansion of the random variables from the vector $\mathbf{\Delta}$, or

$$\chi_{i,k} = \sum_{j=0}^{p} a_{j,i,k}\phi_j(\mathbf{\Delta}) \tag{IV.50}$$

The gPC expansion has $p+1$ terms, which can be determined as $p+1 = \frac{(M+1+r)!}{(M+1)!r!}$, where r is the desired order of the polynomials and M is the order of the KL expansion. The resulting basis, ϕ_j, is therefore an orthogonal basis with respect to $M+1$ independent random variables. Therefore, x_i becomes

$$x_i(t,\Delta) = \sum_{k=0}^{M}\left[f_{x_i,k}(t)\sum_{j=0}^{p} a_{j,i,k}\phi_j\right] \tag{IV.51}$$

This can be rewritten as

$$x_i(t,\Delta) = \sum_{j=0}^{p} x_{i,j}(t)\phi_j \tag{IV.52}$$

where $x_{i,j}(t) = \sum_{k=0}^{M} f_{x,k}(t)a_{j,k}$. Because the covariance of x_i is unknown, the functions $f_{x,k}$ are unknown as well. Therefore, we can utilize the variables $x_{i,j}$ as the states of a differential equation and solve for these as we have done in previous sections. With the equations in this form, the Galerkin projection utilized throughout the paper can

now be used to arrive at the projected dynamics. These have the form

$$\begin{aligned}
\dot{x}_{1,m} &= x_{2,m} \\
\dot{x}_{2,m} &= -x_{1,m} + \frac{1}{\langle \phi_m, \phi_m \rangle} \left(\sum_{i=0}^{p} \sum_{j=0}^{p} \mu_i x_{2,j} e_{ijm} - \right. \\
&\quad \sum_{i=0}^{p} \sum_{j=0}^{p} \sum_{k=0}^{p} \sum_{l=0}^{p} \mu_i x_{1,j} x_{1,k} x_{2,l} e_{ijklm} + \\
&\quad \left. \langle w, \phi_m \rangle + \langle u, \phi_m \rangle \right)
\end{aligned}$$

The terms for these expressions are the same as those obtained previously with the exception being the term $\langle w, \phi_m \rangle$. This term is the projection onto the forcing. Because the forcing terms are first order in Δ_k, in general this term will only be non-zero for M terms. For most sets of orthogonal polynomials in one variable (and in particular the traditional sets), the random variable Δ corresponds to ϕ_1. When these sets are generalized to multiple random variables, Δ_j corresponds to ϕ_{j+1} where $j = 0$ corresponds to the parametric uncertainty and $j = 1, \ldots M$ corresponds to the KL variables. Therefore the inner product can be written as

$$\langle w, \phi_m \rangle = \sum_{j=1}^{M} \sqrt{\lambda_j} f_j(t) \langle \phi_m^2 \rangle \delta_{(j+1),m}$$

As an example, consider the same cost function used in the previous section in eqn. (IV.40) subject to the constraints given in eqn. (IV.41), namely an initial constraint and constraints on the final expected value.

We now solve the same optimal control problem that we solved previously, except with a stochastic forcing term. For this example, we consider a uniform noise input with covariance $R(t_1, t_2) = e^{-\frac{1}{20}|t_2 - t_1|}$. The eigenfunctions of this covariance can be found analytically for a finite time interval (in our case $t \in [0, 5]$ and the first three corresponding eigenvalues are $\lambda_1 = 4.61$, $\lambda_2 = 0.23$, and $\lambda_3 = 0.06$. Because the eigen-

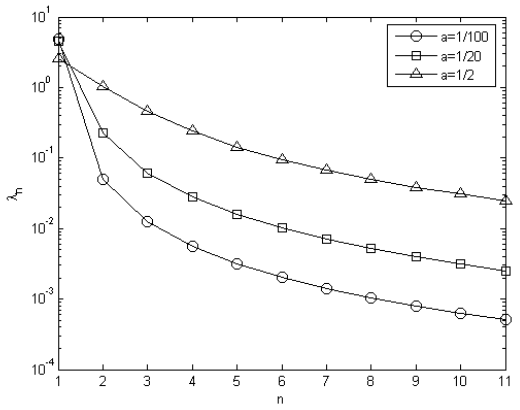

Fig. 20. Eigenvalues (λ_n) of the KL expansion for various window lengths ($1/a$).

values decay as the number of terms is increased, only the first few terms are needed to obtain a good approximation. This is because the eigenfunctions are orthonormal and therefore have unit amplitude. For our case, the eigenfunctions are sines and cosines. Figure 20 shows the eigenvalues of the first 11 terms of the KL expansion. For larger correlation window sizes (smaller values of a), the first eigenfunction is dominant as one would expect. For a window size of $a = 1/20$, the first term is several orders of magnitude larger than the second term, meaning for this example we can create a good approximation by only including the first term.

Furthermore, to reduce the problem size and complexity we use only polynomials up to order $r = 2$, meaning that we have $p = 5$. To test the accuracy of the solution, we examine the expected trajectory of x_1 and x_2 along with the variance of each one. These are compared to Monte-Carlo simulations for various values of Δ_0 and colored noise input.

Figure 21(a) shows the optimized trajectories of each state along with the control. The trajectory in red is the expected trajectory (corresponding to $x_{i,0}$) and those in blue are the remaining states corresponding to $x_{i,k}$ with $k \geq 1$. This figure also shows

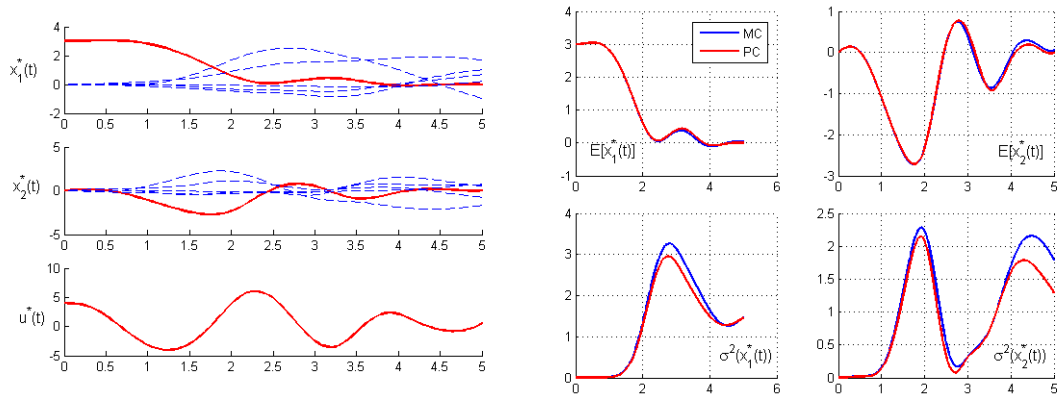

(a) Optimal gPC trajectories for the Van der Pol oscillator with stochastic forcing

(b) Verification of stochastic optimal control law using Monte-Carlo simulations.

Fig. 21. Comparison of trajectories obtained from gPC expansion and Monte-Carlo simulations for 2^{nd} order gPC expansion

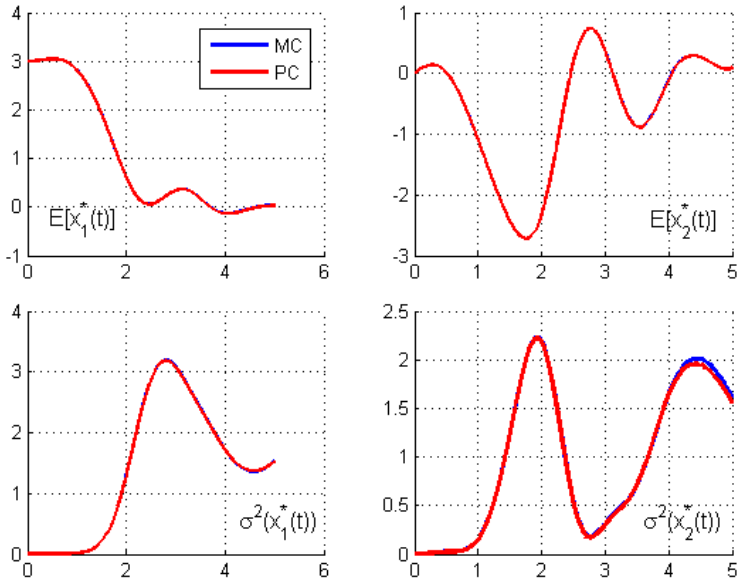

Fig. 22. Comparison of trajectories obtained from gPC expansion and Monte-Carlo simulations for 8^{th} order polynomials.

the open loop optimal control solution. To determine the accuracy of the optimal solution and it's predicted expected values and variances, we compare it to a Monte-Carlo simulation with the same control input. The Monte-Carlo solution utilizes uniformly distributed values of $\mu \in [0, 1]$ as well as a uniformly distributed colored noise, $w \in [-1, 1]$ where the covariance is given by $R(t_1, t_2) = e^{-\frac{1}{20}|t_2 - t_1|}$. Figure 21(b) shows the comparison of the optimal control solutions of $\mathbf{E}[x_1^*]$ and $\mathbf{E}[x_2^*]$ using gPC to the Monte-Carlo solution. The expected values predicted by gPC are accurate when compared to the Monte-Carlo solution. The predicted variances of each state are also shown. These are also accurate, although there is some error, especially in x_2. The inaccuracy in the variance estimates is a result of the low-order PC approximation that is used. If we increase the polynomial order, the accuracy in the variance estimate can be drastically improved. Figure 22 shows the expected value

as well as the variance estimates for the PC system when a polynomial order of 8 is used. Here the variance estimates are much closer to the Monte Carlo results. This result demonstrates that for PC systems to capture variance accurately, higher-order polynomials are usually required. While using higher order polynomials is helpful for prediction purposes, it can make the optimal control problem much more difficult to solve. Solving these more complex problems is a topic of future research. It is important to note that the optimal solution for the problem with stochastic forcing is not identical to that of the previous (parameter uncertainty only) case. This is in large part due to the nonlinearities in the problem.

E. Summary

In this chapter, we have solved stochastic optimal control problems for linear and nonlinear systems using the concept of Polynomial Chaos. The gPC expansion allows us to analyze linear and nonlinear stochastic differential equations in a deterministic framework. For infinite horizon linear optimal control problems, feedback laws are determined for several different choices of a feedback strategy. The other major result presented in this chapter involves the framing of a stochastic trajectory generation problem as a deterministic optimal control problem. This allows us to use well known techniques to solve this problem. In addition, a method of incorporating uncertainty in the form of a stochastic process was also introduced. Combining the KL expansion with the gPC approach enabled the generation of optimal trajectories for systems with parametric uncertainty as well as correlated stochastic forcing. These problems are very difficult to solve using a sampling based approach.

CHAPTER V

RECEDING HORIZON CONTROL

A. Introduction

Generating optimal state and control trajectories for constrained linear and nonlinear systems has been a topic of interest for researchers for a long time. While there have been many tools developed to generate optimal control solutions for linear and nonlinear systems, only under certain assumptions is it possible to obtain analytical feedback solutions. This problem is made more complex with the addition of constraints to the control requirements as well as the state trajectories. Often times, the only method of solving such problems is to find a numerical solution which is generally open loop and difficult to solve for long horizon lengths. To help alleviate some of these difficulties and adapt to changes in system behavior the idea of receding horizon control was developed.

Receding horizon control, also known as model predictive control, has been popular in the process control industry for several years [49, 50]. It is based on the simple idea of repetitive solution of an optimal control problem and updating states with the first input of the optimal command sequence. The repetitive nature of the algorithm results in a state dependent feedback control law. The attractive aspect of this method is the ability to incorporate state and control limits as hard or soft constraints in the optimization formulation. When the model is linear, the optimization problem is quadratic if the performance index is expressed via a $\mathcal{L}_2$-norm, or linear if expressed via a $\mathcal{L}_1/\mathcal{L}_\infty$-norm. Issues regarding feasibility of online computation, stability and performance are largely understood for linear systems and can be found in [51, 52, 53, 54]. For nonlinear systems, stability of RHC methods is guaranteed

by using an appropriate control Lyapunov function [55, 56]. For a survey of the state-of-the-art in nonlinear receding horizon control problems the reader is directed to reference [57].

More recently, the receding horizon control strategy is being extended into the realm of stochastic systems. This extension arises out of a need to create control laws that are robust to probabilistic system uncertainty. Traditional receding horizon laws perform best when modeling error is small as in many cases certain types of system uncertainty can lead to oscillatory behavior [58]. Furthermore, it is possible that even with slight uncertainty, the control strategy may not be robust [59]. Consequently, many approaches have been taken to improve robustness of the policy in the presence of unknown disturbances [60, 61, 62, 63, 64]. Many of these approaches involve the computation of a feedback gain to ensure robustness. The difficulty with this approach is that, even for linear systems, the problem can become more difficult to solve from a computational standpoint. This is because the feedback gain transforms the quadratic programming problem into a nonlinear programming problem. While the area of robust receding horizon control is not necessarily a new one, approaching the problem from a stochastic standpoint has only recently aroused interest. In particular, there have been many approaches that seek to determine solutions to receding horizon problems for stochastic systems [65, 66, 67, 68, 69]. These approaches deal with systems under parametric uncertainty that appears as a white noise process. There is little work on stochastic receding horizon control when uncertainty in the system parameters is governed by a random variable, as opposed to a white process.

In this chapter, we present a receding horizon methodology for linear systems with uncertainty that appears as functions of a random variable in the system matrices. This approach guarantees stability of the approximated system when modeled using the polynomial chaos technique that we have described throughout the work.

We begin by presenting the receding horizon policy and discussing the implementation of different types of constraints in terms of our gPC states. The receding horizon strategy is developed for linear discrete time systems with stochastic parametric uncertainty. Next we present a proof for the policy and finally we present several examples that highlight the implementation issues associated with the method. In particular we present three different policies which can be used depending on the types of measurements collected from the actual system or family of systems.

B. Stochastic Receding Horizon Control

Here we present the formulation of the receding horizon problem for linear systems in terms of the states of the gPC system. In particular, we discuss various implementation issues that may arise when dealing with constraints and prove stability of the methodology.

1. Receding Horizon Policy

In this work, we are interested in determining stable solutions to control problems for discrete-time systems of the form

$$x(k+1,\Delta) = A(\Delta)x(k,\Delta) + B(\Delta)u(k) \tag{V.1}$$

where $x(k) \in \mathbb{R}^n$ are the states of the system at time k and $u(k) \in \mathbb{R}^m$ is the control vector at time k. In particular, we assume that the uncertainty of the system Δ is a random variable governed by a given probability distribution. We will assume that the full state information is available for feedback. As we have done throughout the work, we can express this linear equation in terms of gPC states. The dynamics then

become

$$\mathbf{X}(k+1) = \mathbf{A}\mathbf{X}(k) + \mathbf{B}\mathbf{U}(k) \tag{V.2}$$

Consider the following receding horizon policy computed from initial state, x,

$$\mathcal{P}(x): \qquad V_N^* = \min V_N(\{x(k)\}, \{u(k)\}) \tag{V.3}$$

$$\text{subject to}:$$

$$x(k+1,\Delta) = A(\Delta)x(k,\Delta) + B(\Delta)u(k) \quad k = 0,\ldots,N-1 \tag{V.4}$$

$$x(0) = x \tag{V.5}$$

$$u(k) \in \mathbb{U} \quad k = 0,\ldots,N-1 \tag{V.6}$$

$$x(k) \in \mathbb{X} \quad k = 0,\ldots,N \tag{V.7}$$

$$x(N) \in \mathbb{X}_f \subset \mathbb{X} \tag{V.8}$$

The optimization is performed over the horizon length, N. In the above expression $\mathbb{U}$ and $\mathbb{X}$ are feasible sets on $u(k)$ and $x(k)$ with respect to control and state constraints. The set $\mathbb{X}_f$ is a terminal constraint set. A key assumption is that within the terminal set, there exists a feasible stabilizing control strategy. This will be described in more detail later. The control $u(k)$ may be deterministic or stochastic depending on how it is determined. If state feedback is used, the control $u(k)$ will be a stochastic variable. At the beginning of each horizon, we will assume that the state is known exactly or

$$\mathbf{E}[x(0)] = x(0) \tag{V.9}$$

The cost function V_N is given by

$$V_N = \mathbf{E}\left[\sum_{k=0}^{N-1} x^T(k,\Delta)Qx(k,\Delta) + u^T(k)Ru(k)\right] + C_f(x(N)) \tag{V.10}$$

where $C_f(x(N))$ is a terminal constraint. Unlike traditional receding horizon policies where $u(k)$ is determined directly, we will assume a specific structure for $u(k)$. The

control at each time step will be determined by

$$u(k) = \bar{u}(k) + K_k \left(x(k) - \mathbf{E}[x(k)] \right) \tag{V.11}$$

The main reason for this structure is that in general, an open loop control strategy cannot be used to effectively stabilize an entire family of systems. If the system matrix were stable for all values of Δ, then even with $u(k) = 0$ the family of systems would be stable, but might incur high cost. For unstable systems this is not the case and driving an expected value to zero does not ensure stability of the entire family of systems. Therefore, in general we require use of a feedback gain to ensure stability for the entire family of systems.

With the control law in equation (V.11), the system dynamics become

$$x(k+1) = A(\Delta)x(k) + B \left(\bar{u}(k) + K_k \left(x(k) - \mathbf{E}[x(k)] \right) \right) \tag{V.12}$$

When written in terms of the gPC states, these equations become

$$\mathbf{X}(k+1) = \mathbf{A}\mathbf{X}(k) + \mathbf{B} \left(\bar{U}(k) + \left(K_k \otimes I_{p+1} \right) \left(\mathbf{X}(k) - \bar{X}(k) \right) \right) \tag{V.13}$$

where $\bar{U}(k) = \bar{u}(k) \otimes [1 \ \mathbf{0}_{1\times p}]^T$ and $\bar{X} = \mathbf{E}[x(k)] \otimes [1 \ \mathbf{0}_{1\times p}]^T$. For the gPC system, the expected value of $x(k)$ is given by the first term in the gPC expansion, or $x_0(k)$. Therefore, $\bar{X}(k) = x_0(k) \otimes [1 \ \mathbf{0}_{1\times p}]^T$. Because the system is written in terms of gPC states, the cost function becomes

$$\begin{aligned} V_N \ = \ & \sum_{k=0}^{N-1} \Big[\mathbf{X}^T(k) \bar{Q} \mathbf{X}(k) + \left(\bar{U}^T(k) + \left(\mathbf{X}^T(k) - \bar{X}^T(k) \right) \left(K_k^T \otimes I_{p+1} \right) \right) \bar{R} \left(\bar{U}(k) + \right. \\ & \left. \left(K_k \otimes I_{p+1} \right) \left(\mathbf{X}(k) - \bar{X}(k) \right) \right) \Big] + C_f(x(N)) \end{aligned} \tag{V.14}$$

In the above expressions $\bar{Q} = Q \otimes W_0$ and $\bar{R} = R \otimes W_0$. In other stochastic receding horizon implementations, the terminal cost is written as an expectation of a function

of the final state, $x(N)$. The receding horizon policy that we present requires the final state to be in a given terminal region where there exists a feasible, stabilizing control law. Unlike other implementations [70], we implement this constraint specifically in terms of the gPC states as

$$C_f(x(N)) = \mathbf{X}^T(N) P \mathbf{X}(N) \tag{V.15}$$

where $\mathbf{X}(N)$ is a vector of the terminal gPC states and P is a $n(p+1) \times n(p+1)$-dimensional matrix that is determined from the terminal control law. In this manner the expected cost of the stochastic system can be expressed in terms of deterministic gPC states. This will allow us to utilize a standard methodology to prove the stability of the control strategy.

2. State and Control Constraints

In this section we present the state and control constraints for the receding horizon policy and expand on the expressions in equations (V.6) and (V.7).

a. Expectation Constraints

In general for stochastic systems, it is difficult to handle control and state constraints. Typically, constraints are enforced on the expected values of the state and control. We consider constraints of the following form

$$\mathbf{E}\left[x^T(k) H_{i,x} x(k) + G_{i,x} x(k)\right] \leq \alpha_{i,x} \quad i = 1 \ldots N_x \tag{V.16}$$

$$\mathbf{E}\left[u^T(k) H_{i,u} u(k) + G_{i,u} u(k)\right] \leq \alpha_{i,u} \quad i = 1 \ldots N_u \tag{V.17}$$

$$\mathbf{E}\left[\begin{bmatrix} x(k) \\ u(k) \end{bmatrix}^T H_{i,xu} \begin{bmatrix} x(k) \\ u(k) \end{bmatrix} + G_{i,xu} \begin{bmatrix} x(k) \\ u(k) \end{bmatrix}\right] \leq \alpha_{i,xu} \quad i = 1 \ldots N_{xu} \tag{V.18}$$

for $k = 0 \ldots N$. In these expressions, $H_{i,x} \succeq 0$, $H_{i,u} \succeq 0$, and $H_{i,xu} \succeq 0$. These constraints are on the *expected value* of the quadratic functions. Instead of requiring that the constraint be met for all trajectories, they instead imply that the constraints should be satisfied on average. This means that there may be some trajectories that violate the constraints with finite probability. Following a procedure similar to the previous chapters, we express these constraints in terms of the gPC states. The constraints become

$$\mathbf{X}(k)\bar{H}_{i,x}\mathbf{X}(k) + G_{i,x}x_0(k) \leq \alpha_{i,x} \quad i = 1 \ldots N_x \tag{V.19}$$

$$\mathbf{U}(k)\bar{H}_{i,u}\mathbf{U}(k) + G_{i,u}\bar{u}(k) \leq \alpha_{i,x} \quad i = 1 \ldots N_u \tag{V.20}$$

$$\begin{bmatrix} \mathbf{X}(k) \\ \mathbf{U}(k) \end{bmatrix}^T \bar{H}_{i,xu} \begin{bmatrix} \mathbf{X}(k) \\ \mathbf{U}(k) \end{bmatrix} + G_{i,x} \begin{bmatrix} x_0(k) \\ \bar{u}(k) \end{bmatrix} \leq \alpha_{i,xu} \quad i = 1 \ldots N_{xu} \tag{V.21}$$

where $\bar{H}_{i,x} = H_{i,x} \otimes W_0$, $\bar{H}_{i,u} = H_{i,x} \otimes W_0$, and $\bar{H}_{i,xu} = H_{i,xu} \otimes W_0$. Furthermore, the stochastic control vector $\mathbf{U}(k)$ is given by $\mathbf{U}(k) = \bar{U}(k) + (K_k \otimes I_{p+1})\left(\mathbf{X}(k) - \bar{X}(k)\right)$. When $H_{i,u} = 0$, the constraint is linear and constraints on the control only act on the expected open loop control $\bar{u}(k)$.

b. Covariance Constraints

In many practical applications, it is desirable to constrain the variances of the trajectory at each time step. One means of achieving this is to use a constraint of the form

$$\mathrm{Tr}\left(\mathbf{E}\left[(x(k) - \mathbf{E}[x(k)])(x(k) - \mathbf{E}[x(k)])^T\right]\right) \leq \alpha_{\sigma^2} \tag{V.22}$$

In terms of the gPC states, this becomes

$$\mathbf{X}^T(k)Q_{\sigma^2}\mathbf{X}(k) \leq \alpha_{\sigma^2} \tag{V.23}$$

where $Q_{\sigma^2} = I_n \otimes (W_0 - FF^T)$. In terms of the gPC states, this condition is equivalent to constraining the trajectories to an ellipsoid about the expected value ($W_0 - FF^T$ is a singular matrix). This type of constraint highlights the power of the gPC approach in that it allows us to frame variance and covariance constraints in terms of convex constraints of gPC states. If it is desired to constrain only the variance of a particular state, the constraint can be written as

$$\mathbf{E}\left[(x_i(k) - \mathbf{E}[x_i(k)])^2\right] \leq \alpha_{i,\sigma^2} \tag{V.24}$$

where the term i is used to denote the specific state with which the constraint is concerned. This in turn can be written in terms of the gPC states as

$$\mathbf{X}^T(k) Q_{i,\sigma^2} \mathbf{X}(k) \leq \alpha_{i,\sigma^2} \tag{V.25}$$

where $Q_{i,\sigma^2} = \text{diag}\,(\delta_{i,p}) \otimes W_0 - FF^T$. The expression $\delta_{i,p}$ denotes a vector of length p, consisting of all zeros with a one located at the i^{th} element. The diag$(\cdot)$ term denotes a diagonal matrix with the argument as the diagonal. The composition of the Q_{i,σ^2} matrix is such $\mathbf{X}^T(k) Q_{i,\sigma^2} \mathbf{X}(k) = \mathbf{X}_i^T(k)(W_0 - FF^T)\mathbf{X}_i(k)$ where $\mathbf{X}_i(k)$ is a vector of the gPC states corresponding to the i^{th} state.

c. Probability One Constraints

In many applications, it might be desirable to enforce constraints almost everywhere in Δ. For example, if RHC were used to determine optimal paths for a path planning problem, we would desire that the vehicle avoid obstacles with probability one. In general for stochastic systems, this is not possible because the information available is generally only mean and variance of the states and controls. The only means to obtain this information traditionally is to use a Monte-Carlo technique and ensure that the trajectories of each sample satisfy the constraints. This involves generating

a series of trajectories as part of the optimization routine and ensuring that each of these satisfy the state and control constraints. For systems modeled using gPC, if the parameter variation (and hence the associated probability distribution) is bounded, then we have a means of imposing constraints with probability one. First consider constraints imposed on a single state or control variable such as

$$P(x(k,\Delta) \leq \gamma_{x,ub}) = 1 \tag{V.26}$$

$$P(x(k,\Delta) \geq \gamma_{x,lb}) = 1 \tag{V.27}$$

$$P(u(k,\Delta) \leq \gamma_{u,ub}) = 1 \tag{V.28}$$

$$P(u(k,\Delta) \geq \gamma_{u,lb}) = 1 \tag{V.29}$$

In general, there may be a set of measure zero in Δ where these constraints are violated. However, when the states and controls are modeled as continuous polynomials in Δ, the constraints must hold for all Δ. This is summarized by the following proposition.

Proposition V.1 *Let $x(k,\Delta)$ and $u(k,\Delta)$ be modelled as continuous polynomials in Δ. Then the constraints in (V.26)-(V.29) must hold for all Δ.*

Proof To prove this proposition, we will show it is true first for (V.26). We know that $P(x(k,\Delta) \leq \gamma) = 1 \Rightarrow P(x(k,\Delta) > \gamma) = 0$. Let $\bar{\Delta}$ exist such that $P(\bar{\Delta}) = 0$ and $x(k,\bar{\Delta}) = \sum_{i=0}^{p} x_i(k)\phi_i(\bar{\Delta}) > \gamma$. We know

$$x(k,\bar{\Delta}) = \sum_{i=0}^{p} x_i(k)\phi_i(\bar{\Delta}) > \gamma \Rightarrow x(k,\bar{\Delta}) = \gamma + \epsilon$$

where $\epsilon > 0$. By continuity of the polynomials, ϕ_i, the state, $x(k,\Delta)$, is continuous with respect to Δ. Therefore, $\exists$ a δ such that $|\bar{\Delta} - \tilde{\Delta}| < \delta \Rightarrow |x(k,\bar{\Delta}) - x(k,\tilde{\Delta})| < \epsilon$. In other words, $\forall\ \tilde{\Delta} \in \mathcal{B}(\bar{\Delta},\delta)$, $x(k,\tilde{\Delta}) > \gamma$. Here, $\mathcal{B}(\bar{\Delta},\delta)$ is an open ball of radius δ

centered at $\bar{\Delta}$. Therefore,

$$\begin{aligned} P(x(k,\Delta) > \gamma) &= P(\tilde{\Delta} \in \mathcal{B}(\bar{\Delta},\delta)) = \int_{\Delta} \mathbf{1}_{\tilde{\Delta}\in\mathcal{B}(\bar{\Delta},\delta)} f(\Delta)\, d\Delta \\ &= \int_{\Delta\in\mathcal{B}(\bar{\Delta},\delta)} f(\Delta)\, d\Delta > 0 \end{aligned}$$

Because the state is a continuous polynomial, $\mathcal{B}(\bar{\Delta},\delta)$ has a non-empty interior, thus the above inequality is strict. This means

$$0 < P(x(k,\Delta) > \gamma) = 1 - P(x(k,\Delta) \leq \gamma) \Rightarrow P(x(k,\Delta) \leq \gamma) < 1$$

Thus by contradiction, the proposition is proven. The other three constraint can be proven in the same manner.■

The benefit of the gPC framework is that it gives us a means of writing out the state and control trajectories as known functions of the random variable, Δ. In other words, we can write $x(k) = \sum_{i=0}^{p} x_i(k)\phi_i(\Delta)$ and $u(k) = \bar{u}(k) + K_k\left(\sum_{i=0}^{p} x_i(k)\phi_i(\Delta) - x_0(k)\right)$. As a result of the previous proposition, the constraints in equations (V.26)-(V.29) can be written as

$$x(k,\Delta) = \sum_{i=0}^{p} x_i(k)\phi_i(\Delta) \leq \gamma_{x,ub} \tag{V.30}$$

$$x(k,\Delta) = \sum_{i=0}^{p} x_i(k)\phi_i(\Delta) \geq \gamma_{x,lb} \tag{V.31}$$

$$u(k,\Delta) = \sum_{i=0}^{p} u_i(k)\phi_i(\Delta) \leq \gamma_{u,ub} \tag{V.32}$$

$$u_k(\Delta) = \sum_{i=0}^{p} u_i(k)\phi_i(\Delta) \geq \gamma_{u,lb} \tag{V.33}$$

Because these constraints must hold for all $\Delta \in \Omega$, without loss of generality, we can replace them with maximum and minimum values of $x(k)$ and $u(k)$ for upper

bounds and lower bounds respectively. The constraints can then be written as

$$\max_{\Delta\epsilon\Omega} x(k,\Delta) = \max_{\Delta\epsilon\Omega} \sum_{i=0}^{p} x_i(k,\Delta) \quad \leq \quad \gamma_{x,ub} \tag{V.34}$$

$$\min_{\Delta\epsilon\Omega} x(k,\Delta) = \min_{\Delta\epsilon\Omega} \sum_{i=0}^{p} x_i(k,\Delta) \quad \geq \quad \gamma_{x,lb} \tag{V.35}$$

$$\max_{\Delta\epsilon\Omega} u(k,\Delta) = \max_{\Delta\epsilon\Omega} \sum_{i=0}^{p} u_i(k,\Delta) \quad \leq \quad \gamma_{u,ub} \tag{V.36}$$

$$\min_{\Delta\epsilon\Omega} u(k,\Delta) = \min_{\Delta\epsilon\Omega} \sum_{i=0}^{p} u_i(k,\Delta) \quad \geq \quad \gamma_{u,lb} \tag{V.37}$$

The functions, $\phi_i(\Delta)$ are known, bounded functions of Δ (boundedness follows from Δ being constrained to a finite interval). In general we will assume that the polynomials are constrained such that $\phi_i(\Delta) \epsilon [-1, 1]$. This is a valid assumption as it is always possible to normalize ϕ_i so that this is the case. As an example, figure 23 shows the first six Legendre polynomials on the interval $\Delta \epsilon [-1, 1]$. It is clear that these

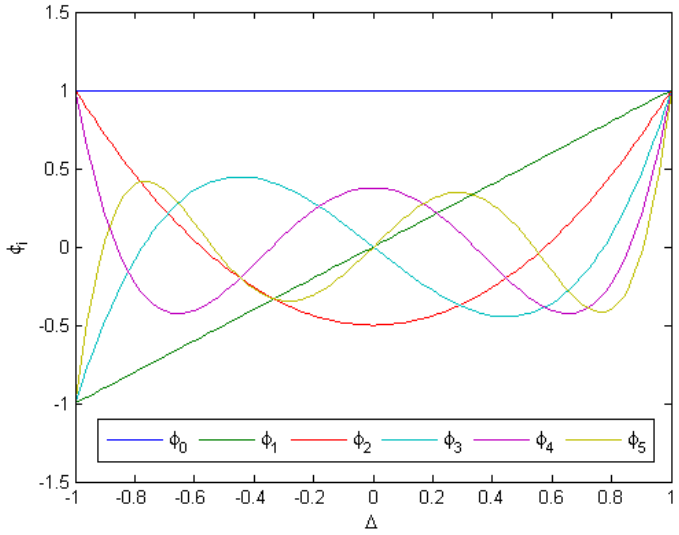

Fig. 23. Legendre polynomials as a function of Δ on the interval $[-1, 1]$

polynomials are bounded on the interval and that they are also bounded by -1 from below and $+1$ from above. Therefore the problems posed in equations (V.34-V.37)

have solutions. When there are a small number of ϕ_i terms and only one random variable, Δ, these can be solved analytically. However, this would require finding the zeros of the derivative of the function $x(k, \Delta)$ (a polynomial in Δ) which is in general difficult problem to solve. We therefore present several alternative methods to approximate the solution to equations (V.34-V.37).

Method 1: One approach is to use bounds of the form

$$\begin{aligned}
\mathbf{X}_0(k) + \sum_{i=1}^{p} |\mathbf{X}_i(k)| &\leq \gamma_{x,ub} \\
\mathbf{X}_0(k) - \sum_{i=1}^{p} |\mathbf{X}_i(k)| &\leq \gamma_{x,lb} \\
\mathbf{U}_0(k) + \sum_{i=1}^{p} |\mathbf{U}_i(k)| &\leq \gamma_{u,ub} \\
\mathbf{U}_0(k) - \sum_{i=1}^{p} |\mathbf{U}_i(k)| &\leq \gamma_{u,lb}
\end{aligned}$$

This bound will always be conservative and the presence of the $|\cdot|$ operator makes this nonlinear.

Method 2: A second method of approximating the constraints is to only enforce them at specific values of Δ. For linear systems, this amounts to enforcing the constraints for values of Δ that correspond to the minimum and maximum values of the parameter. For example if the system matrix is such that

$$A = \begin{bmatrix} -0.9 + \Delta & -.5 \\ 1 & 0 \end{bmatrix}$$

For this system, we have plotted trajectories of the fist state corresponding to various values of Δ in figure 24. The extremal uncertainty values in the A matrix occur for $\Delta = 1$ and $\Delta = -1$. The trajectories corresponding to these values of Δ are displayed as thick blue lines and are labelled in the figure. We can see that the trajectories for these values of Δ make up a good approximate bound throughout the simulation. However,

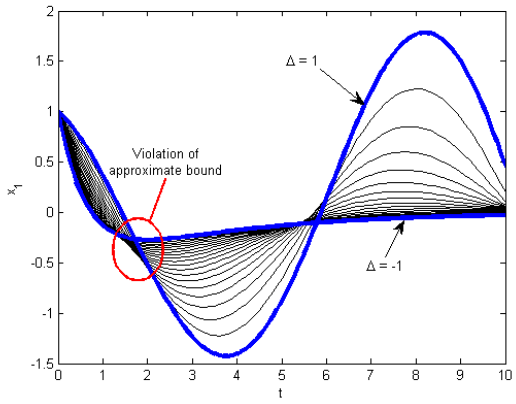

Fig. 24. Trajectories generated for various values of Δ and their bounds approximated at extreme values of Δ

there are points where this approximate bound is violated. This is demonstrated by the circled region of the figure. This method is more computationally efficient than the previous method as it results in linear constraints, but this comes at the cost of making errors in the approximation. Since this approximation makes it possible for the bounds to be violated by some systems, if this method is to be used, it is necessary to be overly conservative in determining constraints.

Method 3: A final method is to enforce the constraints on a grid of Δ values. Define a grid of Δ values

$$\mathcal{D} = \{\Delta_1, \Delta_2, \ldots, \Delta_{n_d}\} \tag{V.38}$$

For every constraint in equations (V.34-V.37), we set up n_d new constraints, each evaluated at Δ_i, for $i = 1, \ldots, n_d$. In other words, we write the constraints as

$$\begin{aligned} x(k, \Delta_i) &= \sum_{j=0}^{p} \mathbf{X}_j(k)\phi(\Delta_i) \quad \leq \quad \gamma_{x,ub} \\ x(k, \Delta_i) &= \sum_{j=0}^{p} \mathbf{X}_j(k)\phi(\Delta_i) \quad \geq \quad \gamma_{x,lb} \\ u(k, \Delta_i) &= \sum_{j=0}^{p} \mathbf{U}_j(k)\phi(\Delta_i) \quad \leq \quad \gamma_{u,ub} \\ u(k, \Delta_i) &= \sum_{j=0}^{p} \mathbf{U}_j(k)\phi(\Delta_i) \quad \geq \quad \gamma_{u,lb} \end{aligned}$$

for $i = 1, \ldots, n_d$. This has the advantages of being less conservative than method 1 as well as being more accurate than method 2. The disadvantage of this method is that it adds a large number of constraints to the system. While enforcing the constraints in this manner requires a form of "sampling", the usage of gPC methods still retains an advantage over Monte-Carlo methods because enforcing these constraints does not require generation of a large family of trajectories. Instead the gPC trajectories can be used directly to generate the "sampled" data.

Remark V.2 *Expectation and variance constraints result in first and second order constraints on the gPC states. As implemented in this section, probability constraints retain a "sampling" implementation that is similar to the traditional robust control approach. This is presented for completeness and to demonstrate that the gPC approach retains the ability to enforce more traditional types of constraints while having the advantage of simple enforcement of expectation and variance constraints.*

3. Stability of the RHC Policy

At this point, we are ready to show stability for the receding horizon policy $\mathcal{P}(x)$ when it is applied to the gPC system. Before proceeding a few assumptions must be

made about the cost function and system constraints.

Assumption 1 *Let the terminal cost matrix satisfy $P \succ 0$ and let there exist a control $u^{\infty}(k) = K_{\infty}x(k)$ such that for all $x(k) \in \mathbb{R}^n$*

$$\mathbf{X}^T(k)P\mathbf{X}(k) \geq \mathbf{E}\left[x^T(k)Qx(k) + \left(u^{\infty}(k)\right)^T Ru^{\infty}(k)\right] + \mathbf{X}^T(k+1)P\mathbf{X}(k+1) \quad \text{(V.39)}$$

where $x(k+1) = A(\Delta)x(k) + B(\Delta)u^{\infty}(k)$ which when written in terms of the gPC dynamics (see eqn. (V.2)) gives $\mathbf{X}(k+1) = \mathbf{A}\mathbf{X}(k) + \mathbf{B}\left(K_{\infty} \otimes I_{p+1}\right)\mathbf{X}(k)$.

This assumption guarantees that the system is stabilizable with respect to a constant gain control. In addition, it guarantees that without control constraints, the system under the control policy u^{∞} is globally asymptotically stable. We next make an assumption about the terminal constraint ($x(N) \in \mathbb{X}_f$). In particular, we need to ensure that the control strategy satisfying assumption 1 is feasible when the terminal constraint is met.

Assumption 2 *The terminal constraint is given by*

$$\mathbf{X}^T(N)P\mathbf{X}(N) \leq \beta \quad \text{(V.40)}$$

and the parameter β is such that for any family of trajectories at time N, $x(N, \Delta)$, (corresponding to $\mathbf{X}(N)$) satisfying equation (V.40), the state trajectory $x(k)$ (and corresponding $\mathbf{X}(k)$) under the terminal control $u^{\infty}(k)$ in Assumption 1 will be feasible for the state and control constraints for all $k \geq N$.

The formulation of the terminal cost as $\mathbf{X}^T(k)P\mathbf{X}(k)$ is more general than a cost of

the form $\mathbf{E}[x^T(k)\hat{P}x(k)]$ with $\hat{P} = \hat{P}^T \succ 0$. An expected cost formulation will result in a structure imposed on P of the form $P = \hat{P} \otimes W_0$. This constraint on the structure of the terminal cost matrix is restrictive and as a result of this imposed structure makes the determination of a terminal controller more difficult.

These two assumptions guarantee that once the system trajectories enter a given ellipsoid, there will exist a feasible linear state feedback controller to bring a family of trajectories (corresponding to $\mathbf{X}(N)$) to the origin. In essence this constraint defines a region in which all possible trajectories must be contained.

Remark V.3 *If the terminal constraint is satisfied then we are guaranteed that at time N the gPC states lie in an ellipsoid. This translates to a constraining the final value of the systems for all Δ. This is possible because the parameter uncertainty is dependent on a random variable not on a white noise process. When a system has uncertainty that is dependent on a white noise process (particularly if the parameter variation has the ability to be unbounded), this might induce a jump outside of the constraint space. Because the uncertain parameter is governed by a random variable, it is in effect constant for each individual system, meaning that this type of behavior is not possible.*

These assumptions will enable us to prove a stability for a stochastic receding horizon policy in a similar manner to the traditional methodology [71]. The result is summarized in the following theorem.

Theorem V.4 *Consider the receding horizon policy $\mathcal{P}(x)$ where the dynamics are governed by that of the gPC system in equation(V.2). If Assumptions 1 and 2 hold*

and a feasible solution exists for x_0, then for the stochastic gPC dynamics,

1. *The feasible set is positively invariant.*
2. *The resulting control policy is asymptotically stable.*

Proof The stability proof will be performed for the projected (gPC) system.

1. To prove the invariance of the feasible set, we define the following sequences. Let the optimal control sequence and state sequences be defined as $\mathbf{U}^* = \{\mathbf{U}^*(0), \mathbf{U}^*(1), \ldots, \mathbf{U}^*(N-1)\}$ and $\mathbf{X}^* = \{\mathbf{X}^*(0), \mathbf{X}^*(1), \ldots, \mathbf{X}^*(N)\}$. By assumption, these sequences are feasible ($\mathbf{U}^* \in \mathbb{U}$ and $\mathbf{X}^* \in \mathbb{X}$). To show invariance of the feasible set, consider the feasibility of the system after one iteration of the map. The projected state after one iteration is $\mathbf{X}(1) = \mathbf{A}\mathbf{X}(0) + \mathbf{B}\mathbf{U}(0)$. Now define sets $\tilde{\mathbf{U}} = \{\mathbf{U}^*(1), \ldots, \mathbf{U}^*(N-1), \mathbf{U}^\infty(N)\}$ and $\tilde{\mathbf{X}} = \{\mathbf{X}^*(1), \ldots, \mathbf{X}^*(N), \mathbf{X}^\infty(N+1)\}$ where $\mathbf{U}^\infty(N) = (K_\infty \otimes I_{p+1})\mathbf{X}_N^*$ (the terminal control policy) and $\mathbf{X}^\infty(N+1) = \mathbf{A}\mathbf{X}^*(N) + \mathbf{B}\mathbf{U}^\infty(N)$. Though these trajectories may not be optimal solutions of V_N, the iterated sets are feasible by assumptions 1 and 2. Therefore positive invariance of the feasible set is proven.
2. Next, we prove asymptotic stability of the control policy. We will use the cost function $V_N^*(x)$ as a Lyapunov function. Consider a trajectory starting at x, satisfying the assumptions of the theorem. The trajectory at the next time step is given by $x^+ = Ax + Bu$ where u is the first control input in the sequence obtained from the receding horizon policy. Define the state and control sequences

$$\{\tilde{x}\} = \{\sum_{i=0}^{p} \mathbf{X}_i^*(1)\phi_i, \ldots, \sum_{i=0}^{p} \mathbf{X}_i^\infty(N+1)\phi_i\}$$

$$\{\tilde{u}\} = \{\sum_{i=0}^{p} \mathbf{U}_i^*(1)\phi_i, \ldots, \sum_{i=0}^{p} \mathbf{U}_i^\infty(N)\phi_i\}$$

$$\{x^*\} = \{\sum_{i=0}^{p} \mathbf{X}_i^*(0)\phi_i, \ldots, \sum_{i=0}^{p} \mathbf{X}_i^*(N)\phi_i\}$$

$$\{u^*\} = \{\sum_{i=0}^{p} \mathbf{U}_i^*(0)\phi_i, \ldots, \sum_{i=0}^{p} \mathbf{U}_i^*(N-1)\phi_i\}$$

Examining the difference between $V_N^*(x^+)$ and $V_N^*(x)$ gives

$$\begin{aligned} V_N^*(x^+) - V_N^*(x) &\leq V_N(\{\tilde{x}\},\{\tilde{u}\}) - V_N(\{x^*\},\{u^*\}) \\ &= V_N(\tilde{\mathbf{X}},\tilde{\mathbf{U}}) - V_N(\mathbf{X}^*,\mathbf{U}^*) \\ &= -\mathbf{X}^T(0)\bar{Q}\mathbf{X}(0) - \mathbf{U}(0)\bar{R}\mathbf{U}(0) + \mathbf{X}^T(N)\bar{Q}\mathbf{X}(N) \\ &\quad +\mathbf{U}^T(N)\bar{R}\mathbf{U}(N) - \mathbf{X}^T(N)P\mathbf{X}(N) + \mathbf{X}^T(N+1)P\mathbf{X}(N+1) \end{aligned}$$

The inequality is a result of $V_N^*(x^+)$ being optimal and $V_N(\{\tilde{x}\},\{\tilde{u}\})$ being simply a feasible solution. The definition of $\tilde{\mathbf{X}}$ and $\tilde{\mathbf{U}}$ result in cancellations for all terms except those corresponding to time $k = 0$ and $k = N$. We now utilize Assumption 1 to obtain

$$\begin{aligned} V_N^*(x^+) - V_N^*(x) &\leq -\mathbf{X}^T(0)\bar{Q}\mathbf{X}(0) - \mathbf{U}^T(0)\bar{R}\mathbf{U}(0) \leq -\mathbf{X}^T(0)\bar{Q}\mathbf{X}(0) \\ &\leq -\lambda_{min}(\bar{Q})\|\mathbf{X}(0)\|^2 \end{aligned}$$

The matrix $\bar{Q}$ is positive definite, thus the right hand side is strictly less than zero for all $\mathbf{X}(0) \neq 0$. The functions $V_N(x)$ and $V_N(x^+)$ can be rewritten in terms of gPC states to give the resulting asymptotic stability guarantee for the coefficients.

■

The theorem shows that the states of the gPC system go to zero asymptotically when a receding horizon policy is employed.

4. RHC Policy Description

In this section we will describe three receding horizon policies that can be shown to be stable via the preceding arguments. The two policies will depend on the type of constraints employed. If linear expectation constraints are employed then we will use a policy that utilizes open loop generation of the gPC states and the expected value of the state vector. When expectation constraints are not employed, then we can implement the receding horizon policy in a more traditional fashion. This distinction is made as a result of feasibility issues with various types of constraints. Consider the sample trajectories shown in figure 25. At time 0, the initial condition is known

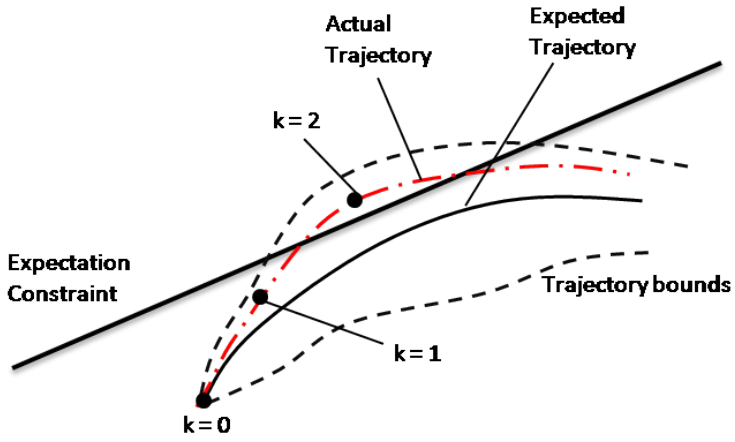

Fig. 25. Sample trajectory paths to demonstrate possible constraint violations

exactly. Therefore, the initial condition is in fact the expected value of the state at time 0. As time progresses, the mean and trajectory bounds are indicated on the figure. At time $k = 2$, though the expectation constraint is satisfied there are some trajectories that violate the constraint. In the figure, we use the red curve (denoted "Actual Trajectory" in the figure) to denote a system trajectory for a specific value of Δ. Assume that the actual system follows this red curve. If at time 2, a measurement were taken and this was set to be the new expected value, then this state would be

in violation of the constraint and thus the feasibility conditions in the proof would be violated. For this reason the gPC states must be generated by open loop simulation of the gPC system to obtain accurate estimates of the expected value for the entire family of systems.

When the constraints are enforced on the actual state values or in the form of variance constraints, then it is possible to use a more traditional receding horizon policy. In this implementation, whenever the receding horizon controls are recalculated, the gPC states will be reset and the current state will be deemed the expected value at time 0. This reflects a more realistic implementation. The main issue of importance for this implementation is to ensure that when the new state is taken to be the initial variable in the RHC policy, there still exists a feasible control law. We will now briefly describe the two policies that will be employed.

a. Policy A

The first receding horizon strategy we discuss differs from traditional RHC policies in that utilizes open loop terms as well as a closed loop term. The actual control law is given by

$$u(k) = \bar{u}(k) + K_k \left(x(k) - \mathbf{E}[x(k)] \right)$$

In this control law, $\bar{u}(k)$ and $\mathbf{E}[x(k)]$ must be either measured or computed. If the control strategy is implemented simultaneously on a family of systems, then it would be possible to estimate the distribution and thus take measurements of the gPC states. If the control strategy is implemented on a single system, this is not possible and we must in turn rely on open-loop estimation of the statistics to obtain the control law. This is accomplished by an open-loop simulation of the gPC states

that begins at the system initial condition at time 0. At each time step, the values of $\bar{u}(k)$, $\mathbf{E}[x(k)]$, and K_k are taken from the simulation of the gPC system. The specific value of $x(k)$ is taken from a measurement of the states of the actual system. The terms coming from the RHC framework are in some sense all open loop as they depend upon iteration of the gPC dynamics. The gPC dynamics by their formulation include all of the modeled uncertainty, so they are in this sense robust. The diagram in figure 26 provides insight into this control strategy. The term $x(0)$ represents the

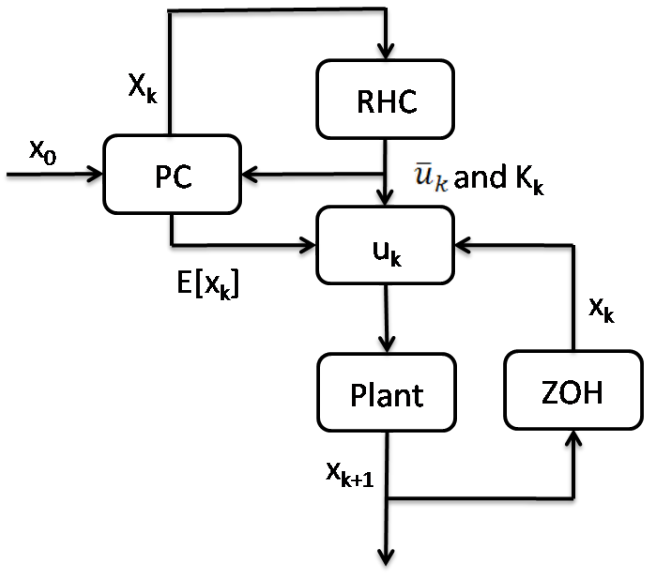

Fig. 26. Receding horizon strategy with open loop statistics prediction

initial condition when the control strategy is applied. This is used to initialize the generation of the statistics and gains for the control strategy. At each step using the gPC data new values of $\bar{u}(k)$ and K_k are generated from the RHC policy and these coupled with $\mathbf{E}[x(k)]$ are used to compute the control for the plant. The only feedback comes in the form of $x(k)$. This strategy avoids the feasibility problem that results from the application of expectation constraints but requires many of the quantities to be generated in an open-loop manner.

b. Policy B

Here we discuss a receding horizon policy that is more traditional in the sense that it does not rely on open-loop generation of statistics. In Policy A, we assumed that the measurements were available for all Δ simultaneously. This could be the result of state measurements for the entire family of systems or the result of open-loop simulation of the entire family. In Policy B we will not take measurements for a family of systems. Instead, when the receding horizon law is recomputed, we will take a measurement for a *single* system and compute a new control assuming all systems start from this newly measured value. The important consideration for this policy is the impact of the reset of the state values on the feasibility of the next iteration. Namely, we need to ensure that when the expected value is reset to the current value, the control strategy for the next RHC iteration is indeed feasible. Figures 27(a) and 27(b) demonstrate the response of the system under the receding horizon policy at two separate time instances. Figure 27(a) demonstrates a sample response at time 0. At time 2, the optimization process is restarted from the new point (as shown in figure 27(b)). When this occurs, the current state is set as the expected value as it is a measured quantity. We therefore start the new policy with the family of systems originating at this point. For this policy to meet the conditions of the previous proof, we must show that when the reset is performed there still exists a feasible solution.

Because the uncertainty in the family of systems is governed by a random variable, it is a constant with respect to time. This is crucial to the feasibility of policy B. To verify the feasibility of the policy we must keep in mind that the uncertainty in the actual system corresponds to a single value of Δ for all time. As a result the controls determined at the start of the algorithm will produce a feasible solution throughout

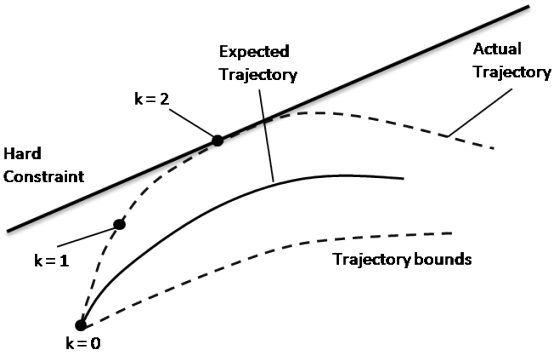

(a) System trajectories under RHC policy at time 0

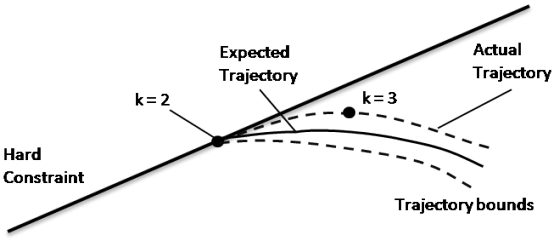

(b) System trajectories under RHC policy after update at time 2

Fig. 27. First two steps of receding horizon feedback policy

the horizon. Denote the gPC states at time k corresponding to the policy computed at time 0 by $\mathbf{X}^0(k)$ and the controls as $\mathbf{U}^0(k)$. Now, these states and controls give the states and controls at time k as functions of Δ, or

$$\begin{aligned} \mathbf{X}^0(k) &\Rightarrow x^0(k,\Delta) \\ \mathbf{U}^0(k) &\Rightarrow u^0(k,\Delta) \end{aligned}$$

For each value of Δ, there is therefore a feasible solution for the state and control. The difficulty occurs with the recomputation of the new control law at a time k. Let $\hat{\Delta}$ be the value of Δ corresponding to the actual system. If the RHC policy is recomputed at time k, then $x^k(k) = x^0(k,\hat{\Delta})$. The new initial state $x^k(k)$ is not dependent on

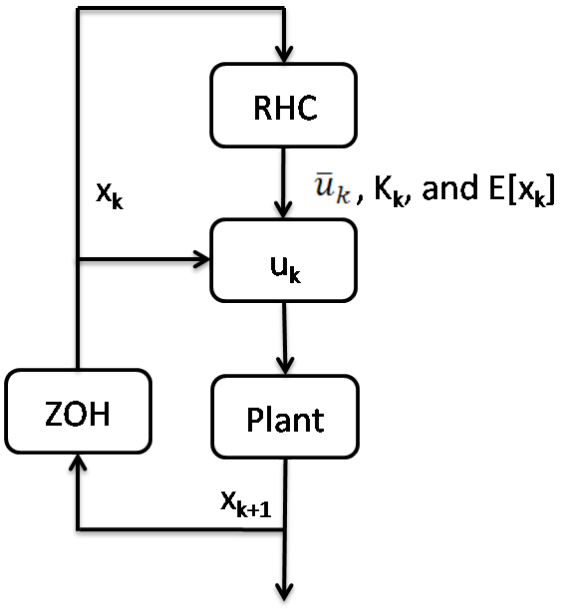

Fig. 28. Block diagram of "closed loop" receding horizon policy

Δ. For $\Delta = \hat{\Delta}$ (the actual system) we can ensure feasibility for this specific value of Δ by setting $u^k(k+j, \hat{\Delta}) = u^0(k+j, \hat{\Delta})\ \forall j \geq 0$ and computing appropriate $\bar{u}^k(k+j)$ and K^k_{k+j} values. However, while this ensures feasibility for the actual system, it does not ensure feasibility for all values of Δ with an initial condition of $x^0(k, \hat{\Delta})$. It is therefore not possible to guarantee feasibility of the policy in general. Generally, this situation can occur when state and control bounds are very strict but if the problem is well posed this does not occur.

The feedback control policy described in this section can be represented by the diagram in figure 28. As the figure demonstrates, this policy is more traditional than policy A. The feed-forward or open-loop terms $\bar{u}(k)$ and $\mathbf{E}[x(k)]$ as well as the gain K_k are provided from the optimally predicted policy.

c. Policy C

To alleviate the possibility of an infeasible solution that can occur using Policy B, we propose a hybrid policy. This policy is the same as Policy B but with one exception. When the RHC optimal solution is recomputed at a time k, if a feasible solution exists Policy B is utilized. If a feasible solution does not exist, the control strategy from the previous RHC computation is utilized. Because we assume the existence of an initial feasible solution, this strategy is always feasible. In the worst-case, this means that the initial RHC strategy will be employed and the control will use open-loop generation of $\bar{u}(k)$, K_k, and $\mathbf{E}[x(k)]$ until the terminal region is reached (for at most N steps). This strategy, however guarantees stability. This hybrid approach also allows for Expectation constraints to be employed.

C. Examples

In this section, we will consider two different examples that will highlight the RHC policies presented in the previous section.

1. Example 1

For the first example, consider the following linear system (which is similar to that considered in [70]).

$$x(k+1) = (A + G(\Delta))x(k) + Bu(k) \tag{V.41}$$

where

$$A = \begin{bmatrix} 1.02 & -0.1 \\ .1 & .98 \end{bmatrix} \quad B = \begin{bmatrix} 0.1 \\ 0.05 \end{bmatrix}$$
$$G = \begin{bmatrix} 0.04 & 0 \\ 0 & 0.04 \end{bmatrix} \Delta$$

The system in consideration is open-loop unstable and the uncertainty appears linearly in the G matrix. In this example, the uncertainty Δ will assumed to be in the range $[-1, 1]$ and the actual value of Δ is governed by a uniform distribution. As a result, Legendre polynomials will be utilized. Polynomials up to 4^{th} order will be used to formulate the control (this corresponds to $p = 4$). For this example, we will place an expectation constraint on $x(k)$ of the form

$$\mathbf{E}\left[\begin{bmatrix} 1 & 0 \end{bmatrix} x(k)\right] \geq -1$$

In terms of the gPC states, this corresponds to

$$\begin{bmatrix} 1 & \mathbf{0}_{1\times 2p+1} \end{bmatrix} \mathbf{X}(k) \geq -1$$

Because of the expectation constraint, we will be required to utilize the open-loop RHC policy to solve this problem. This means that the statistics of the problem will be predicted in open-loop as described by Policy A.

To implement the receding horizon policy, we will need to design a terminal control that will ensure the stability of the policy inside of a terminal region. This can be accomplished using the techniques described in Chapter III of this work, so it will not be discussed here. The cost matrices used to determine the optimal control

policy are

$$Q = \begin{bmatrix} 2 & 0 \\ 0 & 5 \end{bmatrix} \qquad R = 1$$

With this information, we can now design a receding horizon policy to bring the system to the origin while keeping the constraints satisfied. To simulate the system, the RHC policy is determined at each step using open-loop simulation of the gPC dynamics. For each system corresponding to each value of Δ, the resulting control law is used to control the system. Figure 29 shows the phase plane response of the systems corresponding to each value of Δ. The figure demonstrates a few

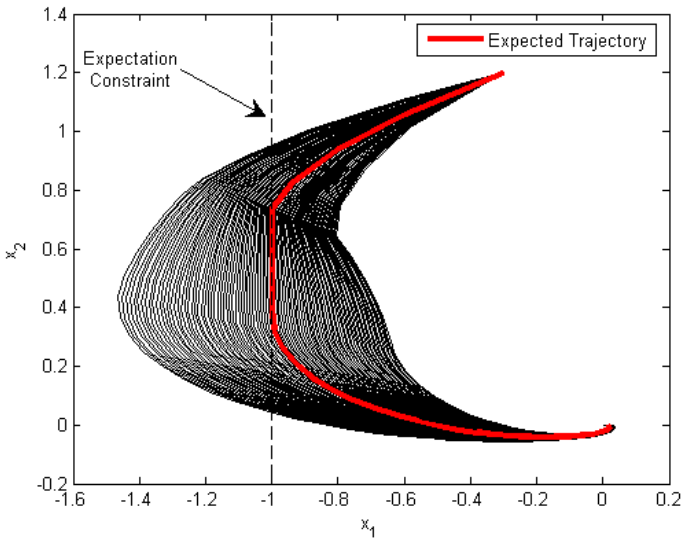

Fig. 29. Trajectories for open loop RHC policy for various values of $\Delta \in [-1, 1]$

important concepts that are associated with stochastic receding horizon control. It is important to note that not all of the *individual* trajectories satisfy the constraint. This is because the constraint has been enforced as an expected (or average) value. Therefore, the constraint is not necessarily satisfied for any single system, but is only satisfied on average. For this reason, if we were using the Policy B, the problem would

quickly become infeasible if the actual trajectory corresponded to one that violated the constraint. Figure 30 shows the mean predicted by gPC compared to the actual

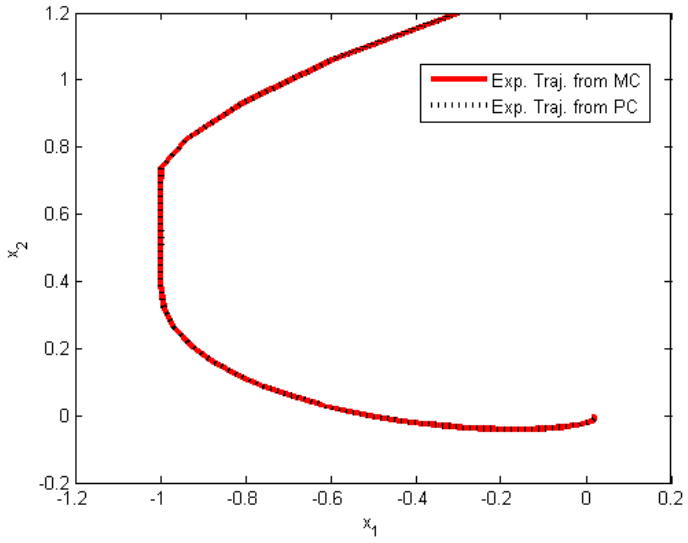

Fig. 30. Expected trajectories for open loop RHC policy obtained by Monte Carlo simulation and predicted by gPC

mean obtained from Monte-Carlo simulation of the closed loop system. The figure demonstrates that the mean tracks very well and is predicted very accurately. This gives confidence that the policy will work very well, even though its statistics have been generated in an open loop fashion.

To highlight the difference between the two policies presented, this example is again solved but with probability one constraints using Policy B. For this example instead of the expectation constraint considered above, we will use the constraint

$$P\left(\begin{bmatrix} 1 & 0 \end{bmatrix} x(k) \geq -1\right) = 1$$

Because this translates to a constraint on the gPC expansion of $x(k)$, it must hold for all values of Δ. For this example, several approaches to enforcing this can be taken. Because the problem is small and there are only a small number of states,

we choose to test the maximum value of $x(k)$ when it is evaluated on a grid of Δ values. The phase plane response of the system is shown in figure 31. Unlike the

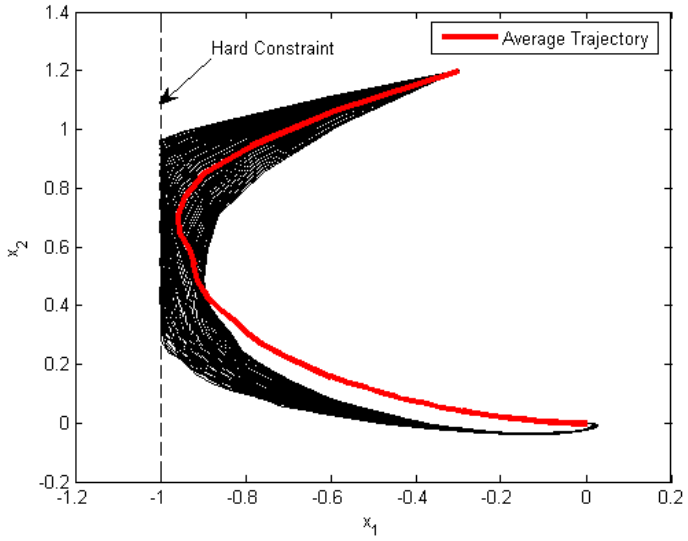

Fig. 31. Trajectories for closed loop RHC policy for various values of $\Delta \in [-1, 1]$

responses of figure 29, there are no trajectories that violate the constraint. This is to be expected as the constraint has been changed from an expectation constraint to a probability one constraint. Because of the enforcement of this constraint, the cost is much higher for systems corresponding to values of Δ that violate the constraint in figure 29. Furthermore, these systems take much longer to reach the origin. The other notable difference in this figure involves the average trajectory. It should be noted that no systems actually follow this trajectory. This is in large part because the systems that are less likely to violate the constraint converge to the origin much faster than those for which the constraint is active. The result is a large variation in the system response at each time step.

This variation helps illustrate the conceptual difference between the two approaches. Policy A treats the variation of systems in the same instant in time. It

is concerned with the *simultaneous* performance of a family of systems. If measurements for all systems are available, then these measurements can be used to calculate the pdf of the family of systems meaning that open loop generation of statistics will not be required. Policies B and C are concerned with the performance of a *single* system. For this implementation, the uncertainty is merely used to help predict and optimize the actual system trajectory given information about its current state. For most physical systems, this will be the policy of choice as multiple systems will not be asked to perform the same tasks in the same manner all at the same time. As the example demonstrates, the gPC approximation has enabled the design of a control strategy that drives an unstable system to the origin even in the presence of large (predicted) variations in plant dynamics.

2. Example 2

The above example illustrates the difference between the two types of control strategies discussed in this work. Now, as a more real-world example, consider an autopilot design for an F-16 aircraft. The design will be performed for the linearized short period dynamics of the aircraft with first-order actuator dynamics included.

$$\dot{x} = Ax + Bu \tag{V.42}$$

The system states are given by $x = [\alpha, q, \delta_e]$ where α is the angle of attack, q is the pitch rate, and δ_e is the angle of the pitch actuator (in degrees). The control input

into the system is an actuator command, $u = \delta_{ec}$. The system matrices are given by

$$A = \begin{bmatrix} -.6398 & .9378 & -0.0014 \\ (-1.5679) & (-0.8791) & (-0.1137) \\ 0 & 0 & -20.2 \end{bmatrix}$$

$$B = \begin{bmatrix} 0 & 0 & -20.2 \end{bmatrix}^T$$

The terms in parenthesis, $(\cdot)$, refer to the terms for which there is uncertainty. For this case, we assume a 20% linear uncertainty in these terms. The uncertainty is assumed to be constant (not time varying) and the value of the perturbation will be governed by a uniform distribution. For this example, we assume that all of the system states are available and measured accurately. Because the receding horizon formulation is done in discrete time, we will need to discretize the system to obtain a difference equation. This is accomplished by applying a zero order hold to the input and output of the system at a sampling time of T_s. The system then becomes

$$x(k+1) = A_d x(k) + B_d u(k) \tag{V.43}$$

where

$$A_d = e^{AT_s}$$

$$B_d = \int_{\tau=0}^{T_s} e^{A(T_s-\tau)} B$$

For this problem, we assume that the input and output zero order holds are sampled at a rate of 50 Hz. Using this sampling rate, the A_d and B_d matrices for the short

period dynamics of the F-16 become

$$A_d = \begin{bmatrix} 0.9870 & 0.0185 & 0 \\ -0.0309 & 0.9823 & -0.0019 \\ 0 & 0 & 0.6676 \end{bmatrix}$$

$$B_d = \begin{bmatrix} 0 \\ -0.0004 \\ 0.3324 \end{bmatrix}$$

Because the model originates as a continuous time model, we must also translate the uncertainty from the continuous time model to variation in the discrete time model. While it is possible to determine the mapping of the uncertainty through the exponential mapping, we will instead employ an approximation. For small sampling times, we can write

$$x(k+1) \approx x(k) + A(\Delta)T_s x(k)$$

Since the uncertainty varies linearly, we can write $A(\Delta) = A + \Delta\tilde{A}$. This means $x(k+1) \approx (I + (A + \Delta\tilde{A})T_s)x(k)$ and therefore the uncertainty appears linearly in the discrete system but is additionally scaled by T_s.

For this example, the open loop policy will not be employed, only the closed loop policy. The Q and R matrices are given by

$$Q = \begin{bmatrix} 100 & 0 & 0 \\ 0 & 1 & 0 \\ 0 & 0 & 0.01 \end{bmatrix}$$

$$R = 0.01$$

These same Q and R matrices can be used in the manner described in Chapter IV

to design the terminal control strategy for the aircraft. A terminal constraint is also placed on the aircraft to ensure that it always travels to a point where there is a stabilizing controller. This is designed to be an ellipsoid where all trajectories within meet constraints when the terminal control strategy is applied. It is important to ensure that for any control strategy, the response of the actuators is smooth and there are no large oscillations in the actuator response. For this reason, a control designer must take special care to ensure that the design not only meets traditional performance specifications, but that it meets pilot approval. For an autopilot, this is not as important, but it is important to ensure that the response is smooth (especially the actuator response) and that the usage of the actuators is fairly small. In general for autopilot designs, the position or rate limits imposed on actuators are accounted for by ensuring gains are small. However if there is a large amount of error, this can still lead to rate limiting. As such, we can use the receding horizon strategy to ensure stability while ensuring that control position limits are not exceeded. To ensure this, we will place the control constraint

$$u^2(k) \leq 1.5^2$$

meaning that the actuator command is constrained to be within ±1.5 degrees of trim. As mentioned in the previous section, this can be enforced using the gPC states by testing the constraint at various values of Δ to ensure that it is satisfied. To demonstrate the control method, the aircraft is perturbed to an angle of attack 6 degrees from trim and the receding horizon strategy is used to bring the aircraft back to trim. Figure 32 shows the responses of each of the states of the aircraft to the angle of attack perturbation. The response of the aircraft is generated for twenty values of Δ in the interval $[-1, 1]$. The angle of attack response is shown in the top portion, the pitch rate is shown in the middle and the actuator response is shown on the bottom.

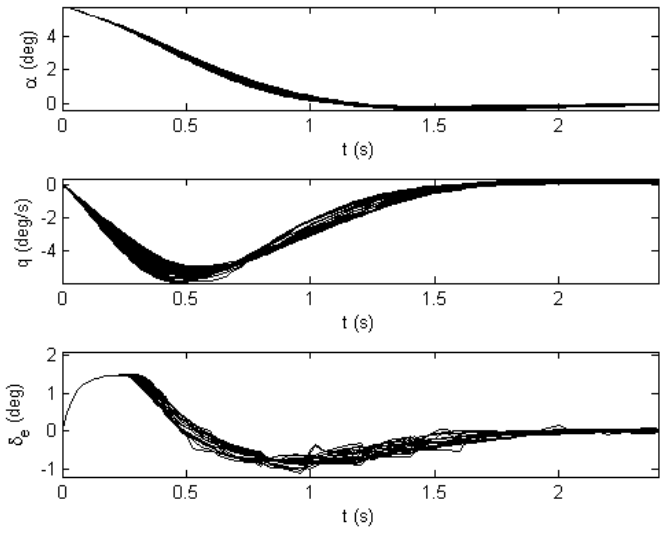

Fig. 32. Response of the linearized F-16 model under RHC control for twenty values of $\Delta \in [-1, 1]$ with control constraint

The actuator response is smooth and it does not violate the constraint for any of the trajectories. The angle of attack and pitch rate also demonstrate very smooth responses for each of the systems. It is important to note that other than resetting the distribution every time a new solution of the RHC policy is generated (every 0.1 seconds), there is no alteration to the control design for any value of Δ. Therefore, the RHC policy is able to provide robust stability for any *modelled* uncertainty governed by any probability distribution provided that feasibility conditions are satisfied and a terminal controller exists. Another important consideration when designing the receding horizon strategy is the horizon length. For the preceding example, a horizon length of 1 second was used with the control implemented for the first 5 steps or 0.1 seconds. We now examine the effect of shortening the horizon length. While the terminal constraint guarantees stability (so long as the problem is feasible), shortening the horizon length can alter the control response. In particular, when the value of the horizon length is shortened, this can lead to an oscillatory response in the control [72].

This can be partially attributed to the interaction between the terminal cost function and the integral cost. As an example consider the unconstrained response of the F-16 to the same angle of attack perturbation of 6 degrees. When a horizon length of 1 second is used, the control responses are smooth as shown in figure 33. When the

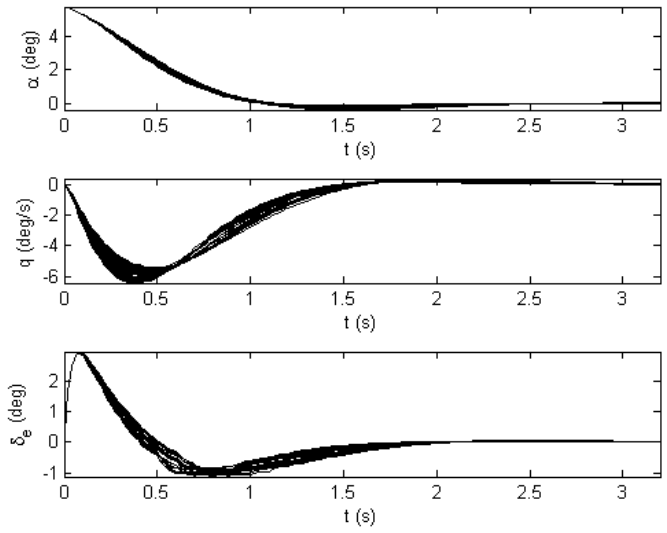

Fig. 33. Unconstrained response of the linearized F-16 model under RHC control for twenty values of $\Delta \in [-1, 1]$ with horizon length of 1 second

horizon length is reduced to 0.6 seconds the system responses are demonstrated by those in figure 34. While the angle of attack and pitch rate responses are smooth, oscillation is observed in the actuator command. The oscillation that is observed is caused by the resetting of the distribution at each of the time steps as well as the recalculation of the optimization problem at each of these steps. While this does not lead to any instability in the aircraft response, it is undesirable as it may lead to structural vibrations in the aircraft.

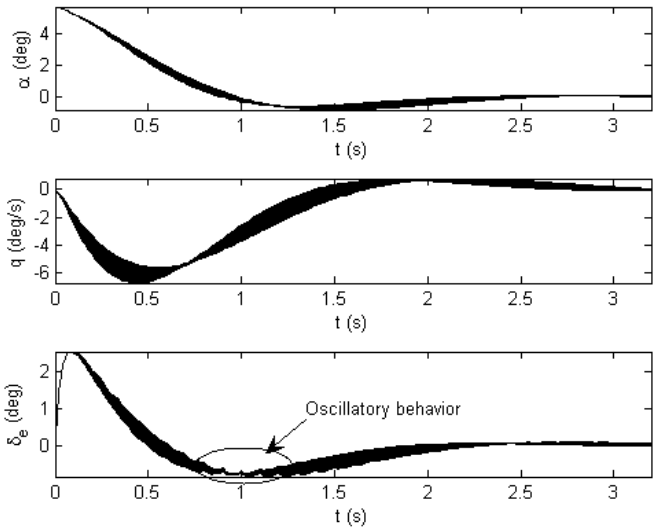

Fig. 34. Unconstrained response of the linearized F-16 model under RHC control for twenty values of $\Delta \in [-1, 1]$ with horizon length of 0.6 seconds

D. Summary

In this section a receding horizon control strategy was developed for linear discrete time stochastic systems. We have used the concept of Polynomial Chaos to frame stochastic problem in a deterministic setting and guarantee stability with an RHC approach. Additionally, because the gPC expansion gives us a deterministic solution to the stochastic problem we are able to enforce constraints that would be difficult to enforce in more traditional approaches. The ability of the control strategy to effectively stabilize the stochastic system is demonstrated with several examples.

CHAPTER VI

STABILITY OF STOCHASTIC SYSTEMS

A. Introduction

Up until this point, we have only examined the stability of the states of the gPC system. At this point, the question naturally arises, "What does the stability of the gPC approximation imply about the stability of the original stochastic system?" In this section, we will attempt to answer these questions.

We will refer to the *projected system* as the system obtained after the Galerkin projection of the dynamics onto the polynomial basis. For linear systems, this is

$$\mathcal{S}_{pc}^{l}: \quad \dot{\mathbf{X}} = \mathbf{A}\mathbf{X} \tag{VI.1}$$

and for nonlinear systems this is

$$\mathcal{S}_{pc}^{nl}: \quad \dot{\mathbf{X}} = \mathbf{F}(\mathbf{X}) \tag{VI.2}$$

where $\mathbf{X}$ has been defined in equation (III.22). For stability analysis, we consider open loop systems. In general, this will apply to closed loop systems as well since they can be written in one of the forms given above. The *pre-projected system* will be defined as the system before the Galerkin projection is performed, or

$$\hat{\mathcal{S}}_{p}^{l}: \quad \dot{\hat{x}}_p - \hat{A}_p(\Delta)\hat{x}_p = R_l(t,\Delta) \tag{VI.3}$$

for linear systems and

$$\hat{\mathcal{S}}_{p}^{nl}: \quad \dot{\hat{x}}_p - \hat{f}_p(\hat{x}_p,\Delta) = R_{nl}(t,\Delta) \tag{VI.4}$$

for nonlinear systems where $\hat{x}_p(t,\Delta) = \sum_{i=0}^{p} \mathbf{X}_i(t)\phi_i(\Delta)$, $\hat{A}_p(\Delta) = \sum_{i=0}^{p} A_i\phi_i(\Delta)$, and

$\hat{f}(\hat{x}_p, \Delta)$ corresponds to the nonlinear function when all parameters that depend on the random variable Δ have been written in terms of a gPC expansion. The terms $R_l(t, \Delta)$ and $R_{nl}(t, \Delta)$ are residue terms that account for the approximation error. The system, $\mathcal{S}^l$ is related to $\hat{\mathcal{S}}_p^l$ by taking the Galerkin projection of the system onto $\{\phi_0, \phi_1, \ldots, \phi_p\}$ and setting the projection of the residue to zero, or

$$\langle \dot{\hat{x}}_p - \hat{A}_p(\Delta)\hat{x}_p, \phi_i \rangle = \langle R_l(t, \Delta), \phi_i \rangle = 0$$

for $i = 0, 1, \ldots, p$. The nonlinear counterparts are related in a similar fashion. Next, we define the *approximate system* as the system obtained by approximating the system dynamics with the finite dimensional polynomial basis. This system is written as

$$\hat{\mathcal{S}}^l : \quad \dot{\hat{x}} = \hat{A}_p(\Delta)\hat{x} \tag{VI.5}$$

for linear systems and

$$\hat{\mathcal{S}}^{nl} : \quad \dot{\hat{x}} = \hat{f}_p(\hat{x}, \Delta) \tag{VI.6}$$

for nonlinear systems. Where $\hat{A}_p$ and $\hat{f}_p$ are the same as those in $\hat{\mathcal{S}}_p^l$ and $\hat{\mathcal{S}}_p^{nl}$ respectively. Finally, the *actual system* is the original stochastic system, or

$$\mathcal{S}^l : \quad \dot{x} = A(\Delta)x \tag{VI.7}$$

for the linear case and

$$\mathcal{S}^{nl} : \quad \dot{x} = f(x, \Delta) \tag{VI.8}$$

for the nonlinear case. At this point, we are ready to present stability and convergence properties of each of these systems.

B. Convergence Results

Now we present certain convergence properties that relate $\hat{\mathcal{S}}^l$ and $\hat{\mathcal{S}}^{nl}$ to $\mathcal{S}^l$ and $\mathcal{S}^{nl}$ respectively. The first result is to demonstrate the finite-time convergence of the solution of $\hat{\mathcal{S}}^l$ to the solution of $\mathcal{S}^l$ as $p \to \infty$. We start with a scalar linear system.

Proposition VI.1 *Consider the linear system given by $\dot{x} = a(\Delta)x$ and assume that the initial state, x_0 is known. The solution of this equation is given by $x(t, \Delta)$. Let an approximate system be governed by $\dot{\hat{x}} = \hat{a}_p(\Delta)\hat{x}$ with its solution as $\hat{x}(t, \Delta)$. Assume that $\hat{a}_p(\Delta)$ converges to $a(\Delta)$ in the mean squared sense (Cameron-Martin [13]) and that all moments of a and $\hat{a}_p$ are finite. Then for a finite time, t, $\hat{x}(t, \Delta) \to x(t, \Delta)$ in the $\mathcal{L}_2$ sense.*

Proof To prove this, we use the solution of x for each value of Δ, or

$$x(t, \Delta) = e^{a(\Delta)t}x_0$$

For the rest of the proof, we will let $a := a(\Delta)$ and $\hat{a} := \hat{a}_p(\Delta)$. The approximate solution is given by

$$\hat{x}(t, \Delta) = e^{\hat{a}t}x_0 = (1 + \hat{a}t + \frac{(\hat{a}t)^2}{2} + \ldots)x_0$$

Now, consider

$$\mathbf{E}[|x - \hat{x}|^2] \quad = \quad \mathbf{E}[|e^{at}x_0 - e^{\hat{a}t}x_0|^2] = \mathbf{E}[|e^{at} - e^{\hat{a}t}|^2]x_0^2$$

Since x_0 does not depend on Δ, it can be taken outside of the expectation operator. Furthermore, we represent the exponential terms with their Taylor series approxima-

tions to obtain

$$\begin{aligned}
\mathbf{E}[|e^{at} - e^{\hat{a}t}|^2] &= \mathbf{E}[|1 + (at) + (at)^2/2 + \ldots - 1 - (\hat{a}t) - (\hat{a}t)^2/2 - \ldots|^2] \\
&= \mathbf{E}[|at - \hat{a}t + 1/2(at)^2 - 1/2(\hat{a}t)^2 + \ldots|^2] \\
&\leq \mathbf{E}[|at - \hat{a}t|^2] + \mathbf{E}[|(at)^2 - (\hat{a}t)^2|^2] + \ldots \\
&= \mathbf{E}[|a - \hat{a}|^2]t^2 + \mathbf{E}[|a^2 - \hat{a}^2|^2]t^4 + \ldots \qquad \text{(VI.9)}
\end{aligned}$$

Now, $\mathbf{E}[|a - \hat{a}|^2] \to 0$ as $p \to \infty$ by assumption. Now consider $\mathbf{E}[|a^2 - \hat{a}^2|^2]$.

$$\begin{aligned}
\mathbf{E}[|a^2 - \hat{a}^2|^2] &\leq \mathbf{E}[|a^2||a^2 - \hat{a}^2|] + \mathbf{E}[|\hat{a}^2||a^2 - \hat{a}^2|] \\
&\leq \mathbf{E}[|a^2||a - \hat{a}||a + \hat{a}|] + \mathbf{E}[|\hat{a}^2||a - \hat{a}||a + \hat{a}|] \\
&\leq \mathbf{E}[\hat{a}^4|a + \hat{a}|^2]^{1/2}\mathbf{E}[|a - \hat{a}|^2]^{1/2} \\
&\quad + \mathbf{E}[a^4|a + \hat{a}|^2]^{1/2}\mathbf{E}[|a - \hat{a}|^2]^{1/2} \qquad \text{(VI.10)}
\end{aligned}$$

In the above derivation, we have made use of the Minkowski inequality and the Schwartz inequality. Finally, the term $\mathbf{E}[a^4|a + \hat{a}|^2]^{1/2}$ by the Schwartz inequality and again the Minkowski inequality becomes

$$\mathbf{E}[a^4|a + \hat{a}|^2]^{1/2} \leq \mathbf{E}[a^8]^{1/4}\mathbf{E}[|a + \hat{a}|^4]^{1/4} \leq \mathbf{E}[|a|^4]^{1/4}\mathbf{E}[|\hat{a}|^4]^{1/4} < \infty$$

This is because moments of a and $\hat{a}$ are finite. In turn, this implies that (VI.10) can be written as

$$\mathbf{E}[|a^2 - \hat{a}^2|^2] \leq C_0\mathbf{E}[|a - \hat{a}|^2]^{1/2}$$

where C_0 is a finite constant. The right-hand side of this expression tends to zero as $p \to \infty$ by assumption. Derivation of the remaining terms in equation (VI.9) is similar and will result in terms on the right-hand side of (VI.9) which all tend to zero as $p \to \infty$ for finite t. This in turn implies that $\hat{x}$ tends to x in the mean squared

sense. This completes the proof. ■

Therefore for scalar systems, over a finite time, the solution of $\hat{\mathcal{S}}^l$ converges to the solution of the $\mathcal{S}^l$ as $p \to \infty$. This case easily extends to the higher dimensional case.

Proposition VI.2 *Consider the linear system given by* $\dot{x} = A(\Delta)x$ $(x \in \mathbb{R}^n)$ *and assume that the initial state,* x_0 *is known. Assume that* $\hat{A}_p(\Delta)$ *converges to* $A(\Delta)$ *in the mean squared sense (Cameron-Martin [13]) and that all moments of* $A(\Delta)$ *and* $\hat{A}_p(\Delta)$ *are finite, then for a finite time,* t, $\hat{x}(t,\Delta) \to x(t,\Delta)$ *in the* $\mathcal{L}_2$ *sense.*

Proof The proof of this is similar to that of the previous proposition and is therefore omitted. ■

The above proposition depends upon the finite moment assumption for the values of $A(\Delta)$ and $\hat{A}(\Delta)$. The next result utilizes the continuous dependence of the solution $x(t,\Delta)$ on $A(\Delta)$ to prove convergence in probability.

Proposition VI.3 *Consider the linear system given by* $\dot{x} = A(\Delta)x$ *with random initial state,* $x_0(\Delta)$. *Assume that* $\hat{A}_p(\Delta)$ *converges to* $A(\Delta)$ *in the mean squared sense and* $\hat{x}_{0,p}(\Delta)$ *converges to* $x_0(\Delta)$ *in the mean squared sense as* $p \to \infty$. *Then for any given time,* t, $\hat{x}(t,\Delta)$ *converges to* $x(t,\Delta)$ *in probability.*

Proof For each value of Δ, the evolution of $x(\Delta)$ is governed by $x = e^{A(\Delta)T}x_0(\Delta)$. Similarly, for each value of Δ, denote $\hat{x}_p$ as the solution to

$$\dot{\hat{x}} = \hat{A}_p\hat{x}$$

Since $\hat{A}_p(\Delta) \to A(\Delta)$ in the mean squared sense, this implies that they also converge in probability [26]. Because $e^{(\cdot)}$ is a continuous function of its arguments, then $e^{\hat{A}_p(\Delta)t} \to e^{A(\Delta)t}$ in probability for each value of t by Corollary 6.3.1 in [26]. Also, since

$\hat{x}_{0,p}(\Delta) \to x_0(\Delta)$ in the $\mathcal{L}_2$ sense, this implies they converge in probability. Finally, we know that since the terms $e^{\hat{A}_p(\Delta)t}$ and $\hat{x}_{0,p}(\Delta)$ converge in probability to $e^{A(\Delta)t}$ and $x_0(\Delta)$ respectively,

$$\hat{x}_p = e^{\hat{A}_p t}\hat{x}_{0,p} \xrightarrow{P} e^{A(\Delta)t}x_0(\Delta) = x$$

This completes the proof. ■

This difference between proposition VI.3 and propositions VI.1 and VI.2 is the type of convergence. The convergence in proposition VI.2 is $\mathcal{L}_2$ which is stronger and implies convergence in probability. This comes at the added cost of assuming all moments are finite, which is generally the case for the systems we consider. Proposition VI.3 makes no such assumptions but only guarantees convergence in probability, which is weaker. The above propositions relate $\mathcal{S}^l$ to $\hat{\mathcal{S}}^l$. In many cases, we might be able to model $A(\Delta)$ exactly using a gPC expansion in which case these are not needed. Furthermore, these propositions do not give us a means of relating the gPC projected system ($\mathcal{S}^l_{pc}$) to $\mathcal{S}^l$ or even $\hat{\mathcal{S}}^l$. To relate the results obtained in the previous chapters using the gPC expansion to those of the $\mathcal{S}^l$ and $\mathcal{S}^{nl}$, we will need to develop additional results.

To assess the convergence of $\hat{x}_p$ (governed by the dynamics of $\mathcal{S}^l_{pc}$ and $\mathcal{S}^{nl}_{pc}$) to the states of $\mathcal{S}^l$ and $\mathcal{S}^{nl}$, we will again return to a first order linear system. When the $A(\Delta)$ matrix is a polynomial function of Δ, then we can express $A(\Delta)$ exactly with a gPC expansion. For illustration purposes, we will assume that $a(\Delta) = \hat{a}_p(\Delta) = a_0\phi_0 + a_1\phi_1$.

Then the actual solution for each value of Δ becomes

$$\begin{aligned} x &= e^{(a_0\phi_0+a_1\phi_1)t}x_0 \\ x &= \Big(1+(a_0\phi_0+a_1\phi_1)t+\frac{1}{2}(a_0\phi_0+a_1\phi_1)^2t^2+\frac{1}{3!}(a_0\phi_0+a_1\phi_1)^3t^3 \\ &\quad +\frac{1}{4!}(a_0\phi_0+a_1\phi_1)^4t^4+\frac{1}{5!}(a_0\phi_0+a_1\phi_1)^5t^5+\ldots\Big)x_0 \end{aligned} \tag{VI.11}$$

Because orthogonal polynomials span the space of all polynomials, it is always possible to express products of polynomials as linear combinations of the basis functions. In fact, because x is a function of the random variable Δ with finite second moment, it can be approximated x to arbitrary accuracy in the mean squared sense by $\hat{x}_p = \sum_{j=0}^{\infty}\mathbf{X}_j\phi_j$ [13]. To determine the coefficients, $\mathbf{X}_j$, we take the projection of this solution onto the basis ϕ_j, which gives

$$\langle x,\phi_0\rangle = \Big(1+a_0t+\frac{1}{2}a_0^2t^2+\frac{1}{2}a_1^2\langle\phi_1^2\rangle t^2+\frac{1}{3!}a_0^3t^3+\frac{1}{3!}a_0a_1^2\langle\phi_1^2\rangle t^3+\ldots\Big)x_0 \tag{VI.12}$$

$$\langle x,\phi_1\rangle = \Big(a_1\langle\phi_1^2\rangle t+a_0a_1\langle\phi_1^2\rangle t^2+\frac{1}{2}a_0^2a_1\langle\phi_1^2\rangle t^3+\frac{1}{3!}a_1^3\langle\phi_1^4\rangle t^3+\ldots\Big)x_0 \tag{VI.13}$$

In the above expression, we have assumed $\langle\phi_0^2\rangle = 1$. Taking the time derivative of the response x, we get

$$\dot{x} = (a_0\phi_0+a_1\phi_1)+(a_0\phi_0+a_1\phi_1)^2t+\frac{1}{2}(a_0\phi_0+a_1\phi_1)^3t^2\ldots$$

Projecting this onto $\phi_0(\Delta)$ gives

$$\langle\dot{x},\phi_0\rangle = a_0+a_0^2t+a_1^2\langle\phi_1^2\rangle t+\frac{1}{2}a_0^3t^2+\frac{3}{2}a_0a_1^2\langle\phi_1^2\rangle t^2+\ldots \tag{VI.14}$$

Examining the first few terms of this expression and comparing them to the terms of $\langle x,\phi_0\rangle$ and $\langle x,\phi_1\rangle$, we can see that the following expression is obtained by simplifying equation (VI.14).

$$\langle\dot{x},\phi_0\rangle = a_0\langle x,\phi_0\rangle + a_1\langle x,\phi_1\rangle \tag{VI.15}$$

The above expression is in fact exact for the usual sets of orthogonal polynomials (Jacobi, Hermite, Legendre, etc.). If we were to continue the process, we would find

$$\begin{aligned}
\langle \dot{x}, \phi_1 \rangle &= a_1 \langle \phi_1^2 \phi_0 \rangle \frac{\langle x, \phi_0 \rangle}{\langle \phi_0^2 \rangle} + a_0 \langle \phi_1^2 \rangle \frac{\langle x, \phi_1 \rangle}{\langle \phi_1^2 \rangle} + a_1 \langle \phi_1^2 \phi_2 \rangle \frac{\langle x, \phi_2 \rangle}{\langle \phi_2^2 \rangle} \\
\langle \dot{x}, \phi_2 \rangle &= a_1 \langle \phi_1^2 \phi_2 \rangle \frac{\langle x, \phi_1 \rangle}{\langle \phi_1^2 \rangle} + a_0 \langle \phi_2^2 \rangle \frac{\langle x, \phi_2 \rangle}{\langle \phi_2^2 \rangle} + a_1 \langle \phi_1 \phi_2 \phi_3 \rangle \frac{\langle x, \phi_3 \rangle}{\langle \phi_3^2 \rangle} \\
&\vdots \\
\langle \dot{x}, \phi_p \rangle &= a_1 \langle \phi_{p-1} \phi_1 \phi_p \rangle \frac{\langle x, \phi_{p-1} \rangle}{\langle \phi_{p-1}^2 \rangle} + a_0 \langle \phi_p^2 \rangle \frac{\langle x, \phi_p \rangle}{\langle \phi_p^2 \rangle} + a_1 \langle \phi_1 \phi_p \phi_{p+1} \rangle \frac{\langle x, \phi_{p+1} \rangle}{\langle \phi_{p+1}^2 \rangle} \\
&\vdots
\end{aligned}$$

Writing these expressions in a matrix form gives

$$\begin{bmatrix} \langle \dot{x}, \phi_0 \rangle \\ \langle \dot{x}, \phi_1 \rangle \\ \langle \dot{x}, \phi_2 \rangle \\ \vdots \end{bmatrix} = \begin{bmatrix} a_0 & a_1 & 0 & 0 & 0 & \cdots \\ a_1 \frac{\langle \phi_1^2 \phi_0 \rangle}{\langle \phi_0^2 \rangle} & a_0 \frac{\langle \phi_1^2 \rangle}{\langle \phi_1^2 \rangle} & a_1 \frac{\langle \phi_1^2 \phi_2 \rangle}{\langle \phi_2^2 \rangle} & 0 & 0 & \cdots \\ 0 & a_1 \frac{\langle \phi_1^2 \phi_2 \rangle}{\langle \phi_1^2 \rangle} & a_0 \frac{\langle \phi_2^2 \rangle}{\langle \phi_2^2 \rangle} & a_1 \frac{\langle \phi_1 \phi_2 \phi_3 \rangle}{\langle \phi_3^2 \rangle} & 0 & \cdots \\ \vdots & \vdots & \vdots & \vdots & \vdots & \vdots \end{bmatrix} \begin{bmatrix} \langle x, \phi_0 \rangle \\ \langle x, \phi_1 \rangle \\ \langle x, \phi_2 \rangle \\ \vdots \end{bmatrix} \tag{VI.16}$$

From here, we can see a clear tri-diagonal structure emerge. This will be the case for any orthogonal polynomials when the system uncertainty is linear in Δ. This series can be extended to infinite terms and if this is done, we can see that the resulting solution in fact converges to the original x because the set of polynomials makes up a Hilbert space. This means that in the limit, this projection approach captures the behavior of the original system ($\mathcal{S}^l$). If we relate this back to the gPC approximations that were determined in previous chapters and replace $\langle x, \phi_j \rangle$ by $\mathbf{X}_j$ we will find that the system matrix we have determined from this procedure is exactly the matrix determine by performing the gPC approximation. If we truncate the series at p, this is equivalent to setting $\langle x, \phi_{p+1} \rangle = 0$ for all time. We can see that this will induce errors in the equations of motion for $\langle \dot{x}, \phi_j \rangle$ with $j \leq p$ and that this error will

in fact enter in through the p^{th} equation in (VI.16). However, because the system matrix has a banded structure, this means the states have a cascaded effect and the error must pass through all of the previous states to influence the first few terms. Furthermore, because the gPC expansion exhibits exponential convergence [15] when the proper polynomials are used, we expect the terms associated with the higher order projections to be small. For stable systems, this error will indeed die out quickly.

The previous example shows that given enough terms in the gPC expansion, the equations of motion of the states in $\hat{\mathcal{S}}_p^l$ and $\mathcal{S}_{pc}^l$ begin to converge to those of $\mathcal{S}^l$. For the next result, we will assume this convergence and show that if this is true, then if in finite time the projected system is driven to zero, then the actual system will also be driven to zero in the mean squared sense. This is summed up in the following proposition.

Proposition VI.4 *Let $\hat{x}_p = \sum_{i=0}^{p} \mathbf{X}_i \phi_i$ be the approximation of x determined from solution of $\mathcal{S}_{pc}$ with dimension p. If we assume that the solution of the projected system, $\hat{x}_p$ converges to the solution of the $\hat{x}$ in the mean squared sense and all moments of A and $\hat{A}$ are finite, then*

$$x_p(t, \Delta) \xrightarrow{\mathcal{L}_2} x(t, \Delta)$$

for a given value of t.

Proof To test the convergence, we examine the limit as $p \to \infty$ of

$$\begin{aligned} \mathbf{E}[(\hat{x}_p - x)^2]^{1/2} &= \mathbf{E}[(\hat{x}_p - \hat{x} + \hat{x} - x)^2]^{1/2} \\ &\leq \mathbf{E}[(\hat{x}_p - \hat{x})^2]^{1/2} + \mathbf{E}[(\hat{x} - x)^2]^{1/2} \end{aligned}$$

Now, the first term tends to zero by assumption and the second term tends to zero by proposition VI.2. This completes the proof. ■

While this result demonstrates convergence, if it were to be used for stability it would require the system matrix to be of infinite dimension so its practical usage is limited. The benefit of this proposition is that it gives us confidence that if our system approximation is valid, then the behavior of the real system should match our truncated system for short times. We will discuss another approach to showing this later.

While the propositions in this section provide converge results between the various systems, the convergence is only guaranteed for a given time. For finite-time problems such as a trajectory generation problem, these results are useful. However, for stability analysis we are concerned about the system behavior as $t \to \infty$. Therefore, we will need to take another approach to relate the stability of $\mathcal{S}_{pc}^{l}$ and $\mathcal{S}_{pc}^{nl}$ to $\mathcal{S}^{l}$ and $\mathcal{S}^{nl}$.

C. Stability Results

In the previous section, discussion was centered around convergence of the gPC approximation for finite time. In this section we will relate the behavior of the projected system to the behavior of the actual system as $t \to \infty$. The first result provided will be a general result that relates the stability of $\mathcal{S}_{pc}^{nl}$ and $\mathcal{S}_{pc}^{l}$ to the actual states of $\hat{\mathcal{S}}_{p}^{nl}$ and $\hat{\mathcal{S}}_{p}^{l}$ respectively.

Proposition VI.5 *Let $\mathcal{S}_{pc}^{l}$ (or $\mathcal{S}_{pc}^{nl}$) be asymptotically stable for all orders of approximation, p, then the response of the state $\hat{x}_p$ converges to 0 in the mean squared ($\mathcal{L}_2$) sense with respect to Δ as $t \to \infty$.*

Proof The solution of $\hat{\mathcal{S}}_p$ converges to zero in the mean-squared sense as $t \to \infty$ if

$\lim_{t\to\infty} \mathbf{E}[(\hat{x}_p - 0)^2] \to 0$. We can write this as

$$\begin{aligned}
\lim_{t\to\infty} \mathbf{E}[(\hat{x}_p - 0)^T(\hat{x}_p - 0)] &= \lim_{t\to\infty} \mathbf{E}[\hat{x}_p^T \hat{x}_p] \\
&= \lim_{t\to\infty} \mathbf{E}\left[\left(\sum_{i=0}^{p} \mathbf{X}_i^T \phi_i\right)\left(\sum_{j=0}^{p} \mathbf{X}_j \phi_j\right)\right] \\
&= \lim_{t\to\infty} \sum_{i=0}^{p}\sum_{j=0}^{p} \mathbf{X}_i^T \mathbf{X}_j \int_{\mathcal{D}_\Delta} \phi_i \phi_j f(\Delta)\, d\Delta \\
&= \lim_{t\to\infty} \mathbf{X}(t)^T (I_n \otimes W)\mathbf{X}(t)
\end{aligned}$$

where W has been defined in equation (IV.4). But, we know that the projected system is asymptotically stable, so $\lim_{t\to\infty} \mathbf{X}^T(I_n \otimes W)\mathbf{X} = 0$. This completes the proof. ■

The result is straightforward, but is presented to illustrate an important point. This is that stability of the $\mathcal{S}_{pc}$ **does not** imply stability of the $\hat{\mathcal{S}}_p$ (and later also $\mathcal{S}$) for **all** Δ. The stability guarantees are instead given in the $\mathcal{L}_2$ sense, meaning that there may be some measure zero subset $\Delta \in \Omega$ where the result does not hold. By definition of measure zero, these values will have zero probability of occurring.

To show stability of the actual system we will need to understand the relationship between the Galerkin projection of the system and the Hilbert projection of the system. The Galerkin projection of the system can be obtained by assuming the system trajectories have the form

$$x(t, \Delta) = \sum_{i=0}^{\infty} \mathbf{X}_i(t)\phi_i(\Delta) \tag{VI.17}$$

This series is truncated at p to get an approximate solution ($\hat{x}_p$). The residue of the projection of the dynamics onto each polynomial direction is set to zero to determine the equations of motion for each $\mathbf{X}_i$. This can be expressed as

$$\langle \sum_{i=0}^{p} \dot{\mathbf{X}}_i \phi_i - A(\Delta)\left(\sum_{i=0}^{p} \mathbf{X}_i \phi_i\right),\, \phi_j \rangle = 0 \tag{VI.18}$$

This gives us the familiar equations of motion for the coefficients $\mathbf{X}$

$$\dot{\mathbf{X}}_j \langle \phi_j^2 \rangle = \sum_{i=0}^{p} \langle A(\Delta)\mathbf{X}_i \phi_i, \phi_j \rangle \tag{VI.19}$$

This gives us $p+1$ equations (one for each $j = 0, 1, \ldots, p$). By assumption, we are dealing with systems with finite second order moments. This translates to systems that are in $\mathcal{L}_2(\Delta)$. The space of all orthogonal functions over Δ makes up a Hilbert space and the sequence of all orthogonal functions is complete. By the projection theorem, we can compute the Hilbert projection to this subspace of orthogonal functions [73]. This projection is in fact the best in the mean squared sense. Let $x(t, \Delta)$ correspond to the true solution. We have denoted $\hat{x}_p(t, \Delta)$ as the approximation obtained from solution of the equations of motion associated with the Galerkin projection. We will denote $\bar{x}(t, \Delta)$ as solution obtained from equations of motion associated with the Hilbert (minimum distance) projection. This projection is obtained by

$$\langle x(t, \Delta), \phi_i \rangle = \bar{x}_i \tag{VI.20}$$

We can write the true solution as

$$x(t, \Delta) = \bar{x}(t, \Delta) + \epsilon = \sum_{i=0}^{p} \bar{x}_i \phi_i + \epsilon \tag{VI.21}$$

It is important to note that by the projection theorem, $\langle \epsilon, \phi_i \rangle = 0$ for $i = 0, \ldots, p$. If we take the derivative of the Hilbert projection, we arrive at

$$\langle \dot{x}(t, \Delta), \phi_i \rangle = \dot{\bar{x}}_i \tag{VI.22}$$

For linear systems, this becomes

$$\langle A(\Delta)x(t, \Delta), \phi_i \rangle = \dot{\bar{x}}_i \tag{VI.23}$$

We now state the following Lemma.

Lemma VI.6 *Assume that the system $\mathcal{S}^l_{pc}$ is asymptotically stable for all p as $p \to \infty$ and that the error in the Hilbert projection is bounded ($\epsilon \leq \epsilon_\infty$). Then the Galerkin projection tends toward the Hilbert Projection as $p \to \infty$ and $t \to \infty$. Moreover, the actual stochastic system is stable for all Δ in the $\mathcal{L}_2$ sense.*

Proof We begin by examining the evolution of the error between the Galerkin and Hilbert projections. This is given by

$$\langle \dot{x}(t,\Delta), \phi_j \rangle - \dot{\mathbf{X}}_j \langle \phi_j^2 \rangle = \langle A(\Delta)x(t,\Delta), \phi_j \rangle - \langle A(\Delta)\hat{x}_p(t,\Delta), \phi_j \rangle \tag{VI.24}$$

Now, we can define $e_i = \bar{x}_i - \mathbf{X}_i$. Furthermore, recall $x(t,\Delta) = \sum_{i=0}^{p} \bar{x}_i \phi_i + \epsilon$. Performing these substitutions gives

$$\dot{e}_j = \frac{1}{\langle \phi_j^2 \rangle} \sum_{i=0}^{p} \langle A(\Delta) e_i \phi_i, \phi_j \rangle + \frac{1}{\langle \phi_j^2 \rangle} \langle A(\Delta)\epsilon, \phi_j \rangle$$

These can be rewritten as

$$\dot{\mathbf{e}} = \mathbf{A}\mathbf{e} + \langle A(\Delta)\epsilon, \phi_j \rangle$$

where $\mathbf{e}$ is a vector of e_j terms and $\mathbf{A}$ is the same matrix obtained from the gPC projection of order p. Recall that $\langle \epsilon, \phi_j \rangle = 0$ for $j \leq p$. Now, we know that $\mathbf{A}$ is stable, so we can write the solution for the error directly in terms of the error in the Hilbert projection, ϵ.

$$\mathbf{e} = e^{\mathbf{A}t}\mathbf{e}_0 + \int_0^t e^{\mathbf{A}(t-\tau)} \langle A(\Delta)\epsilon, \phi_j \rangle \, d\tau$$

Thus, the error between the projections is related to the error in the Hilbert projection. The first term, $e^{\mathbf{A}t}\mathbf{e}_0 \to 0$ as $t \to \infty$ by stability of $\mathbf{A}$. If $\epsilon(t) \leq \epsilon_\infty$, then we know that $|\langle A(\Delta)\epsilon, \phi_j \rangle| \leq C_0 \epsilon_\infty$. This coupled with the stability of $\mathbf{A}$ means that the second term tends to a constant function of ϵ_∞ as $t \to \infty$. This gives

$$\lim_{t \to \infty} |\mathbf{e}| \leq C_1 \epsilon_\infty$$

where $|\cdot|$ is applied element-wise and C_1 is a vector. Therefore the error is in fact bounded and proportional to the bound on ϵ. As the accuracy of the Hilbert projection is increased, the error decreases and the Galerkin projection tends toward the Hilbert projection as $t \to \infty$.

Now, $\hat{x}_p(t, \Delta) \in \mathcal{L}_2(t) \times \mathcal{L}_2(\Delta)$, where $\mathcal{L}_2(\Delta)$ is with respect to the random variable Δ and $\mathcal{L}_2(t)$ is over $t \in [0, \infty)$. Because both of these spaces are Banach spaces, every Cauchy Sequence has its limit in the product space. Therefore, because the $\hat{x}_p \to \bar{x}$ as $p \to \infty$ and as $t \to \infty$, $\bar{x} \in \mathcal{L}_2(t) \times \mathcal{L}_2(\Delta)$. By the same argument, $x \in \mathcal{L}_2(t) \times \mathcal{L}_2(\Delta)$ since $\bar{x} \to x$ as $p \to \infty$. Additionally, since $\hat{x}_p \to 0$ as $t \to \infty$ for all p, it's limit must also tend to zero. This means that the actual stochastic system does in fact decay to zero asymptotically. ■

The previous lemma requires the assumption that there is a bound on the error in the Hilbert projection for all time. When the actual system is stable or bounded, assumption is not restrictive. This assumption is justified because the Lemma above deals with case where the gPC system is stable. Since the gPC system is stable, when we increase the number of terms, the evolution of ϵ is included in $\mathbf{A}$ and this matrix is stable by assumption. We now discuss the case when ϵ is not bounded.

Lemma VI.7 *Assume that $\mathcal{S}^l$ is unstable such that in at least one polynomial direction, $|x_i| \to \infty$. Then $\mathcal{S}^l_{pc}$ will be unstable after some finite number of terms.*

Proof We can without loss of generality write $x = \sum_{i=0}^{\infty} x_i \phi_i$ since the basis functions form a complete set in Δ. Furthermore, the Hilbert projection is equivalent to taking the first p terms of this expansion. The Hilbert projection gives

$$\dot{\bar{\mathbf{X}}} = \mathbf{A}\bar{\mathbf{X}} + \sum_{i=p+1}^{\infty} \langle A(\Delta)\phi_i \Phi \rangle x_i$$

where $\bar{\mathbf{X}}$ corresponds to the vector of terms of the Hilbert projection, and Φ is a vector of ϕ_j's for $j = 0, \ldots, p$. The terms for $i \geq p+1$ correspond to ϵ in the previous arguments. If the system is unstable then by assumption, at least one x_i must tend to infinity. If this is the case, we can without loss of generality assume that this direction corresponds to some ϕ_k. Now, if all other directions are stable and $p \geq k$, this implies $\mathbf{A}$ is unstable for all $p \geq k$. Another way of approaching this is to write the system in a matrix form

$$\begin{bmatrix} \dot{\bar{\mathbf{X}}} \\ \dot{\boldsymbol{\epsilon}} \end{bmatrix} = \begin{bmatrix} \mathbf{A} & \mathbf{A}_{x\epsilon} \\ \mathbf{A}_{\epsilon x} & \mathbf{A}_{\epsilon\epsilon} \end{bmatrix} \begin{bmatrix} \bar{\mathbf{X}} \\ \boldsymbol{\epsilon} \end{bmatrix}$$

Again, the matrix $\mathbf{A}$ is the matrix obtained from gPC. Now, if this system is unstable then there are at most a finite number of upper left hand blocks that have all negative eigenvalues [74]. This means that there will be at most a finite number of terms in the gPC expansion required to determine that the original system is unstable.■

The above Lemma tells us that if $\mathcal{S}^l$ is unstable, $\mathcal{S}^l_{pc}$ will be unstable. This means that if the gPC system remains stable for as $p \to \infty$, the original system is stable as well. The main difficulty in the previous Lemma is the assumption that at least one x_i must tend to infinity. Because the expansion is infinite, it is also possible to have $x \to \infty$ and have each $x_i < \infty$. When this occurs for infinite terms, the expansion will also be infinite. This case, however, does not make sense for linear systems. For a linear system, the only possible equilibrium point is the origin. For linear systems, non-zero steady state values in the state can only be achieved when the system matrix has a zero eigenvalue. Furthermore, we would require that the initial condition $x_0 = \sum_{x_{i,0}\phi(\Delta)}$ to be infinite with $x_{i,0} < \infty$. However, this means the

initial condition would not have a finite second moment as

$$\mathbf{E}[(x_0 - \mathbf{E}[x_0])^T(x_0 - \mathbf{E}[x_0])] = \sum_{i=0}^{\infty} x_i^T x_i \langle \phi_i^2 \rangle = \infty$$

This violates the basic assumptions of the gPC expansion and is therefore not a practical situation.

Finally, we introduce one final Lemma.

Lemma VI.8 *Assume that $\mathcal{S}^l$ is asymptotically stable, then $\mathcal{S}^l_{pc}$ will be stable for all truncations of order p.*

Proof As in the previous Lemma, write the system matrix of the Hilbert projection and its associated error as the following.

$$\begin{bmatrix} \dot{\bar{\mathbf{X}}} \\ \dot{\boldsymbol{\epsilon}} \end{bmatrix} = \begin{bmatrix} \mathbf{A} & \mathbf{A}_{x\epsilon} \\ \mathbf{A}_{\epsilon x} & \mathbf{A}_{\epsilon\epsilon} \end{bmatrix} \begin{bmatrix} \bar{\mathbf{X}} \\ \boldsymbol{\epsilon} \end{bmatrix}$$

If $\mathcal{S}^l$ is asymptotically stable, then every upper left-hand block of this matrix above must have negative eigenvalues [74]. Therefore for every truncation p, $\lambda(\mathbf{A}) < 0$ and therefore $\mathcal{S}^l_{pc}$ must be stable. This completes the proof. ■

The two previous lemmas allow us to use a contradiction argument to assess the stability of $\mathcal{S}^l$ in terms of the stability of $\mathcal{S}^l_{pc}$. If $\mathcal{S}^l_{pc}$ is stable for all p, then it is not possible for the original system to be unstable as Lemma VI.7 provides a contradiction. Similarly, if $\mathcal{S}^l_{pc}$ is unstable then we can determine that the $\mathcal{S}^l$ is not asymptotically stable by drawing a contradiction from Lemma VI.8.

D. Summary

This chapter has provided preliminary results for linking the stability of the gPC system to that of the actual stochastic system. It should be noted that when we

discuss stability for the actual system, there is always a possibility that there may be a measure zero set of Δ for which the system is not stable. It should also be noted that in reality many of the stability and convergence results require conditions to be enforced as $p \to \infty$. These conditions are not possible to test in practice. The goal of this chapter is to provide confidence that the results obtained from the gPC expansion are accurate when enough terms are used and that results obtained from analysis of $\mathcal{S}_{pc}^{l}$ can be applicable to $\mathcal{S}^{l}$. Extending these results to include more rigor and strengthening them is a topic of future research. In particular, these ideas open the door for analysis of controllability, observability, and optimality. Extending these ideas to nonlinear systems is also a topic of future research.

CHAPTER VII

CONCLUSIONS

A. Dissertation Summary

This dissertation has presented a novel framework for solving stochastic stability analysis and control problems in a deterministic setting. These problems arise out of a need to assess the stability of and design control laws for systems that have uncertainty in their dynamics. In practice, the dynamics of a system are not known perfectly and the system parameters may be estimated to within some associated probability distribution. The traditional control design approach is to design a control law for the average value of the uncertain parameters and ensure robustness for the entire range of parameter variation. This approach, however, does not take into account the likelihood of the value of the uncertain parameter. This can generally lead to conservative control laws that place a large amount of weight on outcomes with low probability. As a result, a control designer might wish to increase performance for parameter ranges with high probability and sacrifice performance for parameter values that occur with low probability.

In general, these stochastic stability and control problems can be difficult to solve analytically. As a result, sampling based methods are usually employed to approximate and solve such problems. Unfortunately, these methods can require the solution of large problems that do not have analytical solutions.

The main focus of this work is the use of the generalized Polynomial Chaos (gPC) expansion to transform the solution of stochastic problems into the solution of deterministic problems. In this manner, we are able to solve stochastic stability and control problems using well-known and well-established methodologies. In this

dissertation, the gPC approach has been used to solve a number of stability and control problems with high accuracy.

In order to apply the gPC expansion to dynamic system analysis, we first developed a general framework for the modelling of gPC systems. A general system formulation for transforming the stochastic problem into a deterministic problem was presented. We have shown that linear systems can be written as linear systems in higher dimensional state space and that polynomial systems can be written as polynomial systems of the same order in higher dimensional state space.

After developing a methodology for the transformation of a stochastic system into a deterministic system of higher dimension, we then developed stability conditions for linear open and closed loop systems as well as nonlinear systems. These conditions were demonstrated with several examples and the ability of the gPC approximation to accurately predict the statistical behavior of the stochastic system was demonstrated.

Next, conditions for the solution of stochastic optimal control problems were developed. We are interested in solving minimum expectation problems of the Bolza form. Several feedback laws for the solution of infinite horizon linear minimum expectation control problems have been developed. Additionally, a framework for solving open-loop optimal control problems was also developed. These were demonstrated with several examples.

Additionally, a framework for solving the stochastic receding horizon control problem was presented. Here we developed several receding horizon policies that guarantee the stability of the stochastic system using the gPC approach. These enabled us to compute control strategies for stochastic dynamic systems with different types of state and control constraints.

Finally, we developed preliminary results that justify the use of the gPC approach and relate the stability of the gPC system to that of the original stochastic system

that we have approximated. In general we have presented several convergence results and demonstrated the link between the stability of the original stochastic system and that of the gPC system for linear systems.

B. Future Work

1. Controllability and Observability

Many of the conditions that have been developed in this dissertation present sufficient conditions for determining optimal control laws. However, we have not discussed the controllability of these stochastic systems. The feasibility conditions guarantee that if the system is uncontrollable, then the uncontrollable modes are stable and thus a solution to the optimization problems exists. However, an important problem is that of determining conditions for understanding the controllability (and observability) of the original stochastic systems in terms of the controllability (and observability) of the gPC projected system.

2. Computational Efficiency

The largest drawback of the gPC approach is the higher dimensional state space that results from the Galerkin projection. When high accuracy is needed or when there are multiple random variables, the number of polynomials can become very large. For linear systems, this is not extremely challenging. However, for nonlinear systems this becomes a computational problem. For polynomial systems, the gPC projection results in equations of motion involving higher order tensors. It is possible that the structure can be exploited to reduce computational complexity and improve the speed of simulation. Additionally, the large number of states created by the gPC approximation can make the solution of nonlinear optimization problems very

difficult. This is also a topic of future research.

3. RHC Formulation

The stochastic RHC formulation presented in Chapter V presents a generalized strategy for solving stochastic RHC problems. Although the strategy is effective, additional steps should be taken to reduce the computational time of the strategy and formulate the problem in such a way that on-line solution of the problem is possible. Furthermore, this strategy should be extended to nonlinear systems. Additionally, the probability one constraints discussed in the RHC chapter can be extended to cover more general cases of the form, $P(x \in \mathcal{A}) \geq \bar{P}$. To further develop this formulation, a better means of handling these constraints (and associated the indicator function) should be developed.

4. Robust Control

The approach in this work should be compared to traditional robust control methodologies. A fair comparison will require formulation of stochastic problems in the frequency domain. This can then be used to improve the tendency of robust control methods to be conservative. This provides a means of further developing the concept of risk-sensitive control.

REFERENCES

[1] E. Wong, *Stochastic Processes in Information and Dynamical Systems.* New York, NY: McGraw-Hill, 1971.

[2] R. E. Skelton, T. Iwasaki, and K. M. Grigoriadis, *A Unified Algebraic Approach to Linear Control Design.* Bristol, PA: Taylor and Francis, 1997.

[3] R. F. Stengel, "Some effects of parameter variations on the lateral-directional stability of aircraft," *AIAA Journal of Guidance and Control*, vol. 3, no. 2, pp. 124–131, April 1980.

[4] R. F. Stengel and L. Ryan, "Stochastic robustness of linear time-invariant control systems," *IEEE Transactions on Automatic Control*, vol. 36, pp. 82–87, Jan 1991.

[5] Q. Wang and R. F. Stengel, "Robust nonlinear flight control of a high-performance aircraft," *IEEE Transactions on Control Systems Technology*, vol. 13, no. 1, pp. 15–26, January 2005.

[6] Q. Wang and R. F. Stengel, "Probabilistic control of nonlinear uncertain dynamic systems," in *Probabilistic and Randomized Methods for Design Under Uncertainty*, G. Calafiore and F. Dabbene, Eds. New York, NY: Springer, 2006, pp. 381–414.

[7] B. R. Barmish, C. M. Lagoa, and P. S. Shcherbakov, "Probabilistic enhancement of robustness margins provided by linear matrix inequalities," in *Proceedings of the 34th Annual Allerton Conference on Communication, Control and Computing*, Monticello, IL, 1996, pp. 160–169.

[8] B. R. Barmish, "A probabilistic robustness result for a multilinearly parameterized H_∞ norm," in *Proceedings of the 2000 American Control Conference*, vol. 5, Chicago, IL, June 2000, pp. 3309–3310.

[9] B. T. Polyak and R. Tempo, "Probabilistic robust design with linear quadratic regulators," *Systems & Control Letters*, vol. 43, pp. 343–353, 2001.

[10] Y. Fujisaki, F. Dabbene, and R. Tempo, "Probabilistic design of LPV control systems," *Automatica*, vol. 39, pp. 1323–1337, Dec 2003.

[11] B. Lu and F. Wu, "Probabilistic robust control design for an f-16 aircraft," in *Proceedings of the AIAA Guidance, Navigation, and Control Conference and Exhibit*. San Francisco, CA: AIAA, August 2005.

[12] N. Wiener, "The homogeneous chaos," *American Journal of Mathematics*, vol. 60, no. 4, pp. 897–936, 1938.

[13] R. H. Cameron and W. T. Martin, "The orthogonal development of non-linear functionals in series of fourier-hermite functionals," *The Annals of Mathematics*, vol. 48, no. 2, pp. 385–392, 1947.

[14] D. Lucor, D. Xiu, and G. E. Karniadakis, "Spectral representations of uncertainty in simulations: Algorithms and applications," in *Proceedings of the International Conference on Spectral and Higher Order Methods*, Uppsala, Sweden, June 2001.

[15] D. Xiu and G. E. Karniadakis, "The wiener–askey polynomial chaos for stochastic differential equations," *SIAM J. Sci. Comput.*, vol. 24, no. 2, pp. 619–644, 2002.

[16] R. Askey and J. Wilson, "Some basic hypergeometric polynomials that generalize jacobi polynomials," *Memoirs Amer. Math. Soc.*, vol. 319, 1985.

[17] T. Y. Hou, W. Luo, B. Rozovskii, and H.-M. Zhou, "Wiener chaos expansions and numerical solutions of randomly forced equations of fluid mechanics," *J. Comput. Phys.*, vol. 216, no. 2, pp. 687–706, 2006.

[18] D. Xiu and G. E. Karniadakis, "Modeling uncertainty in flow simulations via generalized polynomial chaos," *J. Comput. Phys.*, vol. 187, no. 1, pp. 137–167, 2003.

[19] X. Wan, D. Xiu, and G. E. Karniadakis, "Stochastic solutions for the two-dimensional advection-diffusion equation," *SIAM J. Sci. Comput.*, vol. 26, no. 2, pp. 578–590, 2005.

[20] R. G. Ghanem and P. D. Spanos, *Stochastic Finite Elements: A Spectral Approach*. New York, NY: Springer-Verlag Inc., 1991.

[21] R. Ghanem and J. Red-Horse, "Propagation of probabilistic uncertainty in complex physical systems using a stochastic finite element approach," *Phys. D*, vol. 133, no. 1-4, pp. 137–144, 1999.

[22] R. Ghanem, "Ingredients for a general purpose stochastic finite elements implementation," *Comput. Methods Appl. Mech. Eng.*, vol. 168, no. 1-4, pp. 19–34, 1999.

[23] F. S. Hover and M. S. Triantafyllou, "Application of polynomial chaos in stability and control," *Automatica*, vol. 42, no. 5, pp. 789–795, 2006.

[24] A. H. Smith, A. Monti, and F. Ponci, "Indirect measurements via a polynomial chaos observer," *IEEE Transactions on Instrumentation and Measurement*,

vol. 56, no. 3, pp. 743–752, June 2007.

[25] A. Monti, F. Ponci, and T. Lovett, "A polynomial chaos theory approach to the control design of a power converter," in *Proceedings of the 35th Annual IEEE Power Electronics Specialist Conference*, Aachen, Germany, June 2004, pp. 4809–4813.

[26] S. Resnick, *A Probability Path.* Boston, MA: Birkhäuser, 1999.

[27] P. Beckmann, *Orthogonal Polynomials for Engineers and Physicists.* Boulder, CO: Golem Press, 1973.

[28] T. Chihara, *An Introduction to Orthogonal Polynomials.* New York, NY: Gordon and Breach Science Publishers, Inc., 1978.

[29] K. B. Datta and M. M. Bosukonda, *Orthogonal Functions in Systems and Control.* River Edge, NJ: World Scientific, 1995.

[30] R. Koekoek and R. F. Swarttouw, "The askey-scheme of hypergeometric orthogonal polynomials and its q-analogue," Department of Technical Mathematics and Information, Delft University of Technology, Technical Report 98-17, 1998.

[31] V. Volterra, *Lecons sur les Equations Integrales et Integro-differentielles.* Paris, France: Gauthier Villars, 1913.

[32] M. Schetzen, *The Volterra and Wiener Theories of Nonlinear Systems.* Melbourne, FL: Krieger Publishing Company, 2006.

[33] S. Kakutani, "Spectral analysis of stationary gaussian processes," in *Proceedings of the Fourth Berkeley Symposium on Mathematical Statistics and Probability.* University of California, 1961, vol. 2, pp. 239–247.

[34] H. Ogura, "Orthogonal functionals of the poisson process," *IEEE Transactions on Information Theory*, vol. 18, pp. 473–481, July 1972.

[35] G. Arfken, *Mathematical Methods for Physicists*, 3rd ed. Orlando, FL: Academic Press, 1985.

[36] M. Loéve, *Probability Theory*, 4th ed. New York, NY: Springer-Verlag, 1977.

[37] H. K. Kushner, *Stochastic Stability and Control.* New York, NY: Academic Press, 1967.

[38] S. P. Meyn and R. L. Tweedie, *Markov Chains and Stochastic Stability.* New York, NY: Springer-Verlag, 1993.

[39] B. J. Debusschere, H. N. Najm, P. P. Pébay, O. M. Knio, R. G. Ghanem, and O. P. L. Maître, "Numerical challenges in the use of polynomial chaos representations for stochastic processes," *SIAM J. Sci. Comput.*, vol. 26, no. 2, pp. 698–719, 2005.

[40] S. Boyd, L. E. Ghaoui, E. Feron, and V. Balakrishnan, *Linear Matrix Inequalities in System and Control Theory.* Philadelphia, PA: Siam, 1994.

[41] P. A. Parrilo, "Structured semidefinite programs and semialgebraic geometry methods in robustness and optimization," Ph.D. dissertation, California Institute of Technology, Pasadena, California, 2000.

[42] A. Papachristodoulou and S. Prajna, "A tutorial on sum of squares techniques for systems analysis," in *Proceedings of the 2005 American Control Conference*, Portland, OR, June 2005, pp. 2686–2700.

[43] A. Papachristodoulou and S. Prajna, "On the construction of lyapunov functions using the sum of squares decomposition," in *Proceedings of the* 41st *Conference on Decision and Control*, Las Vegas, NV, December 2002, pp. 3482–3487.

[44] S. Prajna, A. Papachristodoulou, and P. A. Parillo, "Introducing sostools: A general purpose sum of squares programming solver," in *Proceedings of the* 41st *IEEE Conference on Decision and Control*, Boston, MA, December 2002, pp. 741–746.

[45] S. Prajna, A. Papachristodoulou, P. Seiler, and P. A. Parillo, "New developments in sum of squares optimization and sostools," in *Proceedings of the 2004 American Control Conference*, Boston, MA, June 2004, pp. 5606–5611.

[46] Michal Kocvara and Michael Stingl, *PENBMI*, Version 2.0, 2004. See www.penopt.com.

[47] R. Bhattacharya, " OPTRAGEN: A MATLAB toolbox for optimal trajectory generation," *45th IEEE Conference on Decision and Control*, pp. 6832–6836, 2006.

[48] P. E. Gill, W. Murray, and M. A. Saunders, "SNOPT: An SQP algorithm for large-scale constrained optimization," *SIAM Journal on Optimization*, vol. 12, no. 4, pp. 979–1006, 2002.

[49] S. Qin and T. Badgwell, "An overview of industrial model predictive control technology," *AIChE Symposium Series*, vol. 93, pp. 232–256, 1996.

[50] A. Bemporad and M. Morari, "Robust model predictive control: A survey," Automatic Control Laboratory, Swiss Federal Institute of Technology (ETH),

Physikstrasse 3, CH-8092 Zürich, Switzerland, www.control.ethz.ch, Tech. Rep., 1999.

[51] W. Kwon, "Advances in predictive control: Theory and application," *1st Asian Control Conference, Tokyo*, 1994.

[52] R. Bitmead, M. Gevers, and V. Wertz, *Adaptive Optimal Control: The Thinking Man's GPC*, ser. International Series in Systems and Control Engineering. Englewood Cliffs, NJ: Prentice Hall, 1990.

[53] R. Soeterboek, *Predictive Control: A Unified Approach*, ser. International Series in Systems and Control Engineering. Prentice Hall, 1992.

[54] J. Rodellar and J. Martín Sánchez, *Adaptive Predictive Control*, ser. International Series in Systems and Control Engineering. Upper Saddle River, NJ: Prentice Hall, 1996.

[55] J. Primbs, "Nonlinear optimal control: A receding horizon approach," Ph.D. dissertation, California Institute of Technology, Pasadena, CA, 1999.

[56] A. Jadbabaie, J. Yu, and J. Hauser, "Stabilizing receding horizon control of nonlinear systems: A control lyapunov function approach," *Proceedings of the 1999 American Control Conference*, vol. 3, pp. 1535–1539, 1999.

[57] D. Mayne, J. Rawlings, C. Rao, and P. Scokaert, "Constrained model predictive control, stability and optimality," *Automatica*, vol. 36, pp. 789–814, 2000.

[58] J. Fisher, R. Bhattacharya, and S. R. Vadali, "Spacecraft momentum management and attitude control using a receding horizon approach," in *Proceedings of the 2007 AIAA Guidance, Navigation, and Control Conference and Exhibit*. Hilton Head, SC: AIAA, August 2007, p. Available at http://www.aiaa.org/.

[59] G. Grimm, M. J. Messina, S. E. Tuna, and A. R. Teel, "Examples when nonlinear model predictive control is nonrobust," *Automatica*, vol. 40, pp. 1729–1738, 2004.

[60] S. V. Raković, A. R. Teel, D. Q. Mayne, and A. Astolfi, "Simple robust control invariant tubes for some classes of nonlinear discrete time systems," in *Proceedings of the 45th IEEE Conference on Decision and Control*. San Diego, CA: IEEE, December 2006, pp. 6397–6402.

[61] J. H. Lee and Z. Yu, "Worst-case formulations of model predictive control for systems with bounbded parameters," *Automatica*, vol. 33, no. 5, pp. 763–781, 1997.

[62] B. Kouvaritakis, J. A. Rossiter, and J. Schuurmans, "Efficient robust predictive control," *IEEE Transactions on Automatic Control*, vol. 45, no. 8, pp. 1545–1549, 2000.

[63] M. V. Kothare, V. Balakrishnan, and M. Morari, "Robust constrained model predictive control using linear matrix inequalities," *Automatica*, vol. 32, no. 10, pp. 1361–1379, 1996.

[64] A. Bemporad, "Reducing conservativeness in predictive control of constrained linear systems with disturbances," in *Proceedings of the 37th IEEE Conference on Decision and Control*, vol. 2. Tampa, FL: IEEE, December 1998, pp. 1384–1389.

[65] D. H. van Hessem and O. H. Bosgra, "A conic reformulation of model predictive control including bounded and stochastic disturbances and input constraints," in *Proceedings of the 2002 Conference on Decision and Control*, vol. 4. Las Vegas, NV: IEEE, December 2002, pp. 4643–4648.

[66] D. H. van Hessem and O. H. Bosgra, "Closed-loop stochastic dynamic process optimization under input and state constraints," in *Proceedings of the 2002 American Control Conference*, vol. 3. Anchorage, AK: IEEE, July 2002, pp. 2023–2028.

[67] D. H. van Hessem and O. H. Bosgra, "A full solution to the constrained stochastic closed-loop mpc problem via state and innovations feedback and its receding horizon implementation," in *Proceedings of the 2003 Conference on Decision and Control*, vol. 1. Maui, HI: IEEE, December 2003, pp. 929–934.

[68] D. H. van Hessem and O. H. Bosgra, "Closed-loop stochastic model predictive control in a receding horizon implementation on a continuous polymerization reactor example," in *Proceedings of the 2004 American Control Conference*, vol. 1. Boston, MA: IEEE, July 2004, pp. 914–919.

[69] D. H. van Hessem and O. H. Bosgra, "Lmi-based closed-loop economic optimization of stochastic process operation under state and input constraints," in *Proceedings of the 2001 Conference on Decision and Control*, vol. 5. Orlando, FL: IEEE, December 2001, pp. 4228–4233.

[70] J. A. Primbs and C. H. Sung, "Stochastic receding horizon control of constrained linear systems with state and control multiplicative noise," *In revision for IEEE Transactions on Automatic Control*.

[71] G. C. Goodwin, M. M. Seron, and J. A. D. Doná, *Constrained Control and Estimation: An Optimisation Approach*, ser. Communications and Control Engineering. Berlin: Springer, 2005.

[72] R. Bhattacharya, G. J. Balas, M. A. Kaya, and A. Packard, "Nonlinear receding horizon control of an f-16 aircraft," *Journal of Guidance, Control, and Dynamics*, vol. 25, no. 5, pp. 924–931, 2002.

[73] D. G. Luenberger, *Optimization by Vector Space Methods*. New York, NY: John Wiley and Sons Inc., 1969.

[74] R. A. Horn and C. R. Johnson, *Matrix Analysis*. New York, NY: Cambridge University Press, 1999.

APPENDIX A

SOME COMMON SETS OF ORTHOGONAL POLYNOMIALS

In this section, we cover a few sets of orthogonal polynomials that are used in the gPC framework. In this appendix, we will discuss the weighting functions with which each set of polynomials is orthogonal and relate these to their corresponding probability distribution.

Hermite Polynomials (Gaussian Distribution)

As is mentioned in Chapter II, the concept of Polynomial Chaos was initially developed using Hermite polynomials. These polynomials are orthogonal with respect to the weighting function

$$f(\Delta) = \frac{1}{\sqrt{2\pi}} e^{-\frac{\Delta^2}{2}} \tag{A.1}$$

This weighting function corresponds to a *Gaussian distribution* with zero mean and variance 1. The polynomials themselves can be determined from Rodriguez Formula

$$H_n(\Delta) = (-1)^n e^{\Delta^2/2} \frac{d^n}{d\Delta^n} e^{-\Delta^2/2} \tag{A.2}$$

Table 4 gives the listing of polynomials for $\Delta \in \mathbb{R}^1$ up to 8^{th} order. The domain of these polynomials is $\Delta \in (-\infty, \infty)$. The weighting function above corresponds to unit variance. If a different variance is required there are several methods of dealing with this. One is to change the weighting function to

$$f_\sigma(\Delta) = \frac{1}{\sigma\sqrt{2\pi}} e^{-\frac{\Delta^2}{2\sigma^2}}$$

where σ^2 is the desired variance. This method requires recomputing a new set of orthogonal polynomials. This is equivalent to substituting $\Delta = \hat{\Delta}/\sigma$ into the expres-

Table 4. One-dimensional Hermite polynomials up to 8^{th} order

n	H_n
0	1
1	Δ
2	$\Delta^2 - 1$
3	$\Delta^3 - 3\Delta$
4	$\Delta^4 - 6\Delta^2 + 3$
5	$\Delta^5 - 10\Delta^3 + 15\Delta$
6	$\Delta^6 - 15\Delta^4 + 45\Delta^2 - 15$
7	$\Delta^7 - 21\Delta^5 + 105\Delta^3 - 105\Delta$
8	$\Delta^8 - 28\Delta^6 + 210\Delta^4 - 420\Delta^2 + 105$

sions in table 4 where $\hat{\Delta}$ has variance σ^2. An additional method for using a non-unit variance is to multiply Δ by σ everywhere it appears in the actual equations. It is always possible to write a random variable with non-unit variance in terms of a random variable of unit variance multiplied by a constant (σ).

When the dimension of Δ is greater than one, we can use the weight function corresponding to the multi-dimensional Gaussian distribution. This function is given by

$$f(\Delta) = \frac{1}{(2\pi)^{m/2}} e^{-\frac{\Delta^T \Delta}{2}} \tag{A.3}$$

where $\Delta \in \mathbb{R}^m$. This weight function corresponds to a multivariate Gaussian distribution where all of the random variables are *independent* and therefore have no correlation. If correlation were allowed, then a different weighting function would be required and a different set of polynomials obtained. The polynomials can be obtained by using products of the one-dimensional Hermite polynomials for each Δ_i. For example, the set of second order polynomials are given by $H_2(\Delta_1)$, $H_1(\Delta_1)H_1(\Delta_2)$, and $H_2(\Delta_2)$. Table 5 gives the Hermite polynomials up to 4^{th} order for $\Delta \in \mathbb{R}^2$. For the single dimensional case, the number of polynomials is $p+1$ where p is the desired order. For the multivariate set, the relationship between the number of polynomials and the desired order is given by $N = \frac{(m+p)!}{m!p!}$. For the case above, we have $m = 2$ and $p = 4$ which means we require 15 polynomials ($\hat{H}_n$).

Legendre Polynomials (Uniform Distribution)

Legendre polynomials are orthogonal with respect to the weighting function

$$f(\Delta) = \frac{1}{2} \tag{A.4}$$

Table 5. Two-dimensional Hermite polynomials up to 4^{th} order

n	p	$\hat{H}_n$
0	0	1
1	1	Δ_1
2		Δ_2
3	2	$\Delta_1^2 - 1$
4		$\Delta_1\Delta_2$
5		$\Delta_2^2 - 1$
6	3	$\Delta_1^3 - 3\Delta_1$
7		$\Delta_1^2\Delta_2 - \Delta_2$
8		$\Delta_2^2\Delta_1 - \Delta_1$
9		$\Delta_2^3 - 3\Delta_2$
10	4	$\Delta_1^4 - 6\Delta_1^2 + 3$
11		$\Delta_1^3\Delta_2 - 3\Delta_2\Delta_1$
12		$\Delta_1^2\Delta_2^2 - \Delta_1^2 - \Delta_2^2 - 1$
13		$\Delta_2^3\Delta_1 - 3\Delta_1\Delta_2$
14		$\Delta_2^4 - 6\Delta_2^2 + 3$

for $\Delta \in [-1, 1]$. The weighting function corresponds to a *uniform distribution* for the interval $[-1, 1]$. The Legendre polynomials can be expressed using Rodriguez formula

$$P_n(\Delta) = \frac{1}{2^n n!} \frac{d^n}{d\Delta^n} \left[\left(\Delta^2 - 1 \right)^n \right] \tag{A.5}$$

The polynomials up to 8^{th} order are given in table 6. To extend the one-dimensional

Table 6. One-dimensional Legendre polynomials up to 8^{th} order

n	P_n
0	1
1	Δ
2	$\frac{1}{2}(3\Delta^2 - 1)$
3	$\frac{1}{2}(5\Delta^3 - 3\Delta)$
4	$\frac{1}{8}(35\Delta^4 - 30\Delta^2 + 3)$
5	$\frac{1}{8}(63\Delta^5 - 70\Delta^3 + 15\Delta)$
6	$\frac{1}{16}(231\Delta^6 - 315\Delta^4 + 105\Delta^2 - 5)$
7	$\frac{1}{16}(429\Delta^7 - 693\Delta^5 + 315\Delta^3 - 35\Delta)$
8	$\frac{1}{128}(6435\Delta^8 - 12012\Delta^6 + 6930\Delta^4 - 1260\Delta^2 + 35)$

Legendre Polynomials to multi-variate polynomials, a procedure similar to that employed for Hermite polynomials can be used. When this is the case the multivariate weighting function becomes.

$$f(\Delta) = \frac{1}{2^m} \tag{A.6}$$

where m is the number of independent random variables. Table 7 shows the polynomials in the set for $m = 2$ and polynomials up to 3^{rd}-order. As with the Hermite case, these polynomials are obtained when each random variable is independent.

Table 7. Two-dimensional Legendre polynomials up to 3^{rd} order

n	p	$\hat{P}_n$
0	0	1
1	1	Δ_1
2		Δ_2
3	2	$\frac{1}{2}(3\Delta_1^2 - 1)$
4		$\Delta_1\Delta_2$
5		$\frac{1}{2}(3\Delta_2^2 - 1)$
6	3	$\frac{1}{2}(5\Delta_1^3 - 3\Delta_1)$
7		$\frac{1}{2}(3\Delta_1^2\Delta_2 - \Delta_2)$
8		$\frac{1}{2}(3\Delta_2^2\Delta_1 - \Delta_1)$
9		$\frac{1}{2}(5\Delta_2^3 - 3\Delta_2)$

Jacobi Polynomials (Beta Distribution)

The set of Jacobi Polynomials are orthogonal with respect to the weighting function

$$f(\Delta) = \frac{(\Delta - a)^{\beta}(b - \Delta)^{\alpha}}{(b-a)^{\alpha+\beta+1}B(\alpha+1, \beta+1)} \tag{A.7}$$

for $\Delta \in [a, b]$ where $\alpha, \beta \in \mathbb{R}$ are parameters that determine the shape of the distribution. The Beta function, $B(\cdot, \cdot)$ is defined as

$$B(j, k) = \frac{\Gamma(p)\Gamma(q)}{\Gamma(p+q)} \tag{A.8}$$

The distribution function $f(\Delta)$ corresponds to a Beta distribution. To generate the polynomials for $\Delta \in [-1, 1]$, the Rodriguez formula can be used. This is given by

$$P_n^{(\alpha,\beta)} = \frac{(-1)^n}{2^n n!(1-\Delta)^{\alpha}(1+\Delta)^{\beta}} \frac{d^n}{d\Delta^n}\left[(1-\Delta)^{n+\alpha}(1+\Delta)^{n+\beta}\right] \tag{A.9}$$

Here we have used $a = -1$ and $b = 1$. When $\alpha = \beta = 0$ the Jacobi Polynomials are the Legendre Polynomials and the weighting function becomes constant. This is to be expected as the Beta distribution for $\alpha = \beta = 0$ is the uniform distribution. Table 8 shows the polynomials up to 4^{th} order for $\alpha = \beta = 2$. The products of polynomials and their weights can be used to compute a multivariate in the same manner as for

Table 8. One-dimensional Jacobi polynomials up to 4^{th} order

n	$P_n^{(2,2)}$
0	1
1	3Δ
2	$7\Delta^2 - 1$
3	$15\Delta^3 - 5\Delta$
4	$\frac{1}{16}(495\Delta^4 - 270\Delta^2 + 15)$

the previous sets of orthogonal polynomials.

APPENDIX B

MISCELLANEOUS APPLICATIONS

In this appendix, we will examine the solution to a few problems that can be solved using the PC approach.

Confidence Intervals

The first problem considered is that of ensuring stability or performance in terms of a certain confidence interval. In general throughout this dissertation, we have solved problems in terms of the entire set of Δ. As mentioned previously, for distributions with infinite support this can be an unrealistic problem. In such cases it is better to discuss system properties with respect to a confidence interval. As an example, consider the linear system

$$\dot{x} = Ax + (B\Delta)x$$

where Δ is governed by a Gaussian distribution. Because the system uncertainty is linear in Δ, it is clear that ensuring stability with probability one is not possible. This would be equivalent to ensuring that the eigenvalues of

$$\hat{A} = A + B\Delta$$

were stable for $\Delta \in (-\infty, \infty)$. It is therefore more reasonable to consider stability of the system with respect to some finite probability. Clearly,

$$P(\lambda(\hat{A}) < 0) = P(\{\Delta : \lambda(\hat{A}) < 0\}) = \int_{\Delta} \mathbf{1}_{\lambda(\hat{A}(\Delta))<0}(\Delta) f(\Delta) d\Delta \tag{B.1}$$

where $\mathbf{1}_{\lambda(\hat{A}(\Delta))<0}(\Delta)$ is the indicator function that is 1 when the system is stable and zero otherwise. This statement is valid for any form of $\hat{A}$, not just the linear form

given above. To actually compute this interval, we would be required to numerically compute the values of Δ where this is the case. This is the Monte-Carlo approach. Besides being a computationally difficult problem (especially when the support of Δ is infinite), solution of this problem may not give the results one would expect. For example let the dependence of $\hat{A}$ on Δ be such that

$$\{\Delta : \lambda(\hat{A}(\Delta)) < 0\} = (-\infty, -\epsilon] \bigcup [\epsilon, \infty)$$

where $\epsilon > 0$. In many cases, we might want to ensure that the system is stable with some finite probability $\bar{P}$. If $P(\{(-\infty, -\epsilon] \bigcup [\epsilon, \infty)\}) \geq \bar{P}$, we would say the condition was satisfied. However, from this condition, we can see that at the center of the distribution (our expected value), the condition is not verified. Therefore, simply examining the "Probability of Stability" in this sense is not necessarily the best method for solving the problem we wish to solve. Indeed, in general we wish to ensure that the system is stable with some probability and that the values of Δ for which the condition is not satisfied correspond to the tails of the distribution (or those with the least probability).

Define the set

$$\mathcal{A} = [-\epsilon, \epsilon]$$

where ϵ is some positive constant. In general, the condition we truly wish to satisfy is

$$P(\{\Delta \in \mathcal{A} : \lambda(\hat{A}(\Delta)) < 0)\}) \geq \bar{P}$$

If $P(\{\Delta \in \mathcal{A}\}) = \bar{P}$, then we only need to ensure that $\lambda(\hat{A}(\Delta)) < 0 \ \forall \Delta \in \mathcal{A}$. This is a much easier problem to solve. In general, this can be solved with a sampling based method by taking values of $\Delta \in \mathcal{A}$ and testing these values. However, a non-sampling approach to solving this problem can be accomplished by using the gPC projection.

Instead of using polynomials which are orthogonal over the entire domain of Δ, we create a new set of polynomials that are orthogonal over $\mathcal{A}$. This can be accomplished by using the Gram-Schmidt procedure defined in Chapter II.

To demonstrate this a simple example will be presented. Consider the system

$$\dot{x} = A(\Delta)x$$

where

$$A = \begin{bmatrix} -4+\Delta & -1.5 \\ 1 & 0 \end{bmatrix}$$

Now, we can see that this system will be stable when $\Delta \leq 4$. Assume that Δ is a Gaussian random variable with unit variance. Now, it is not possible for the system to be stable for all values of Δ. However, let us say that we wish to satisfy stability with 95% probability. In such a case we might choose to make sure that the system is stable to within 2σ. To use the gPC approach, we then build a set of polynomials that are orthogonal with respect to the weighting function

$$f(\Delta) = \frac{1}{\sqrt{2\pi}} e^{-\frac{\Delta^2}{2}}$$

for $\Delta \in [-2, 2]$. Using the Gram-Schmidt procedure we can arrive at the set of orthogonal polynomials (up to 4^{th} order) shown in table 9.

These polynomials form an orthonormal basis on the domain of Δ. If we use these polynomials to formulate the corresponding **A** matrix, we find that the eigenvalues of the matrix correspond well to the actual eigenvalues. Figure 35 displays the eigenvalues of the system for the PC expansion as well as the actual eigenvalues of the system. The eigenvalues match very well. As the number of terms is increased, the eigenvalues of the gPC system matrix, **A**, will begin to cover the entire range of the eigenvalues observed by Monte-Carlo. As the figure demonstrates the sys-

Table 9. Polynomials up to 4^{th} order for Gaussian distribution with domain 2σ

n	P_n
0	1
1	Δ
2	$\Delta^2 - 0.7737$
3	$\Delta^3 - 1.8303\Delta$
4	$\Delta^4 - 2.8930\Delta^2 + 0.8222$

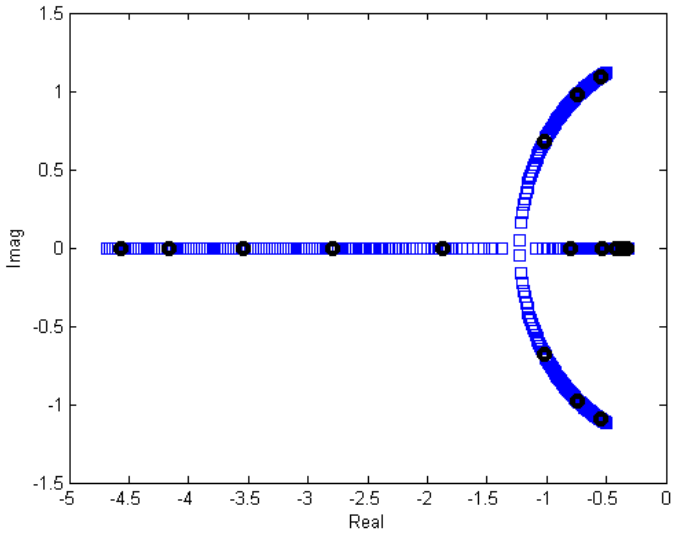

Fig. 35. Eigenvalues of system over 2-σ variation in Δ for gPC approximation and Monte-Carlo prediction

tem is clearly stable with probability greater than or equal to 95%. Beyond simply testing for stability, we can use this framework to design controllers that guarantee performance with a given probability and also to create more risk-sensitive controls.

Multivariate Distributions with Different PDF's

Thus far, the examples presented in this work has assumed that all uncertainty appearing in the equations of motion have the same probability distributions. While on face it seems that this is a necessary assumption, we will show that it is simple to incorporate independent random variables governed by different probability distributions. The difficulty that must be overcome is building a polynomial basis that is orthogonal with respect to the joint probability distribution. As an example consider two independent random variables governed by the distributions $f_1(\Delta_1)$ and $f_2(\Delta_2)$. Because the random variables are independent, the joint probability distribution is simply the product of the these distributions, or $f = f_1(\Delta_1)f_2(\Delta_2)$. To test that this distribution is still in fact a probability distribution, we integrate over the domain of $\Delta = (\Delta_1, \Delta_2)$.

$$\begin{aligned} P(1) &= \int_{\Delta} f \, d\Delta = \int_{\Delta_1}\int_{\Delta_2} f_1(\Delta_1) f_2(\Delta_2)\, d\Delta_2\, d\Delta_1 \\ &= \int_{\Delta_1} f_1(\Delta_1)\, d\Delta_1 \int_{\Delta_2} f_2(\Delta_2)\, d\Delta_2 = 1 \end{aligned}$$

So this joint distribution is in fact a probability distribution. A more theoretically sound way of seeing this is to use the definition of independent random variables. If $\Delta_1, \ldots, \Delta_n$ are independent, then

$$P(\Delta_1, \ldots, \Delta_n) = \prod_{i=1}^{n} P_i(\Delta_i)$$

This justifies our choice of joint distribution. The benefit of this joint distribution is that it allows us to define multivariate polynomials orthogonal to the joint distribution as products of the univariate polynomials associated with each single distribution. The joint distribution is given by $f(\Delta_1, \ldots, \Delta_n) = \prod_{i=1}^{n} f_i(\Delta_i)$. To define the associated gPC expansion, we again return to the two-dimensional case. Let ϕ_i^j correspond

to the i^{th} order polynomial associated with Δ_j and its corresponding probability distribution (weight function). The set of polynomials of order 0 are given by

$$O(0) = \{\phi_0^1, \phi_0^2, \phi_0^1\phi_0^2, \ldots\}$$

For sets of orthogonal polynomials, these are always 1 and thus $\phi_0 = 1$. For the set of first, second, and third order polynomials, the sets of polynomials are given by

$$\begin{aligned} O(1) &= \{\phi_1^1, \phi_1^2\} \\ O(2) &= \{\phi_2^1, \phi_1^1\phi_1^2, \phi_2^2\} \\ O(3) &= \{\phi_3^1, \phi_2^1\phi_1^2, \phi_1^1\phi_2^2, \phi_3^2\} \end{aligned}$$

The factorial relationship for the number of polynomials presented throughout the work holds even with multiple distributions. Because ϕ_i^1 and ϕ_j^2 are functions of different variables, it is easy to see that the orthogonality properties of the single dimensional polynomials carry over to the multidimensional case as well. This can be generalized for the n-dimensional case to obtain orthogonal polynomials with respect to n variables all governed by possibly different distributions. It is also not important for the domain of each variable to be the same as the projections onto each space correspond to multiple integrals over the domain of each random variable. As an example consider a simple linear system $\dot{x} = Ax$ with

$$A = \begin{bmatrix} -1.5 + \Delta_1 & -1.5 + \Delta_2 \\ 1 & 0 \end{bmatrix}$$

where $\Delta_1 \in [-1, 1]$ is governed by a uniform distribution and $\Delta_2 \in [-1, 1]$ is governed by a Beta distribution with $\alpha = \beta = 2$. The polynomials up to third order are given in table 10. With this set of orthogonal polynomials, we are able to predict the system mean and variance of the system response very accurately. Here we use a 4^{th}

Table 10. Two-dimensional polynomials up to 3^{rd} order where Δ_1 is governed by a uniform distribution and Δ_2 is governed by a beta distribution

n	p	ϕ_n
0	0	1
1	1	Δ_1
2		$3\Delta_2$
3	2	$\frac{1}{2}(3\Delta_1^2 - 1)$
4		$3\Delta_1\Delta_2$
5		$7\Delta_2^2 - 1$
6	3	$\frac{1}{2}(5\Delta_1^3 - 3\Delta_1)$
7		$\frac{3}{2}(3\Delta_1^2\Delta_2 - \Delta_2)$
8		$7\Delta_1\Delta_2^2 - \Delta_1$
9		$15\Delta_2^3 - 5\Delta_2$

order expansion (meaning the number of polynomials is 15) to capture the stochastic dynamics.

Figures 36 and 37 display the mean and variances for each state as predicted by the gPC expansion. These lie directly on top of those observed by Monte Carlo simulations. We can see that toward the end of the simulations, there is a small amount of error build up in the variance, but this is many orders of magnitude lower than the variance of the response. For this system, even with fourth order polynomials we are able to predict the interaction between two independent random variables governed by different distributions. Because there are more random variables, accurately predicting the variance requires many more polynomials than for the case when the uncertainty is governed by a single random variable. For linear systems, this increase in dimensionality is not a significant problem (for systems of fairly low order). For

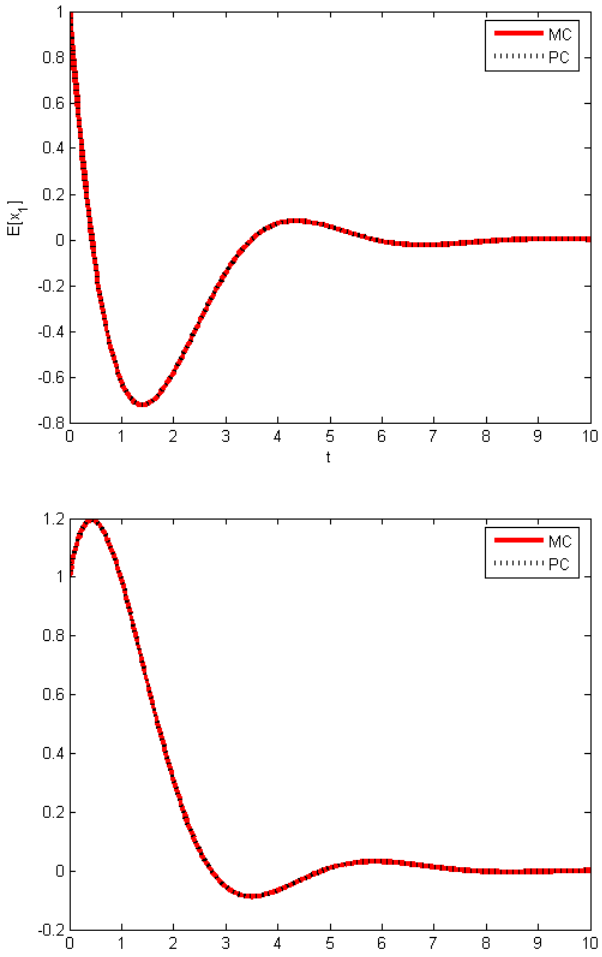

Fig. 36. Expected value of both states of the stochastic system from gPC prediction and Monte-Carlo observation

nonlinear systems, this higher dimensionality can create some difficulty. This example serves to demonstrate the ability of the gPC expansion to handle types of problems that are extremely difficult to handle in a traditional sampling-based framework.

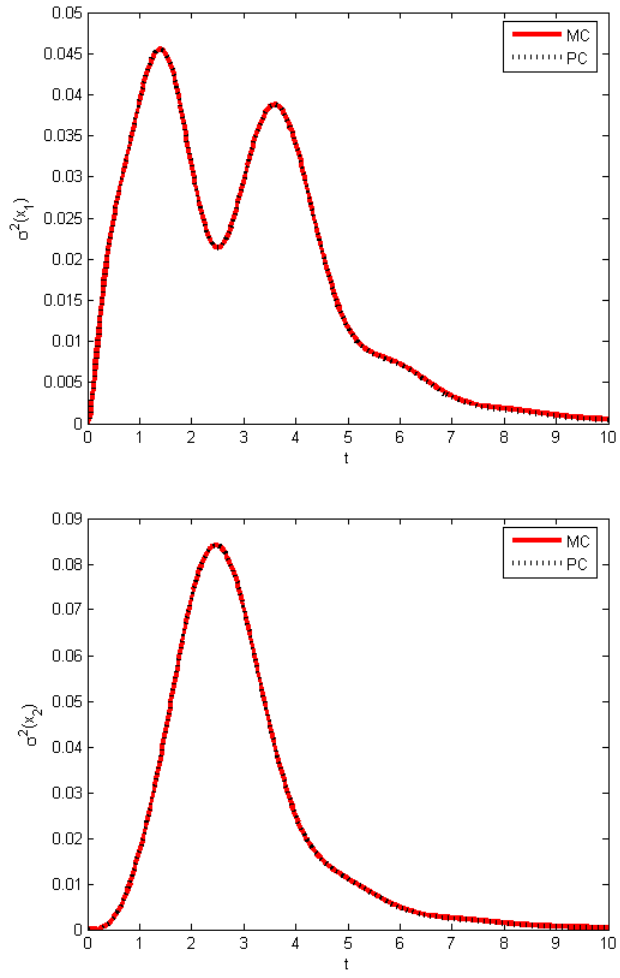

Fig. 37. Variance response of each state of the stochastic system from gPC prediction and Monte-Carlo observation

VITA

James Robert Fisher received his Bachelor of Science in mechanical engineering from Texas A&M University in May 2001. He received a Master of Science in mechanical engineering in December 2004 and his Ph.D. in aerospace engineering in August 2008 also from Texas A&M Univeristy. James has experience working with nonlinear and adaptive control systems, neural networks, nonlinear optimal control, and stochastic systems analysis and control. James is currently working for Raytheon Missile Systems in Tucson, Arizona developing guidance and control algorithms for research systems. He can be reached at the address:

Department of Aerospace Engineering
H.R. Bright Building, Rm. 701, Ross Street - TAMU 3141
College Station TX 77843-3141